Institute für Theoretische Physik
Fakultät Mathematik und Naturwissenschaften
Technische Universität Dresden

Wavefunction-based method for excited-state electron correlations in periodic systems

— application to polymers —

Dissertation
zur Erlangung des
Doktorgrades der Naturwissenschaften
(Doctor rerum naturalium)

vorgelegt von
Viktor Bezugly
geboren am 7. Juli 1976 in Charkow

Dresden 2004

Eingereicht am 17. Dezember 2003

1. Gutachter: Prof. Dr. Peter Fulde

2. Gutachter: Dr. habil. Uwe Birkenheuer

3. Gutachter: Prof. Dr. Hermann Stoll

Verteidigt am 25. Februar 2004

Abstract

In this work a systematic method for determining correlated wavefunctions of extended systems in the ground state as well as in excited states is presented. It allows to fully exploit the power of quantum-chemical programs designed for correlation calculations of finite molecules.

Using localized Hartree–Fock (HF) orbitals (both occupied and virtual ones), an effective Hamiltonian which can easily be transferred from finite to infinite systems is built up. Correlation corrections to the matrix elements of the effective Hamiltonian are derived from clusters using an incremental scheme. To treat the correlation effects, multireference configuration interaction (MRCI) calculations with singly and doubly excited configurations (SD) are performed. This way one is able to generate both valence and conduction bands where all correlation effects in the excited states as well as in the ground state of the system are taken into account. An appropriate size-extensivity correction to the MRCI(SD) correlation energies is developed which takes into account the open-shell character of the excited states.

This approach is applicable to a wide range of polymers and crystals. In the present work *trans*-polyacetylene is chosen as a test system. The corresponding band structure is obtained with the correlation of all electrons in the system being included on a very high level of sophistication. The account of correlation effects leads to substantial shifts of the "center-of-mass" positions of the bands (valence bands are shifted upwards and conduction bands downwards) and a flattening of all bands compared to the corresponding HF band structure. The method reaches the quantum-chemical level of accuracy.

Further an extention of the above approach to excitons (optical excitations) in crystals is developed which allows to use standard quantum-chemical methods to describe the electron-hole pairs and to finally obtain *excitonic* bands.

Contents

List of abbreviations

1D	one-dimensional
CC	Coupled-cluster
cc-p	correlation consistent (basis set) including polarization functions
CCSD	Coupled-cluster with singly and doubly excited configurations
CI	Configuration interaction
DFT	Density functional theory
EA	Electron affinity
GTO	Gaussian-type orbital
HF	Hartree–Fock
HOMO	Highest occupied molecular orbital
IP	Ionization potential
IS	Incremental scheme
LCAO	Liner combination of atomic orbitals
LDA	Local density approximation
LMO	Localized molecular orbital
LUMO	Lowest unoccupied molecular orbital
LME	Local matrix element
MP2	Møller–Plesset perturbation theory in second order
MR	Multireference
MRCI	Multireference configuration interaction
SD	Single and double excitations
SCF	Self-consisted field
tPA	*trans*-polyacetylene
VDZ	Valence double zeta
VTZ	Valence triple zeta
WO	Wannier orbital

Chapter 1

Introduction

The study of electronic properties of solids was constantly a hot topic in physics over many decades. Various different approximations, e.g. the free-electrons model, the tight-binding method and others (see, e.g. [Z72]), were tried to get qualitative description of the electron states in periodic systems. More sophisticated methods aiming already at a quantitative description have been developed since computers have become a common tool of researchers. Among these methods one could distinguish a number of approaches based on the local density approximation (LDA) to density functional theory (DFT) [HK64], [KS65] which are widely used presently in solid-state physics. They allow, in particular, to account for electron correlation effects by locally treating electrons as a homogeneous gas. These methods have become very popular as they provide quantitatively correct results for the ground state of many systems. However, these methods fail to describe correctly the band structure of solids, e.g. they usually give too narrow band gaps for non-conducting systems. To overcome this problem, further improvements of the formalism have been developed. For instance in the last decade the most successive methods became those based on the so-called *GW* approximation [H65].

One of main advantages of methods based on DFT is their relatively small computational cost that opens the possibility to routinely apply them to periodic systems with large unit cells. However, all DFT-based methods are focused on computing

physical ground-state properties of the systems which are related to electron density and avoid calculation of the many-body wavefunction which would provide us with explicite information on the electron correlation in particular materials. Another serious disadvantage of DFT methods is the impossibility to control the accuracy of the obtained results and to improve them in a systematic manner. Thus, in the long perspective, an alternative way to study electron states in periodic systems is required.

In parallel to the development of DFT-based approaches, methods which solve the Hartree–Fock (HF) equation for solids were established. They provide single-particle wavefunctions and energies obtained self-consistently with the many-body wavefunction being a superposition of Bloch waves. For this purpose powerful program packages like CRYSTAL [PDR88], [CRY98] have been designed. The use of the variational method to solve the HF equation allows one to reach the desired accuracy within a given set of parameters (such as basis sets, crystal geometry, thresholds for integral values etc.) and a systematic improvement of the basis sets and a reducing of the thresholds leads to further improvement of the results. However, in this approach electrons are considered to experience only a mean interaction field and thus the electron correlation is missing totally. As a result of this, the fundamental band gap of non-conducting materials is substantially overestimated by the HF method.

Let us now turn to quantum chemistry. In this field, an intensive development of methods which start with the HF solution for finite systems and accurately account for electron correlation took place. These methods yield *correlated* wavefunctions and *correlated* energies of finite molecules in good agreement with experimental data. A detailed description of such approaches can be found in, e.g. [SO96] and [LM86]. Among these methods one can distinguish the configuration interaction (CI) methods, the coupled cluster (CC) methods and methods based on the many-body perturbation theory (MBPT) such as the second-order Møller–Plesset (MP2) method which have become standard in quantum chemistry and are implemented in quantum-chemical program packages like MOLPRO [M2000] and GAUSSIAN

[G98].

At first glance, there is no possibility to apply these quantum-chemical methods (which operate with single-electron wavefunctions defined in real space) to extended systems where the states are usually defined in momentum space. However, if one reformulates the HF solution in terms of localized Wannier functions, which are defined in the real space, and considers finite clusters of the crystal, then one can account for correlation effect within this cluster. An electron placed in a localized orbital interacts strongly with electrons in neighbor localized orbitals trying to avoid coming too close to each other. Electrons in farther orbitals are already screened and "felt" via the mean field established in the HF description. Thus, electron correlation is predominantly a local effect, and therefore the electron correlation effects in an entire crystal can be derived from finite clusters. Here, very accurate quantum-chemical methods can be employed. One only needs a scheme to transfer the results from clusters to periodic systems which in fact resembles a Wannier back transformation. This way one gets the *correlated* wavefunction of extended system with which any physical quantity of a system can be calculated. The scheme described above preserves the spirit of *wavefunction-based* methods which consist of a sequence of *well-controlled* approximations and thus allowing to *estimate* and *improve* the accuracy of the final results.

The implementation of this idea has started in the late eighties of the last century and from that time has reached a valuable success. Ground-state and cohesive energies of many covalent and ionic systems have been calculated until now (see e.g. [St92a], [St92b], [PFS95], [PFS96], [DDFS97], [KPFS97], [ASD00a] and [ASD00b]). The approach was also used to study structural properties of polymers ([YKD97] and [AA+99]). In parallel to the study of ground-state properties of extended systems, an approach for the hole states in periodic infinite systems has been developed. To the present moment it was addressed to the valence bands of simple semiconductors, such as diamond, silicon and germanium ([GSF93], [GSF97] and [AFS00]). Further information on the current state of the art of wavefunction-based approaches for

extended systems which employ quantum-chemical methods can be found in the recent review [F02].

Another promising wavefunction-based method appeared recently and has successively been applied to the band structure of LiF (see [AI01], [AF02] and [A02]). In the post-HF step it uses Green's function formalism which is usually not considered as a standard quantum-chemical method. Therefore, we only mention it here briefly.

As one can notice, the wavefunction-based methods for solids described in [GSF93], [GSF97] and [AFS00] study correlation of electrons in occupied orbitals. However, to also obtain correlated *conduction* bands one needs a proper description of correlation effects for states with an additional electron in the virtual space as well. Without this one can not evaluate one of the most fundamental electronic property of insulators and semiconductors, namely the band gap. The main reason of the previous approaches to fail here is the impossibility to construct localized virtual orbitals in clusters (in contrast to occupied orbitals) by standard localization schemes used in quantum chemistry. Therefore, a different approach to localization of virtual orbitals was needed.

Conceptual works [MV97] and [SMV01] on obtaining maximally localized orbitals in periodic systems and implementations of similar ideas in CRYSTAL code ([BZ+01] and [ZWDS01]) convinced us to use localized virtual orbitals obtained in a periodic system as a starting point for the construction of localized virtual molecular orbitals for sufficiently large cluster models of periodic systems. This way we could properly describe states with an attached electron in crystals by means of finite clusters. Thus, we can calculate not only valence but also conduction bands and, therefore, the band gap provided electron correlation effects are accurately and systematically taken into account. This we regard as the main motivation for the present work.

In fact, having obtained the *correlated* band structure we extract from it not only the band gap but also band widths, the ionization potential and the electron affinity

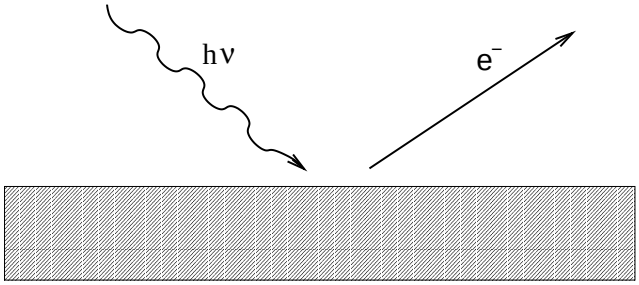

Figure 1.1: A schematic view of photoionization process.

of the system with electron correlation being taken into account. The correlated wavefunction is used implicitely to calculate these quantities. Our approach also allows us to estimate the error bar for each calculated quantity and it provides a way to improve the accuracy further.

All the quantities calculated here can also be measured directly in experiments. To study the band structure of crystals photoionization (Fig. 1.1) and inverse photoionization experiments (Fig. 1.2) can be performed (see e.g. [PS99]).

Ionization potentials IP_n (the valence-band energies) are the difference between the energy of $(N-1)$-electron system with a hole in band n and the energy of the neutral N-electron system. This quantity can be measured by irradiation of light with known frequency on the surface of a crystal and measuring the kinetic energy of the photoemitted electrons: $E_{\mathrm{kin}} = h\nu + (E_0 - {}^{N-1}E_n) = h\nu - \mathrm{IP}_n$.

The inverse process is used to measure the electron affinities EA_m which correspond to the energy which a neutral system gains when an extra electron is accepted in the conduction band m and an $(N+1)$-electron state is formed. Electrons with known kinetic energy are shined onto the surface and the frequency of the emitted light is measured: $h\nu_m = E_{\mathrm{kin}} + (E_0 - {}^{N+1}E_m) = E_{\mathrm{kin}} + \mathrm{EA}_m$. This two experiments give band energies which we aim to calculate theoretically.

Another motivation of this study is to extend the borders of the wavefunction-based approaches to correlated band structures. By this we mean that we would like i) to investigate a system with more complex unit cell than was done before, ii) to use larger basis sets (valence triple zeta) which are necessary in quantum chemistry to

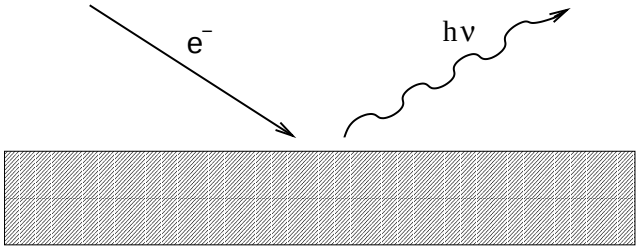

Figure 1.2: A schematic view of inverse photoionization process.

obtain indeed accurate results and which are appropriate for correlation calculation in $(N+1)$-electron systems and iii) to use one of the most accurate and powerful correlation method (the multireference configuration interaction method restricted to singly and doubly excited configurations) available in standard quantum-chemical program packages. The implementation of all the ideas mentioned above put our approach far ahead with respect to other methods for band structure calculations in non-conducting systems.

Yet another goal of our study is to develop an approach which allows to even describe well-bound excitons in crystals. These electron-hole pairs made up by neutral excitations of the electronic structure are rather compact objects and therefore can be treated in real space. Occupied and virtual Wannier orbitals are used for that purpose such that the electron-hole pair can be described in finite clusters of the crystal by standard quantum-chemical methods. Provided, the localized orbitals in such a cluster represent the Wannier orbitals of the crystal well, an appropriate transformation allows to transfer the relevant data on the localized excitonic states from the clusters to the periodic system and excitonic bands can be calculated.

As a test system we have chosen *trans*-polyacetylene (tPA). This is a semiconducting polymer which consists of weakly interacting single chains. Therefore, its highly anisotropic electronic properties can be studied in a one-dimensional system, a tPA single chain. This is a very useful feature for the implementation of our approach to conduction bands in particular because the corresponding localized virtual one-particle orbitals are in fact rather diffuse objects. To study the decay of

the correlation effects with the distance of the involved localized orbitals we need a linearly scaling system.

Also polymers themselves are intriguing systems providing researchers with surprising results. The discovery and development of electrically conductive polymers were appreciated by the Nobel Prize in Chemistry for 2000. One of the experimentally well-studied systems is doped *trans*-polyacetylene. Thus, the sound understanding of the electronic structure of tPA is highly desired. In our work we also aim to answer the question whether electron correlation in polymers can be described properly in a single chain to give results which agree with experimental data for the bulk system. For this purpose, in section 3.1.1, we describe in details the investigated material and further, in section 4.4, we compare results obtained for tPA single chains with existing experimental data on bulk tPA crystals.

The thesis is organized as follows. In Chapter 2 the basic theoretical aspects of our approach are discussed. At the beginning of the chapter we briefly sketch the approximations used in *ab initio* methods. In first sections we consider the solution of the HF equation for infinite systems in terms of Bloch waves and Wannier orbitals and define the local quantities which also show up in infinite systems and clusters and which can be transferred from one to another. In the last two sections we discuss why electron correlations are necessary to be taken into account, the physical meaning of these effects in both neutral and charged systems, and how these correlation effects can be evaluated by the MRCI(SD) method.

Chapter 3 is dedicated to the development of our wavefunction-based approach. First we introduce the structural and electronic properties of the test system. Next we discuss in details how to get localized HF occupied and virtual orbitals in clusters and define the corresponding local matrix elements (LMEs) which are used to calculate the SCF band structure of tPA. In section 3.3 we discuss how to evaluate the correlation corrections to the LMEs by MRCI(SD) method, and the use of an approximate but well controlled scheme for this purpose (namely incremental scheme) is presented in section 3.4. The possibility to reduce the size-extensivity error of

CI(SD) is explored in section 3.5. In the last section of Chapter 3 the way to handle the problem of the emergence of satellite states in cluster models is presented.

In Chapter 4 we summarize and discuss numerical results for *trans*–polyacetylene. There we emphasize the effect of electron correlation on the key quantities of our method, namely the local matrix elements. We use correlation corrected LMEs to plot the correlated band structure from which we get the band gap, IPs, EAs, and band widths of linear tPA. The accuracy of the whole method is explored and the error bars for the calculated quantities are estimated. In section 4.4 we compare our results obtained for the one-dimensional system to experimental data on bulk *trans*–polyacetylene.

In Chapter 5 we introduce a new approach to excitonic states in crystals in terms of singly excited configurations. The method is established and some preliminary results are presented.

In Chapter 6 we conclude and discuss perspectives of our approach.

Chapter 2

Local approach to wavefunctions

In this chapter we would like to discuss the basic theoretical approaches to our study. The ultimate goal of the physicist studying theoretically electronic properties of an atom, a molecule or even a bulk material would be to get a many-body wavefunction which maximally approaches the exact one and contains all the information about the electronic structure, the forces on the nuclei, and other parameters of the system in all its possible states. Unfortunately, obtaining the exact many-body wavefunction is unrealistic. In order to proceed one has either to make some approximations for the wavefunctions and then to calculate the desired quantities with this approximated wavefunctions (and to estimate the emerging errors) or one tries to obtain those quantities directly (avoiding the calculation of wavefunctions) using some tricks or semiempirical methods. In the latter case the question about the achievable accuracy often remains open. When one is interested not only in a qualitative description of a system and the effects in it, but also in accurate quantitative results then the first way seems to be more attractive, even though more complicated. Having chosen this way, one choses the most accurate among all feasible approximations in order to get a realistic description of the system and to reduce the errors to a minimum.

In our study we are aiming at a *correlated* wavefunction of a periodic system (e.g. *trans*-polyacetylene). This means that we introduce some controlled approximations

at the very beginning, then get the wavefunction which is assumed to be very close to the real one, and finally calculate the ground state energy and energies of one-particle states (the band structure). By the term "controlled approximation" we mean that we can both estimate the error bar for the calculated quantities and improve our results to (in principle) any desired accuracy by increasing the computational efforts. Here we mention these approximations.

The first one is the Born–Oppenheimer approximation. The system under consideration consists of nuclei vibrating around their equilibrium positions and electrons filling the space between the nuclei. The Hamiltonian of the system and, correspondingly, its wavefunction depends on coordinates of both all nuclei and all electrons. As electrons are much lighter than nuclei they move much faster and, therefore, can be considered as moving in the field of fixed nuclei (for details we reffer to [Z72], chapter 6.11). Then solving only the "electronic" part of the Hamiltonian one obtains electron eigenfunctions and eigenvalues which depend parametrically on the nuclear coordinates. Having the solution for the electron problem one considers the nuclei as slowly moving in the averaged field of the fast moving electrons and solves the problem of vibration, rotation and translation of the system consistently with the help of electronic solutions. In our work we are concentrating on the electronic problem and consider the nuclei as fixed at their equilibrium positions which we can define e.g. by using experimental data on the structure of a given material. By this we exclude the vibrational and rotational degrees of freedom of finite systems baring in mind, however, the possibility to obtain them by looking at the electronic structure for different positions of the nuclei. This approximation is valid as long as electron-phonon interaction in the system is negligible.

The second point to discuss is the use of basis sets for the electron wavefunctions which are necessary for numerical calculations of electronic structures. We use atomic basis sets since quantum chemistry has demonstrated for many decades that for atoms and molecules this representation gives very accurate results as compared to experimental data. We also have to notice that this basis sets are finite. To set

up an analytic expression for the wavefunction of an electron we use Gaussian-type atomic orbitals (GTO) which are very favourable from the computational point of view. With these GTO basis sets very accurate results can be obtained and the accuracy depends on the number of atomic orbitals in the basis set for each atom and on the number of Gaussians per atomic orbital. Enlarging these numbers leads to tremendous computational efforts when one wants to treat big molecules which in fact limits the size of basis sets. However, at this point we want to emphasize that finite but sufficiently large GTO basis sets can provide reasonable accuracy and are still convenient to use.

In our work we consider systems consisting of light atoms whose atomic numbers are not larger than six. Therefore, we can neglect relativistic effects and consider the spin coordinates of electrons as independent from their spatial ones. Spin-orbital coupling only becomes not negligible for more heavy atoms starting from the atomic number around 30 (see, e.g. §72 in [LL77] and chapter 3.11 in [Z72]). In zero-oder approximation we consider the wavefunction of a system as being the one of an independent particles system where electrons occupy spin orbitals (a function of electron position vector $\mathbf{r}_i$ and spin coordinate σ_i) or alternatively we can say that spatial orbitals (which depend only on $\mathbf{r}_i$) are occupied by pairs of electrons one having spin up and the other having spin down. Such spin orbitals are solutions of a single-particle Hamiltonian in the self-consisted field (SCF) approximation and are represented as linear combinations of atomic orbitals (LCAO). Then, the many-body wavefunction of the whole system is given as the antisymmetrized product of all occupied spin orbitals, the so-called Slater determinant (see e.g. [SO96]). The ansatz to write molecular orbitals as LCAO is also an approximation and is based on the fact that when an electron is placed close to one nucleus its interaction energy with this nucleus is much larger than interaction with all other nuclei. In quantum chemistry the LCAO approximation is very common and considered as being proved empirically to yield very good agreement between experimental data and theoretical results for molecules, once electron correlations are included.

Despite the essentially unavoidable approximations mentioned so far we do not make any approximation for the nuclear potentials and the Coulomb interaction between electrons. The systems are treated as realistic as possible keeping by this the sense of *ab initio* calculations.

As mentioned above we start from the wavefunction of the closed-shell system obtained in the SCF (or HF) approximation. In this approximation the one-particle Hamiltonian is constructed, treating an electron as moving in the field of the fixed nuclei and the averaged field of all the remaining electrons. The set of electron orbitals is obtained as the solution of this problem. Electrons are placed in this orbitals starting from the one with the lowest energy and filling the $N/2$ energetically lowest spatial orbitals where N denotes the number of electrons in the system. All the other orbitals remain unoccupied. The solution is obtained iteratively with the desired precision for the chosen basis sets. We do not want to discuss here the quality of results obtained with such a wavefunction as it is well known from both solid state physics and quantum chemistry that the Hartree–Fock approximation provides a reasonable but not accurate wavefunction and that for some properties it only gives qualitative results. However, it is also known that this wavefunction may serve as a good starting point for further improvement towards the exact wavefunction as long as weakly correlated systems are considered. So, our aim is start from the HF approximation and to go beyond it in order to obtain some good approximation to the correlated wavefunctions of a system and to calculate the ground state energy and energies of the excited states.

Moreover, the system which we refer to is periodic and infinite. Our approach will allow to transfer the data obtained in clusters with standard quantum-chemical program packedges to the infinite system exploiting the local character of electron correlations. For this purpose we have to define local quantities (electron orbitals and matrix elements) which have identical meaning in the clusters and in the infinite systems and to esteblish a scheme to transfer them.

In the first Section we consider the HF solution for infinite systems, namely,

Bloch waves, the ground state energy and the band structure. In Section 2.2 we redefine these quantities in terms of Wannier orbitals. In Section 2.3 we show how those local quantities may be obtained for clusters and how they are transferred to infinite systems to give the band structure. In Section 2.4 we discuss why electron correlation should be taken into account, the physical meaning of this effect and how it is incorporated in our method. There we also define the correlated wavefunction. In Section 2.5 the quantum-chemical correlation method is described: why we have chosen the particular method, its advantages and disadvantages as compeared to other methods, the results which we get by using it and their quality.

2.1 The Hartree–Fock approximation

The electronic *ab initio* Hamiltonian of a solid or molecule in the Born–Oppenheimer approximation is written in the form

$$H_{\text{el}} = -\sum_i \frac{1}{2}\nabla_i^2 - \sum_{i,A} \frac{Z_A}{|\mathbf{r}_A - \mathbf{r}_i|} + \sum_{i<j} \frac{1}{|\mathbf{r}_i - \mathbf{r}_j|} + \sum_{A<B} \frac{Z_A Z_B}{|\mathbf{r}_A - \mathbf{r}_B|} \qquad (2.1)$$

where $\mathbf{r}_i$ and $\mathbf{r}_j$ are the coordinates of electrons, $\mathbf{r}_A$ and Z_A are the fixed coordinates and the atomic number of nucleus A. Atomic (Hartree) units are used here where electron charge e is set to 1. The last term in Eq. (2.1) is the interaction energy between the fixed nuclei and does not affect the electronic eigenfunctions. We omit this term in further consideration bearing in mind that this constant for given geometry must be added to the system total energy at the end.

The many-body wave function for N independent electrons may be written as an antisymmetrized product (or the Slater determinant) of the spin orbitals $\psi_i(\mathbf{r}\sigma)$:

$$\Phi(\mathbf{r}_1\sigma_1;\ldots;\mathbf{r}_N\sigma_N) = \frac{1}{\sqrt{N!}}\begin{vmatrix} \psi_1(\mathbf{r}_1\sigma_1) & \psi_2(\mathbf{r}_1\sigma_1) & \cdots & \psi_N(\mathbf{r}_1\sigma_1) \\ \psi_1(\mathbf{r}_2\sigma_2) & \psi_1(\mathbf{r}_2\sigma_2) & \cdots & \psi_N(\mathbf{r}_2\sigma_2) \\ \vdots & \vdots & \ddots & \vdots \\ \psi_1(\mathbf{r}_N\sigma_N) & \psi_1(\mathbf{r}_N\sigma_N) & \cdots & \psi_N(\mathbf{r}_N\sigma_N) \end{vmatrix}$$

$$\equiv \frac{1}{\sqrt{N!}}\det[\psi_1(\mathbf{r}_1\sigma_1)\ldots\psi_N(\mathbf{r}_N\sigma_N)]. \tag{2.2}$$

Let us denote $\Phi(\mathbf{r}_1\sigma_1;\ldots;\mathbf{r}_N\sigma_N)$ as Φ for the convenience. The expectation value of the ground-state energy of the system is defined as $E_0 = \langle\Phi|H_{\text{el}}|\Phi\rangle$. By optimizing the spin orbitals ψ_i one obtains the lowest value for E_0 under the constraint that spin orbitals ψ_i remain orthogonal to each other and normalized: $\langle\psi_i|\psi_j\rangle = \delta_{ij}$. As the solution of this variational problem the HF single-determinant wavefunction of the many-electron system is obtained. It consists of spin orbitals being eigenfunctions of the self-consistent single-particle Fock operator F:

$$F|\psi_i\rangle = \varepsilon_i|\psi_i\rangle \tag{2.3}$$

where F takes a diagonal form in the representation of the canonical orbitals ψ_i and has the following matrix elements:

$$f_{ij} = \langle\psi_i|h_1|\psi_j\rangle + \sum_{l=1}^{N}\big(\langle\psi_i\psi_l|v_{12}|\psi_j\psi_l\rangle - \langle\psi_i\psi_l|v_{12}|\psi_l\psi_j\rangle\big). \tag{2.4}$$

and electron orbitals ψ_i are obtained self-consistently. In Eq. (2.4) index l counts the occupied orbitals and operators h_1 and v_{12} are defined as

$$h_1 = -\frac{1}{2}\nabla_1^2 - \sum_A \frac{Z_A}{|\mathbf{r}_A - \mathbf{r}_1|} \tag{2.5}$$

and

$$v_{12} = \frac{1}{|\mathbf{r}_1 - \mathbf{r}_2|}. \tag{2.6}$$

The derivation of the equation (2.3) can be found in many textbooks (e.g., in [SO96]).

Getting an analytic solution of the Fock equation (2.3) is not possible in general case and numerical methods have to be used for this purpose. In quantum-chemical program packages the Fock eigenfunctions are obtained iteratively in the form of linear combinations $\psi_i = \sum_j \chi_j \alpha_{ji}$ within a chosen atomic basis sets $\{\chi_j\}$ by varying the coefficients α_{ji} and minimize the ground-state energy of the system. In our study solving the Fock equation is a routine procedure and we do not want to pay too much attention to the details of Hartree–Fock theory. We only want to point out the physical meaning of the eigenvalues in Eq. (2.3). The quantity ε_i represents an energy of an electron occupying the spin orbital ψ_i. It consists of the electron kinetic energy, its potential energy in the field of nuclei and in the mean field of the other electrons. The latter in its turn consists of the Coulomb repulsion energy and the exchange energy which are determined correspondingly by the two last terms in the right-hand side of Eq. (2.4). The N spin orbitals with the lowest orbitals energies are occupied in the ground state. Further we use indices a, b, c,... for these occupied orbitals. The remaining eigenfunctions from (2.3) stay unoccupied in the ground state and are labeled by r, s, t,.... If a statement or a formula is valid for both, occupied and virtual orbitals, we use the indices i, j, k,.... Also for the sake of convenience we use $|i\rangle$ instead of $|\psi_i\rangle$. Multiplying Eq. (2.3) by $\langle i|$ from the left and taking into account Eqs. (2.4)–(2.6) we get an expression for orbitals energies

$$\varepsilon_i = \langle i|h_1|i\rangle + \sum_{b=1}^{N}\big(\langle ib|v_{12}|ib\rangle - \langle ib|v_{12}|bi\rangle\big) \equiv \langle i|h|i\rangle + \sum_{b=1}^{N}\big(\langle ib|ib\rangle - \langle ib|bi\rangle\big) \quad (2.7)$$

where the potential v_{12} is omitted in the matrix element for convenience. In particular we can write the energies for the occupied orbitals as

$$\varepsilon_a = \langle a|h|a\rangle + \sum_{b\neq a}\big(\langle ab|ab\rangle - \langle ab|ba\rangle\big) \quad (2.8)$$

and that for the unoccupied orbitals as

$$\varepsilon_r = \langle r|h|r\rangle + \sum_{b=1}^{N}\big(\langle rb|rb\rangle - \langle rb|br\rangle\big). \tag{2.9}$$

These two quantities are of special interest in our study. Let us look more closely at expressions (2.8) and (2.9). The energy of an electron in an occupied orbital ψ_a (2.8) consists of its kinetic energy, the energy of attraction to the nuclei plus the Coulomb ($\langle rb|rb\rangle$) and exchange ($-\langle rb|br\rangle$) interaction with each of the $N-1$ remaining electrons of the system in the ground state. Therefore we can refer to the value $-\varepsilon_a$ as to an energy which is necessary to pay in order to remove an electron from the occupied orbital ψ_a without changing the rest of the system, that is the ionization potential of the system in the frozen orbital approximation. An unoccupied orbital energy is the sum of kinetic energy of an electron on this orbital, the energy of its attraction to the nuclei and energies of Coulomb and exchange interaction with all N electrons of the system in the ground state as if an additional $(N+1)$-th electron would have been adiabatically added to the system (i.e. in the frozen orbital approximation) on the r-th orbital. Thus, we can regard the value $-\varepsilon_r$ as the energy one gains when adding one electron to the neutral system and placing it into the orbital ψ_r that is by definition the electron affinity. These two statements are known as Koopmans' theorem [Ko34].

To demostrate how these simple relations (2.8) and (2.9) arise from the frozen orbital approximation we provide the proof for this theorem. The ionization potential is the difference between the energy of the system with $N-1$ electron (excited state) and the energy of N-electron system (its ground state)

$$\mathrm{IP} = {}^{N-1}E - E_0 \tag{2.10}$$

and the electron affinity is the difference between the ground state energy and the

energy of $(N+1)$-electron system

$$\mathrm{EA} = E_0 - {}^{N+1}E. \tag{2.11}$$

It is convenient to define state eigenfunctions in the second quantization formalism (especially in the case of infinite systems). Then the ground state wavefunction is written as

$$|\Phi\rangle = \prod_a c_a^\dagger |0\rangle \tag{2.12}$$

where $c_a^\dagger$ is the creation operator for an electron in an occupied spin orbital ψ_a and $|0\rangle$ is the vacuum state. The $(N-1)$-electron state in the frozen orbital approximation is given by

$$|\,{}^{N-1}\Phi_c\rangle = c_c|\Phi\rangle \tag{2.13}$$

and the $(N+1)$-electron state by

$$|\,{}^{N+1}\Phi_r\rangle = c_r^\dagger|\Phi\rangle \tag{2.14}$$

where the operator c_c destroys an electron in occupied spin orbital ψ_c and the operator $c_r^\dagger$ creates an electron in virtual spin orbital ψ_r. Let us note that ${}^{N-1}\Phi_c$ and ${}^{N+1}\Phi_r$ are singe determinants constructed from $N-1$ and $N+1$ spin orbitals with $1/\sqrt{(N-1)!}$ and $1/\sqrt{(N+1)!}$ as normalization factors, respectively. The energies E_0, ${}^{N-1}E_c$ and ${}^{N+1}E_r$ are obtained as the expectation values of these single determinants:

$$E_0 = \langle\Phi \mid H \mid \Phi\rangle = \sum_{a=1}^{N}\langle a|h|a\rangle + \frac{1}{2}\sum_{a=1}^{N}\sum_{b=1}^{N}\big(\langle ab|ab\rangle - \langle ab|ba\rangle\big), \tag{2.15}$$

$${}^{N-1}E_c = \langle {}^{N-1}\Phi_c \mid H \mid {}^{N-1}\Phi_c\rangle = \sum_{a\neq c}\langle a|h|a\rangle + \frac{1}{2}\sum_{a\neq c}\sum_{b\neq c}\big(\langle ab|ab\rangle - \langle ab|ba\rangle\big) \tag{2.16}$$

and

$$
\begin{aligned}
{}^{N+1}E_r &= \langle {}^{N+1}\Phi_r \mid H \mid {}^{N+1}\Phi_r \rangle = \sum_{a=1}^{N} \langle a|h|a\rangle + \langle r|h|r\rangle + \\
&\frac{1}{2}\sum_{a=1}^{N}\sum_{b=1}^{N}\big(\langle ab|ab\rangle - \langle ab|ba\rangle\big) + \sum_{b=1}^{N}\big(\langle rb|rb\rangle - \langle rb|br\rangle\big). \qquad (2.17)
\end{aligned}
$$

The energy for taking an electron out from the spin orbital ψ_c of the neutral system is given by difference between (2.16) and (2.15)

$$
\begin{aligned}
\mathrm{IP}_c &= \sum_{a\neq c}\langle a|h|a\rangle + \frac{1}{2}\sum_{a\neq c}\sum_{b\neq c}\big(\langle ab|ab\rangle - \langle ab|ba\rangle\big) \\
&\quad - \sum_{a=1}^{N}\langle a|h|a\rangle - \frac{1}{2}\sum_{a=1}^{N}\sum_{b=1}^{N}\big(\langle ab|ab\rangle - \langle ab|ba\rangle\big) \\
&= -\langle c|h|c\rangle - \sum_{b\neq c}\big(\langle cb|cb\rangle - \langle cb|bc\rangle\big) = -\varepsilon_c \qquad (2.18)
\end{aligned}
$$

and the energy obtained from adding an electron to the neutral system in the spin orbital ψ_r is given by difference between (2.15) and (2.17)

$$
\mathrm{EA}_r = -\langle r|h|r\rangle - \sum_{b=1}^{N}\big(\langle rb|rb\rangle - \langle rb|br\rangle\big) = -\varepsilon_r. \qquad (2.19)
$$

We have described the $(N+1)$- and $(N-1)$-electron states by single-determinant wavefunctions constructed with frozen (non-relaxed) spin orbitals which are obtained as a solutions of the equation (2.3) for the ground state of N electron system. For the case of finite molecules one should not expect spin orbitals of a neutral system to be the same as in cases of the charged one. For the more apropriate description of the $(N+1)$- and $(N-1)$-electron states in molecules, the so-called ΔSCF approach, one has to solve the corresponding HF equations for the charged open-shell systems and get energies ${}^{N-1}E_c$ and ${}^{N+1}E_r$ from these solutions. Thus, the expressions derived above for $\mathrm{IP_c}$ and $\mathrm{EA_r}$ in the frozen orbital approximation only give approximate results for finite molecules. However, formulas (2.18) and

(2.19) are correct for extended systems where the electrons are delocalized over an infinite volume and hence no orbital relaxation takes place. Here we mean "correct" in the sense of the ΔSCF approach which is purely based on the HF energies.

In a periodic infinite system the single-electron wave functions must obey the translation symmetry of the crystal. This leads to Bloch's theorem which states that each electron eigenfunction translated by a distance $R = na_l$ along a lattice vector should be equal to the original one within an exponential prefactor

$$\psi_k(\mathbf{r} + R\,\mathbf{l}_x) = \mathrm{e}^{ikR}\psi_k(\mathbf{r}) \tag{2.20}$$

where, for simplicity, we only consider a one-dimensional crystal with lattice constant a_l (aligned along the x-axis), n is an integer and the electron states are labeled by a crystal-momentum quantum numbers $k \in [-\pi/a_l; +\pi/a_l]$. The k-dependent eigenvalues of the states form energy bands and the quantity $\varepsilon_{k\nu}$ refers to the energy of an electron in a Bloch state with crystal-momentum k and from the band ν. In the ground state of an insulator or a semiconductor the energetically lowest bands are completely filled (valence bands) and are separated by a gap from the others which are empty (conduction bands). For metals partially filled bands exist in the ground state. We explicitly exclude metals for our approach to correlated wavefunctions in solids and consider systems with band gaps only.

As Koopmans' theorem holds for extended systems the electron energy $\varepsilon_{k\nu}$ of a Bloch wave $\psi_{k\nu}$ is (up to a sign) the ionization potential for taking out an electron from the system ($\mathrm{IP}_{k\nu}$) in case of valence electrons and the energy gain from putting an extra electron into a conduction band which is the electron affinity ($\mathrm{EA}_{k\nu}$). As defined in (2.10) and (2.11) they are the differences of the energies of $(N-1)$- or $(N+1)$-particle system respectively and the neutral N-particle system. These energies are defined as the expectaction values of Hamiltonians for the corresponding single-determinant wavefunctions. Since N, in this case, approaches infinity such a representation of the wavefunction becomes cumbersome and the use of the second quantization formalism seems to be more appropriate here. Then we define the

ground-state wavefunction of the N-particle system as

$$|\Phi\rangle = \prod_{k\nu}^{\text{occ}} c^{\dagger}_{k\nu\uparrow} c^{\dagger}_{k\nu\downarrow} |0\rangle \tag{2.21}$$

where operator $c^{\dagger}_{k\nu\uparrow}$ ($c^{\dagger}_{k\nu\downarrow}$) creates a spin-up (spin-down) electron in a Bloch wave, k runs over the first Brillouin zone and ν counts only the valence bands. The energy of this state is E_0 and is proportional to the volume of the extended system. The $(N-1)$-particle-state wavefunction is obtained by applying an annihilation operator for an electron with crystal-momentum k in the valence band ν and with spin σ to the wavefunction (2.21)

$$|k\nu\sigma\rangle = c_{k\nu\sigma} \mid \Phi\rangle \tag{2.22}$$

and the $(N+1)$-particle-state wavefunction by applying a creation operator $c^{\dagger}_{k\mu\sigma}$ to (2.21)

$$|k\mu\sigma\rangle = c^{\dagger}_{k\mu\sigma} \mid \Phi\rangle \tag{2.23}$$

where the index μ is used to label conduction bands. In this new notation we can define bands as energy differences which depend on k. The valence bands are given by

$$-\text{IP}_{k\nu} = -\langle k\nu\sigma \mid H \mid k\nu\sigma\rangle + E_0 \tag{2.24}$$

and the conduction bands by

$$-\text{EA}_{k\mu} = \langle k\mu\sigma \mid H \mid k\mu\sigma\rangle - E_0. \tag{2.25}$$

At first glance, such a definition of the energy bands looks more complicated as compared to the energies of single-particle states in a crystal $\varepsilon_{k\nu}$ and $\varepsilon_{k\mu}$. However, it will give us the possibility to express $\text{IP}_{k\nu}$ and $\text{EA}_{k\mu}$ as a kind of Fourier transformation of some local matrix elements and to include electron correlation by

affecting these matrix elements which would be not possible if electrons are treated as Bloch waves.

Some alternative approaches to correlated band structure (e.g. based on DFT) are focused on finding an equation analogous to Eq. (2.3) but already containing ground-state correlations. In such schemes the band energies $\varepsilon_{k\nu}$ are usually simply defined as the eigenvalues of a single-particle equation similar to the HF equations. However, these values are not strictly energies of correlated holes or attached electrons and in the DFT framework this approximation usually leads to an underestimation of the band gap of insulators and semiconductors. In contrast, in our method, we calculate separately and explicitly correlated $(N-1)$-, $(N+1)$- and N-particle states and this allows us to see how the system reacts in detail on the presence of an extra charge.

2.2 Wannier orbitals

In the HF approximation an electron is considered as moving in the averaged self-consistent field of all the other electrons. But in reality each particular electron tries to avoid coming too close to its nearest neighbors due to Coulomb repulsion. This effect can not be described on the HF level and is called electron correlation.

In our study we describe the process of adding of an electron to an infinite system or removing it which is equivalent to producing a positive charge. These extra charges are totally delocolized in the extended system since extra electrons (or holes) in crystals are Bloch waves and the response of a system with infinite number of electrons to these extra particles is a pure correlation effect. Alternatively, we can use some mathematically constructed localized orbitals for the electrons and holes and restrict the response of an area around the localized extra charge (localized electron or hole). As a consequence, the correlation problem is reduced to the consideration of a limited number of electrons in a finite part of the crystal. The obtained correlation effect can subsequently be transferred back to Bloch states.

This way we are able to get correlated wavefunctions and correlated band structures. In the present Section we will introduce the localized crystalline orbitals which can be used for that purpose.

The natural choice would be the atomic basis functions however they are not mutually orthogonal in the crystal and are not solutions of the HF problem which we want to start from. The HF eigenfunction of the system, obtained in the form of the single determinant, in turn, has the nice property to be invariant (up to a phase factor) under any unitary transformation of the set of single-particle orbitals which compose it. Hence, a set of spatially localized orthonormal orbitals can be obtained as linear combination of canonical (delocalized) ones

$$\varphi_i = \sum_j \psi_j u_{ji} \tag{2.26}$$

and several localization schemes (finding the unitary matrix u_{ji} which provides the less extended orbitals) have been proposed in quantum chemistry for finite molecules, e.g. [FB60], [ER65], [PM89]. Then, the wavefunction of the whole system can be written as a single determinant over φ_i instead of ψ_i. The total energy of the system obtained as the expectation value of the Hamiltonian with the transformed wavefunction remains unchanged.

In periodic systems the Wannier functions [W34] are known to yield localized electron orbitals if a suitable unitary transformation of the Bloch waves is used:

$$\varphi_{Rn} = \int_{-\pi/a_l}^{\pi/a_l} \mathrm{e}^{-ikR} \sum_{\nu=\nu_1,\ldots,\nu_m} U_{\nu n}^{(k)} \psi_{k\nu} \,\mathrm{d}k \tag{2.27}$$

and details of this step can be found in [E88]. The m Wannier functions φ_{0m} which represent m energy bands $\nu_1, \ldots \nu_m$ are referred to some unit cell (for instance by their centers) and repeated over the whole crystal by primitive translation vectors R. Pairs of spin-up and spin-down electrons from the m bands are said to occupy these repeated Wannier orbitals (WOs). Now the $(N-1)$- and $(N+1)$-particle-state wavefunctions are obtained from the canonical ones $|k\nu\sigma\rangle$ introduced in Section 2.1

by a transformation totally analogous to the Wannier transformation of the Bloch orbitals. The wavefunction of the state with a localized hole is then given by

$$|Rn\sigma\rangle = c_{Rn\sigma}|\Phi\rangle \tag{2.28}$$

where an electron with spin σ is removed from the n-th Wannier orbital centered at the unit cell with lattice vector R (we refer to a one-dimensional crystal here) and the ground-state wavefunction Φ is constructed from Wannier orbitals. Note that due to translational invariance the vector R is not uniquely defined. However by fixing once the reference (or zero) unit cell we eliminate this ambiguity. Analogously, the $(N+1)$-electron states are defined as

$$|Rm\sigma\rangle = c^{\dagger}_{Rm\sigma}|\Phi\rangle \tag{2.29}$$

where m is used to indicate the use of WOs from the conduction bands.

Now we show how energy bands can be obtained from quantities defined in terms of $|Rn\sigma\rangle$ and $|Rm\sigma\rangle$. Analogously to our discourse in Section 2.1 we define "local" matrices of ionization potentials

$$\mathrm{IP}_{R'-R,nn'} = \langle Rn\sigma|H|R'n'\sigma\rangle - \delta_{RR'}\delta nn'E_0 \tag{2.30}$$

and electron affinities

$$\mathrm{EA}_{R'-R,mm'} = -\langle Rm\sigma|H|R'm'\sigma\rangle + \delta_{RR'}\delta mm'E_0. \tag{2.31}$$

Following the results (2.18) and (2.19) their diagonal elements can be regarded as the energy of an electron occupying some Wannier orbital n (or m) in any cell and the off-diagonal elements are considered as hopping matrix elements between orbitals n in the cell R and n' in the cell R'. However, one should always keep in mind, that in reality an electron can not be removed from (or added to) some Wannier orbital. Nevertheless, these matrix elements can be used to obtain the band structure.

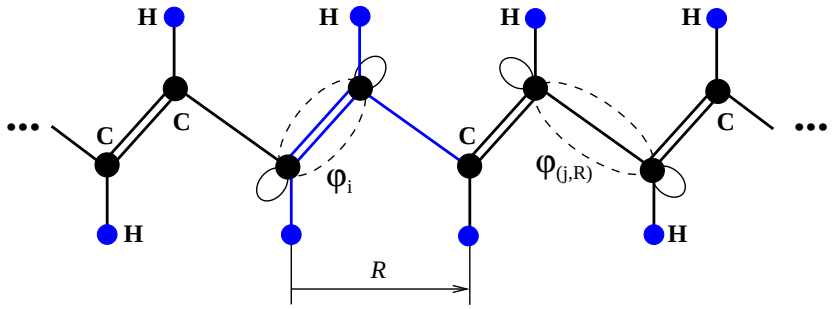

Figure 2.1: Schematic picture of two Wannier orbitals in *trans*-polyacetylene.

Since the quantities (2.30) and (2.31) depend only on the difference $R' - R$ we fix R at the zero cell ($R \equiv 0$). In Fig. 2.1 two occupied Wannier orbitals in *trans*-polyacetylene are shown schematically. The WO φ_i is centered at the zero unit cell (marked by blue bonds). The energy of an electron in this orbital is $-\mathrm{IP}_{0,ii}$. The hopping matrix element between WO φ_i and WO φ_j from the cell at distance R from the reference cell is $-\mathrm{IP}_{R,ij}$. From now on we will refer to $\mathrm{IP}_{R,ij}$ and $\mathrm{EA}_{R,ij}$ as the "local matrix elements" (LMEs).

The energy bands (one-particle energies as a function of the crystal-momentum k) are obtained as eigenvalues of the "back-transformed" matrices

$$\mathrm{IP}_{nn'}(k) = \sum_R \mathrm{e}^{ikR} \mathrm{IP}_{R,nn'} \tag{2.32}$$

and

$$\mathrm{EA}_{mm'}(k) = \sum_R \mathrm{e}^{ikR} \mathrm{EA}_{R,mm'}. \tag{2.33}$$

The matrix elements $\mathrm{IP}_{R,nn'}$ and $\mathrm{EA}_{R,mm'}$ are the key quantities in our method for correlated band structures. Being calculated on the HF level they reproduce the HF band structure. In fact, only a relatively small amount of matrix elements is needed for doing this as the hopping matrix elements decay rapidly with increasing distance R and therefore the infinite summation in Eqs. (2.32) and (2.33) can be terminated at some R_{cut} such that the rest of the sum is negligible with respect to the terms summed up so far.

The effect of electron correlation leads to a change of the matrix elements $\mathrm{IP}_{R,nn'}$ and $\mathrm{EA}_{R,mm'}$ as will be shown in the following chapters. This means that the energy of a correlated hole or attached electron in some localized orbital and also the hopping matrix elements between different sites are not the same as in the HF approximation but contain all the information about the response of the charged $(N-1)$- or $(N+1)$-particle system and the correlation in the ground state. Thus, substituting "correlated" matrix elements $\mathrm{IP}^{\mathrm{corr}}_{R,nn'}$ and $\mathrm{EA}^{\mathrm{corr}}_{R,mm'}$ in Eqs. (2.32) and (2.33) gives the band structure with electron correlations included.

The correlation effect is determined by a variational method in which all unoccupied orbitals are used to construct the variational space. In a crystal there is an infinite amount of virtual orbitals which would lead to an infinitely large variational space and make the calculation not feasible. To arrive at a finite variational space all the unoccupied Bloch waves can be transformed to Wannier orbitals and ordered by their distance from the localized charge and then only WOs up to a certain distance R_{cut} are taken into account. However, firstly, the localization (Wannier transformation) of *all* virtual Bloch orbitals becomes very expensive for rich basis sets and, secondly, WOs corresponding to energetically high Bloch states are spatially rather extended and therefore the cut-off radius R_{cut} has to be chosen large enough that may again lead to infeasible correlation calculations. As an alternative to the set of unoccupied WOs, one can use atomic orbitals with one projected out of the occupied space. This idea is being efficiently implemented in quantum-chemical codes (see e.g. [SHW99] and [WMK03]). These orbitals are perfectly localized and the cut-off radius is reduced to the minimum value but they are (i) not mutually orthogonal and (ii) can not be used to reproduce the HF bands by a suitable unitary transformation.

In our approach we avoid the problem of an infinite variational space by performing the correlation calculations in finite molecules representing a small piece of the periodic system. This implies a finite number of virtual HF orbitals in these molecules.

2.3 One-particle configurations

Here we have come to the crucial point of our method. The matrix elements $\mathrm{IP}_{R,ij}$ and $\mathrm{EA}_{R,ij}$ defined in (2.30) and (2.31) can be obtained (approximately) from calculations in finite molecules. Moreover, electron correlation can be easily incorporated by performing standard quantum-chemical finite-cluster correlation calculations. In the present Section we focus our attention on the first statement.

For understanding this statement the molecular-orbital theory may provide a hint. A bond orbital φ_a between two atoms A and B in a molecule (a localized one-particle wavefunction) is obtained as a linear combination of atomic basis functions with the main contribution centered on these two atoms:

$$\varphi_a = \sum_i \alpha_{A,i}\chi_{A,i} + \sum_i \alpha_{B,i}\chi_{B,i} + \sum_{i,C\neq A,B} \alpha_{C,i}\chi_{C,i} \tag{2.34}$$

with $|\alpha_{A,i}|, |\alpha_{B,i}| \gg \max_{C\neq A,B} |\alpha_{C,i}|$ where $\chi_{A,i}$ is the i-th atomic basis function of atom A and $|\alpha_{C,i}|$ decays rapidly with the distance between the C-th atom and the bond. The same bond one expects to find in a covalent extended system when the same two atoms at the same distance and with similar atomic structure in the neighborhood are considered. Therefore one expects to obtain occupied Wannier orbitals in a crystal which are very similar to the localized occupied spin orbitals in a molecule when this molecule represents some finite part of the crystal provided the same atomic basis sets and the same localization criteria are used for both the molecule and the crystal. The larger the molecule the closer the localized molecular orbital (LMO) in the central part of the molecule are to the relevant WO of the crystal. The LMOs at the edges of the molecule are less similar to the corresponding WOs as the surrounding of the former differs strongly from the surrounding in the crystal.

The matrix elements $\mathrm{IP}_{R,nn'}$ (2.30) are defined in terms of localized crystalline orbitals which are derived from HF solutions for the closed-shell system in the ground state. The diagonal elements $-\mathrm{IP}_{0,nn}$ are the energies $\varepsilon_{0,nn}$ of an electron in the n-th orbital of the reference unit cell which constitutes a generalization of Koopmans'

theorem to the case of localized orbitals. The quantity $\varepsilon_{0,nn}$ depends on the shape of the orbital itself and on the atomic and electronic structure of the close surrounding. If they are similar in the molecule and in the crystal the corresponding orbital energies should coincide.The same statement is valid for the hopping matrix elements in (2.30) when the two localized orbitals and the structure between them do not differ. Thus all the matrix elements which are needed in the restricted summation (2.32) can be obtained from calculations in large enough but finite molecules.

Similar argumentation holds for the unoccupied WOs corresponding to the energetically lowest conduction bands with the distinction that localized unoccupied orbitals in molecules can not be obtained by standard quantum-chemical localization methods, in general. However, in this case the WOs from the periodic system can directly be projected onto a molecule when the structure and the basis sets are identical and can be used as unoccupied LMOs. This technics is described in details in chapter 3.2.2. Here we only emphasize that local matrix elements $\mathrm{EA}_{R,mm'}$ (2.31) can be obtained from calculations in finite molecules as well.

To get the matrix elements (2.30) and (2.31) from molecular calculations an appropriate molecules have to be chosen. The structure of such molecules must contain the appropriate clusters of a crystal under consideration, e.g. those unit cells which are needed to represent the corresponding WOs without noticeable loss of accuracy. Such clusters cut from covalent crystals have dangling bonds which can be saturated by hydrogen atoms. To be more specific let us consider the occupied WOs schematically shown in the Fig. 2.1. There, four unit cells of *trans*-polyacetylene are drawn. The two WOs define the three matrix elements $\mathrm{IP}_{0,ii}$, $\mathrm{IP}_{R,ij}$ and $\mathrm{IP}_{R,jj} \equiv \mathrm{IP}_{0,jj}$. To obtain these matrix elements from a molecule calculation the shown cluster C_8H_8 (with four unit cells) is appropriate and therefore for calculations one can use a C_8H_{10} molecule with the same geometry as the C_8H_8 cluster but with the two cut C–C bonds being substituted by C–H bonds with the same orientation as the C–C bond and a typical C–H bond length. In our investigation of *trans*-polyacetylene we use C_6H_8, C_8H_{10}, $C_{10}H_{12}$ and $C_{12}H_{14}$ molecules which represent

different-size clusters of the infinite chain all being constructed to contain full unit cells such that they can be terminated by single C–H bonds. The size of the chosen cluster is defined by the distance between the relevant WOs and should be as small as possible for cheaper calculations but still big enough to preserve the shape of the WOs and by this the accuracy of the results. These criteria hold for the selection of proper molecules for all kinds of covalent materials, e.g. diamond, silicon, gallium arsenide, polyethylene etc.

Thus, having chosen appropriate molecules we can formally redefine the matrix elements (2.30) and (2.31) in terms of localized molecular orbitals

$$\mathrm{IP}_{IJ}^{\mathrm{mol}} = \langle I|H^{\mathrm{mol}}|J\rangle - \delta_{IJ}E_0^{\mathrm{mol}} \tag{2.35}$$

with

$$|I\rangle = c_I|\Phi^{\mathrm{mol}}\rangle \tag{2.36}$$

and

$$\mathrm{EA}_{I^*J^*}^{\mathrm{mol}} = -\langle I^*|H^{\mathrm{mol}}|J^*\rangle + \delta_{I^*J^*}E_0^{\mathrm{mol}} \tag{2.37}$$

with

$$|I^*\rangle = c_{I^*}^\dagger|\Phi^{\mathrm{mol}}\rangle \tag{2.38}$$

where c_I destroys an electron in an occupied localized molecular orbital named I (a bonding orbital) and $c_{I^*}^\dagger$ creates an electron in an unoccupied localized molecular orbital I^* (an anti-bonding orbital).

Starting from this point we shall refer to local matrix elements as obtained from calculations in molecules. Also we adopt the notations for many-body wavefunctions used in quantum chemistry. In the HF approximation the electronic wavefunction of a molecule in the ground state is written as a Slater determinant (2.2). Since the Slater determinant is essentially (up to a phase factor) invariant under any unitary

transformation of the orbitals we rewrite it in terms of the localized spin orbitals (2.26)

$$\Phi = \frac{1}{\sqrt{N!}} \det[\varphi_1, \ldots, \varphi_N] \tag{2.39}$$

where N is the number of electrons in the molecule. In the HF ground state configuration all occupied spin orbitals φ_a contain an electron and all virtual spin orbitals φ_r are empty. By taking out an electron from an orbital φ_a we produce an $(N-1)$-particle state with the wavefunction

$$\Phi_a = \frac{(-1)^{N-a}}{\sqrt{(N-1)!}} \det[\varphi_1, \ldots, \varphi_{a-1}, \varphi_{a+1}, \ldots, \varphi_N]. \tag{2.40}$$

When an electron is added to the system and placed into the virtual spin orbital φ_r an $(N+1)$-particle state is produced and its wavefunction is

$$\Phi_r = \frac{1}{\sqrt{(N+1)!}} \det[\varphi_1, \ldots, \varphi_N, \varphi_r]. \tag{2.41}$$

We shall call the wavefunctions (2.40) and (2.41) "one-particle configurations" as they correspond to states with one particle (a hole or an electron) being added to the system in the ground state.

Now we would like to show explicitly how local matrix elements are obtained from molecular quantum-chemical calculations on the HF level. As follows from Eqs. (2.35)–(2.41) the LMEs are given in terms of the one-particle configurations as

$$\mathrm{IP}_{ab} = \langle \Phi_a | H^{\mathrm{mol}} | \Phi_b \rangle - \delta_{ab} E_0^{\mathrm{mol}}, \tag{2.42}$$

$$\mathrm{EA}_{rs} = -\langle \Phi_r | H^{\mathrm{mol}} | \Phi_s \rangle + \delta_{rs} E_0^{\mathrm{mol}} \tag{2.43}$$

where

$$E_0^{\mathrm{mol}} = \langle \Phi | H^{\mathrm{mol}} | \Phi \rangle. \tag{2.44}$$

In the following we omit the superscript "mol" since our calculations are always performed in molecules except of the localization of the unoccupied orbitals and there we explicitly distinguish infinite and finite systems. From the HF calculations with the program package MOLPRO [M2000] the total ground-state energy E_0, the canonical HF spin orbitals ψ_i and the Fock matrix (2.4) are obtained. In the representation of the canonical orbitals the Fock matrix has diagonal form

$$f_{ij} = \langle \psi_i | F | \psi_j \rangle = \delta_{ij} \varepsilon_i \tag{2.45}$$

where ε_i are the canonical orbital energy (2.7). By a localization procedure applied to the canonical orbitals one obtains the LMOs (2.26) and the corresponding unitary matrix u_{ji}. Then using Eqs. (2.26), (2.16), (2.10) and (2.18) one can express matrix elements IP_{ab} in terms of calculated quantities:

$$\begin{aligned}
\mathrm{IP}_{ab} &= \langle \Phi_a | H | \Phi_b \rangle - \delta_{ab} E_0 = \langle \sum_i^{\mathrm{occ}} u_{ia} \, {}^{N-1}\Phi_i | H | \sum_j^{\mathrm{occ}} u_{jb} \, {}^{N-1}\Phi_j \rangle - \delta_{ab} E_0 \\
&= \sum_i^{\mathrm{occ}} \sum_j^{\mathrm{occ}} u_{ia} u_{jb} \langle {}^{N-1}\Phi_i | H | {}^{N-1}\Phi_j \rangle - \delta_{ab} E_0 = \sum_i^{\mathrm{occ}} \sum_j^{\mathrm{occ}} u_{ia} u_{jb} \, {}^{N-1}E_i \delta_{ij} - \delta_{ab} E_0 \\
&= \sum_i^{\mathrm{occ}} u_{ia} u_{ib} (E_0 - \varepsilon_i) - \delta_{ab} E_0 = \sum_i^{\mathrm{occ}} u_{ia} \varepsilon_i u_{ib}.
\end{aligned} \tag{2.46}$$

(Here we omitted complex conjugation as molecular HF orbitals are usually real.) Thus, the local matrix elements IP_{ab} obtained on the HF level are in fact the elements of the Fock matrix (with the opposite sign) which is defined in terms of the localized occupied orbitals:

$$\mathrm{IP}_{ab} = -f_{ab} = -\langle \varphi_a | F | \varphi_b \rangle. \tag{2.47}$$

Similarly one gets

$$\mathrm{EA}_{rs} = -\sum_i^{\mathrm{vir}} u_{ir} u_{is} (E_0 + \varepsilon_i) + \delta_{rs} E_0 = -\sum_i^{\mathrm{vir}} u_{ir} \varepsilon_i u_{is}. \tag{2.48}$$

which simply is

$$\mathrm{EA}_{rs} = -f_{rs} = -\langle\varphi_r|F|\varphi_s\rangle. \tag{2.49}$$

In (2.46) index i runs over all occupied canonical orbitals and in (2.48) it counts only relevant virtual ones which means all virtual canonical orbitals which were used for the generating of the virtual LMOs φ_r.

The crystalline matrix elements (2.30) and (2.31) which enter the restricted summations (2.32) and (2.33) can be replaced by the matrix elements (2.46) and (2.48) obtained in molecules, and by this the HF band structure of the corresponding crystal can be calculated. Such a band structure, obtained by LMEs from molecules, can be compared to that obtained from canonical HF calculations for the infinite system, e.g. done by the program package CRYSTAL [CRY98] using identical basis sets and geometries of the crystal and the clusters. Also the LMEs themselves can be compared directly if elements of the Fock matrix in the representation of the WOs can be obtained from the calculations of the infinite system. Such comparisons show how accurate the cluster approach is. In fact, there should be small deviations between the band structure by LMEs on the HF level and that calculated by CRYSTAL because of the truncation in the summations (2.32) and (2.33). When the correlated band structure is obtained by LMEs including correlation corrections one can account for these small deviations as is explained in chapter 4.2.

2.4 Electron correlation effects

Above we have showed how the many-body wavefunction in the HF approximation can be obtained. This approximation serves as a good starting point for the study of electronic properties both in finite molecules and in extended systems providing single-electron orbitals with corresponding orbital energies, the ground state energy of the system, the energies of the $(N+1)$- and $(N-1)$-particle system in different excited states, ionization potentials and electron affinities. However, all these results

can only be considered as approximate since the effect of electron correlation is missing on the HF level.

Let us consider an extended periodic system (a crystal or a polymer chain) in the ground state for which the HF solution is known, in particular the ground-state energy E_0 and the localized electron orbitals (Wannier orbitals). E_0 accounts for the Coulomb repulsion between the electrons only in an averaged way (mean-field approximation). In reality electrons move in accordance to the movement of their neighbor electrons trying to avoid coming too close to each other and to reduce by this the Coulomb repulsion. Consequently, the total energy of the system, E_0, is reduced noticeably. Alternatively, we can describe this effect as charge fluctuations. In a neutral system a dipole may emerge due to local fluctuation of the charge. The system reacts to this by inducing another dipole and gains the energy of the dipole-dipole interaction.

If an additional electron is added to a localized virtual orbital (or removed from some occupied WO) the system reacts on the presence of the extra charge by producing a polarization cloud around it. The main effect of electron rearrangement happens in the close surrounding and decays with increasing distance. Of course, the effect, described above for the neutral system, also takes place in the charged one. Both these effects lead to a substantial reduction of the energy ${}^{N+1}E$ of the $(N+1)$-particle system and the energy ${}^{N-1}E$ of the $(N-1)$-particle system.

As we have seen, electron correlations in the ground state of a system are of van der Waals type and the contribution to the system energy falls rapidly with the distance between dipoles. Therefore, only rather small clusters are needed to properly estimate the correlation contribution to the ground-state energy. Significantly more efforts requires the proper description of electron correlations in the charged system. An accurate treatment of the polarization cloud around the localized extra charge is necessary as this is the main contribution to the correlation corrections to the LMEs. Since electron-dipole interaction decays more slowly than dipole-dipole interaction, larger clusters have to be chosen. Also, one can account separately for

the (relatively small) contribution coming from the polarization of the farther surrounding which is not present in the cluster models. For that purpose the crystal is considered as a polarizable continuum in the presence of a point charge and the approximate formula for the corresponding contribution to the correlation energy is presented in chapter 4.3. Thus, electron correlations have mainly local character and the corresponding corrections to the ground-state energy and the LMEs can be obtained from calculations on finite clusters.

Now we would like to show explicitly how electron correlation is included in quantum-chemical post-HF methods. Solving the Hartree–Fock equations (2.3)–(2.6) not only provides an approximate ground-state wavefunction in the form of a single determinant (2.2) but also one obtains a set of $2 \times N_{\text{bas}}$ spin orbitals (or N_{bas} spatial orbitals) where N_{bas} is the number of atomic basis functions $\{\chi_i\}$, $i = 1, \ldots, N_{\text{bas}}$ for a given molecule. Using these spin orbitals one can select a huge number of different orbital configurations which is of the order of $\binom{2N_{\text{bas}}}{N}$ where $\binom{a}{b}$ is the binomial coefficient. Each of these orbital configurations represents a single determinant referred to simply as "configuration". The HF wavefunction Φ is usually defined as that configuration which gives the lowest (self-consistent) energy E_0 for a given number of electrons in the molecule.

To incorporate correlations in the wavefunction one takes advantage of the fact that the entire set of configurations Φ_I form a basis of the Hilbert space. Hence one can write the "correlated" wave function of the system as the linear combination of single-determinant configurations:

$$\Phi^{\text{corr}} = \Phi + \sum_I \alpha_I \Phi_I \tag{2.50}$$

(here written in the intermediate normalization without a prefactor for Φ). By varying the coefficients α_I one can minimize the energy corresponding to the correlated

wavefunction (2.50)

$$E_0^{\mathrm{corr}} = \frac{\langle \Phi^{\mathrm{corr}} | H | \Phi^{\mathrm{corr}} \rangle}{\langle \Phi^{\mathrm{corr}} | \Phi^{\mathrm{corr}} \rangle}. \tag{2.51}$$

Of course, in practice, one has to truncate the set of configurations somehow. This is the essence of the so-called "configuration interaction" (CI) methods. The obtained energy E_0^{corr} is lower than E_0 from the HF calculations. The same argumentation holds for the wavefunction and the energy of $(N-1)$- and $(N+1)$-particle systems when the $(N-1)$- and $(N+1)$-electron configurations are used, respectively, to construct the multi-determinant wavefunctions.

In fact only for small molecules with a few atoms and small basis sets a variation of all configurations is possible (full CI). For larger systems a drastic reduction of the variational space (the number of involved configurations) must be done. The excited configurations denoted as Φ_I in (2.50) can be sorted by the number of substitutions of occupied spin orbitals in the ground-state configuration by unoccupied ones and the correlated wavefunction (2.50) can be rewritten as

$$\Phi^{\mathrm{corr}} = \Phi + \sum_{ar} \alpha_a^r \Phi_a^r + \sum_{a<b,\, r<s} \alpha_{ab}^{rs} \Phi_{ab}^{rs} + \sum_{a<b<c,\, r<s<t} \alpha_{abc}^{rst} \Phi_{abc}^{rst} + \ldots \tag{2.52}$$

where Φ_a^r, Φ_{ab}^{rs} and Φ_{abc}^{rst} are the excited configurations, subscripts denote the spin orbitals excluded from Φ and superscripts denote the substituting virtual spin orbitals.

The contributions to the correlated wavefunction, associated with configurations with three and more substitutions (so-called excitations), are negligibly small all together compared to those of first three terms on the right-hand side of Eq. (2.52). Therefore, we take into account only the ground-state configuration (the dominant contribution to the correlated wavefunction) and the singly and doubly excited configurations (single-double CI). Note that the singly excited configurations do not contribute directly to the correlation energy of the ground state as they do not couple to the HF ground-state configuration: $\langle \Phi_a^r | H | \Phi \rangle = 0$. This is the statement of

Brillouin's theorem (see, e.g., chapter 3.3.2 in [SO96]) which holds as long as the HF spin orbitals are determined self-consistently. Thus, the second sum in Eq. (2.52) including the double excitations gives the main contribution to correlation energy and includes dipole-dipole interactions.

The correlated wavefunctions for the charged systems can be constructed similarly. For instance, the wavefunction of a system with a *static* hole in a *frozen* orbital φ_a would be written as

$$\Phi_a^{\rm corr} = \Phi_a + \sum_{b\neq a,r} \tilde{\alpha}_{ab}^{\ r} \Phi_{ab}^{\ r} + \sum_{b<c\neq a,\, r<s} \tilde{\alpha}_{abc}^{\ rs} \Phi_{abc}^{\ rs} \tag{2.53}$$

Here both sums give contribution to the energy of the $(N-1)$-electron system. Matrix elements $\langle \Phi_{ab}^{\ r} | H | \Phi_a \rangle$ do not vanish and describe the polarization cloud around an extra charge.

Of course, in reality a hole is delocalized over the entire system and a more general ansatz for the correlated wavefunction of the $(N-1)$-particle system has to be made:

$${}^{N-1}\Phi^{\rm corr} = \sum_a \alpha_a \Phi_a + \sum_{a,b\neq a,r} \alpha_{ab}^{\ r} \Phi_{ab}^{\ r} + \sum_{a,b<c\neq a,\, r<s} \alpha_{abc}^{\ rs} \Phi_{abc}^{\ rs} \tag{2.54}$$

The number of configurations (the number of single determinants) required for this is huge even though we restricted ourselves to singly and doubly excited configurations only. However, we do not need to store the explicitly correlated wavefunction consisting of billions of single determinants since we are rather interested in physical quantities which are obtained with this wavefunction, namely, LMEs like the ones introduced on the HF level (2.42) and (2.43). Below we show how this is done.

First, we turn back to the representation of the HF one-particle configurations in terms of canonical orbitals in which the Fock matrix is diagonal. We denote these configurations as Ψ_i here with an electron being removed from (or added to) the canonical spin orbital ψ_i. The configurations Ψ_i can also be obtained as the linear combinations of the "local" configurations Φ_i: $\Psi_i = \sum_j \Phi_j \, (u^{-1})_{ji}$, because

the canonical spin orbitals can be obtained from the localized ones with the help of the unitary matrix u_{ji} from the localization procedure (2.26): $\psi_i = \sum_j \varphi_j \, (u^{-1})_{ji}$. The correlated counterpart of the HF wavefunction Ψ_i is that *eigenstate* $\Psi_i^{\rm corr}$ of the charged system which resembles the HF configuration Ψ_i the most. It will essentially be composed by local one-particle configurations like the ones in the first sum on the right-hand side of Eq. (2.54) for ${}^{N-1}\Phi^{\rm corr}$. The wavefunctions $\Psi_i^{\rm corr}$ of the $(N-1)$-electron or $(N+1)$-electron system are associated with *total* energies $E_i^{\rm corr}$:

$$H\Psi_i^{\rm corr} = E_i^{\rm corr}\Psi_i^{\rm corr}. \tag{2.55}$$

Next, we formally introduce a one-to-one correspondence between the HF many-particle wavefunctions and their correlated counterparts by the use of a *wave operator* Ω which produces the correlated wavefunctions $\Psi_i^{\rm corr}$ from the HF ones Ψ_i

$$\Psi_i^{\rm corr} = \Omega\Psi_i, \qquad\qquad i = 1, \ldots, d. \tag{2.56}$$

Then, we divide the full space of local configurations Φ_j, $\Phi_{ja}^{\ r}$ and $\Phi_{jab}^{\ rs}$ used to construct the correlated wavefunctions $\Psi_i^{\rm corr}$ into a small subspace $\mathcal{P}$ of dimension d consisting of all SCF one-particle configurations Ψ_i (or equivalently of all local configurations Φ_j) with P being the projector onto this space and its orthogonal complement $\mathcal{Q}$ (with the projector Q), so $P + Q = 1$. The $\mathcal{P}$-space is often called the *model space* (or the space of *model configurations*) and the $\mathcal{Q}$-space is called the *external space*, and accordingly the configurations which belong to the $\mathcal{Q}$-space are called *external configurations*. Thus, the wave operator Ω acts on configurations Ψ_i from the $\mathcal{P}$-space and yields the exact wavefunctions $\Psi_i^{\rm corr}$ from the full Hilbert space.

The HF wavefunctions Ψ_i can be obtained from the correlated counterparts by the back transformation

$$\Psi_i = \Pi \, \Psi_i^{\rm corr}. \tag{2.57}$$

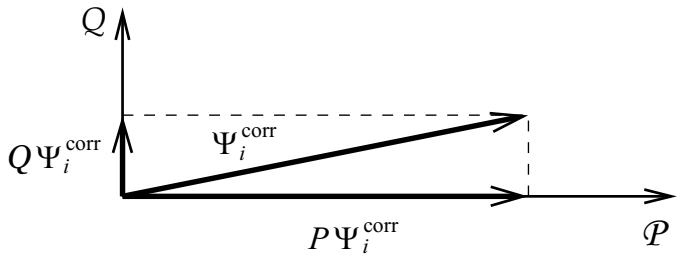

Figure 2.2: Schematic representation of the correlated wavefunction.

Π is an operator acting from the d-dimensional space spanned by the correlated counterparts $\{\Psi_i^{\rm corr}\}_{i=1,\ldots,d}$ to the model space $\mathcal{P}$. It is similar but not identical to the projector P which can be written as

$$P = \sum_{i=1}^{d} |\Psi_i\rangle\langle\Psi_i| \tag{2.58}$$

because the projections $P\Psi_i^{\rm corr}$ are neither perfectly normalized nor mutually orthogonal. In Fig. 2.2 we schematically show a correlated wavefunction $\Psi_i^{\rm corr}$. Both, its projection $P\Psi_i^{\rm corr}$ and the HF counterpart Ψ_i lie in the $\mathcal{P}$-space but differ slightly.

Let us substitute (2.56) into the left-hand side of Eq. (2.55) and act on the obtained equation by the operator Π from the left

$$\Pi H\Omega\Psi_i = \Pi H\Psi_i^{\rm corr} = E_i^{\rm corr}\Pi\Psi_i^{\rm corr} = E_i^{\rm corr}\Psi_i. \tag{2.59}$$

This way we get an eigenvalue equation for Ψ_i and $E_i^{\rm corr}$. Inspired by this relation we define an *effective* Hamiltonian as

$$H^{\rm eff} = \Pi H\Omega. \tag{2.60}$$

It operates fully in the $\mathcal{P}$-space and its eigenvalues are those of the *exact* Hamiltonian (2.55):

$$H^{\rm eff}\Psi_i = E_i^{\rm corr}\Psi_i. \tag{2.61}$$

As the unitary transformation (2.26), which gives the localized HF spin orbitals of a molecule in terms of the canonical ones, is known from the localization procedure we can readily get the matrix elements of H^{eff} in terms of the localized one-particle configurations Φ_i:

$$\begin{aligned} H_{ij}^{\text{eff}} &= \langle\Phi_i|H^{\text{eff}}|\Phi_j\rangle = \langle\sum_{i'} u_{i'i}\Psi_{i'}|H^{\text{eff}}|\sum_{j'} u_{j'j}\Psi_{j'}\rangle \\ &= \sum_{i'}\sum_{j'} u_{i'i}\, u_{j'j}\, E_{i'}^{\text{corr}}\, \delta_{i'j'} = \sum_{i'} u_{i'i}\, E_{i'}^{\text{corr}}\, u_{i'j} \end{aligned} \tag{2.62}$$

where the energies $E_{i'}^{\text{corr}}$ are those obtained in our correlation calculations. To be more precise, these energies as well as the elements of the matrix u_{ij} were calculated by the MOLPRO program package [M2000], [WK88], [KW88], [KW92]. The matrix elements H_{ij}^{eff} defined in Eq.(2.62) differ from the corresponding ones on the HF level H_{ij} and contain electron correlation as far as it is included in the energies $E_{i'}^{\text{corr}}$. Together with the correlated energy of the ground state E_0^{corr} (2.51) the matrix elements of the effective Hamiltonian define the correlated LMEs:

$$\text{IP}_{ab}^{\text{corr}} = H_{ab}^{\text{eff}} - \delta_{ab} E_0^{\text{corr}} \tag{2.63}$$

and

$$\text{EA}_{rs}^{\text{corr}} = -H_{rs}^{\text{eff}} + \delta_{rs} E_0^{\text{corr}} \tag{2.64}$$

which are to be used in (2.32) and (2.33) instead of the SCF ones to give the correlated band structure. Note the similarity of the equations (2.62)–(2.64) with the corresponding ones for the matrix elements IP_{ab} and EA_{rs} on the HF level (2.46) and (2.48).

It should be mentioned here that one can also use P instead of Π and a corresponding wave operator W (which is linked to Ω by $W = \Omega(P\Omega)^{-1}$) to define an

effective Hamiltonian

$$\tilde{H}^{\text{eff}} = PHW. \tag{2.65}$$

Despite the fact that $\tilde{H}^{\text{eff}}$ is non-Hermitian it has the same properties as H^{eff}.

At the end of this section we would like to say a few more words about the wave operator Ω and its inverse Π. They enter the *definition* of the effective Hamiltonian (2.60) however they are not used for obtaining its matrix elements H_{ij}^{eff}. The latter ones are calculated using equation (2.62). Hence, Ω and Π (or P and W) are only introduced formally in our method. Nevertheless, P and W can be constructed by the use of perturbation theory up to any desired accuracy as is comprehensively explained in chapter 9 of Ref. [LM86]. Then the correlated wavefunctions (2.54) can be obtained by applying W to the projection $P\Psi_i^{\text{corr}}$ which is obtained perturbatively as well.

2.5 Multireference configuration interaction method

Above we have used the CI ansatz to write the correlated wavefunction of a many-body system (2.52) and (2.54). However, there are also other correlation methods which use the HF wavefunction as a starting point and excited configurations to construct its correlated counterpart. Here we would like to mention two of them, namely the single and double excitation coupled-cluster (CCSD) method and the second-order Møller–Plesset perturbation (MP2) method. The CCSD method is more successful in ground-state correlation calculations than the single and double configuration interaction (CI(SD)) and both have the advantage that they are size-consistent in contrast to CI(SD). Unfortunately, CCSD and MP2 are not suitable for excited-state calculations.

The CCSD ansatz for the correlated ground-state wavefunction is

$$\Phi_{CC}^{\mathrm{corr}} = \exp\left(\sum_{ar} t_a^r c_a c_r^\dagger + \sum_{a<b,\, r<s} t_{ab}^{rs} c_a c_b c_r^\dagger c_s^\dagger\right)\Phi \tag{2.66}$$

where the operators c_a and c_b ($c_r^\dagger$ and $c_s^\dagger$) destroy (create) an electron in an occupied (unoccupied) spin orbitals φ_a and φ_b (φ_r and φ_s) of the ground-state configuration, respectively. The coefficients t_a^r and t_{ab}^{rs} in Eq. (2.66) are obtained from a set of algebraic equations. The exponential form of $\Phi_{CC}^{\mathrm{corr}}$ implies that the correlated wavefunction of a system consisting of some well separated subsystems is the product of the wavefunctions of these subsystems which is the crucial prerequisite for size-consistency. There is no simple extension of the CC method to multireference (MR) calculations which are needed to describe excited states. Though such an extension of CC became a hot topic in the literature in the last decade, e.g. [PB99], [AMI00], [P03], the MRCC method seems still to be far from the stage of implementation in standard quantum-chemical program packages at the present moment.

The second-order Møller–Plesset perturbation method can be generalized to the multireference case. However, in the perturbation expansion for the correlated wavefunctions and energies of the $(N-1)$- and $(N+1)$-electron systems there are terms which are proportional to

$$\frac{1}{E_i - E_{ja}^{\ r}} \tag{2.67}$$

Here E_i is the SCF energy of some hole (or attached electron) state and $E_{ja}^{\ r}$ is the energy of an SCF configuration with one hole (or attached electron) state plus one electron-hole excitation. It may happen, now, that E_i gets very close to $E_{ja}^{\ r}$ in the case where E_i corresponds to an energetically deep lying hole and $E_{ja}^{\ r}$ corresponds to an energetically high lying hole and a close electron-hole excitation. This situation takes place in systems with relatively small band gap and a strong dispersion of the bands. Such small denominators blow up the correlated energies and lead to wrong results. Therefore, the MP2 method can only be applied to systems with big band

gaps and rather flat bands [ARM98]. Also deep valence bands and high conduction bands can not be treated properly. This problem was discussed in, e.g. [SB96] and [AKS01] where the MP2 method was generalized for crystal-momentum space and could be applied only to the π bands of *trans*-polyacetylene single chains.

As a variant, a hybrid method was used to determine the correlated valence bands of diamond, silicon and germanium in Ref. [GSF93], [GSF97] and [AFS00] where single-excited configurations were incorporated by MRCI(S) and for the double excitations a separate calculation was performed employing quasi-degenerate variational perturbation theory [CD88]. In that case small denominators do not show up. However, the size-consistency problem of MRCI(S) is still present (though reduced as compared to MRCI(SD)) and the contribution of coupling terms between singly- and doubly-excited configurations to the correlation energy is missing totally. Also such a hybrid method is technically more complicated than pure MRCI(SD).

Hence, for our correlation calculations we have chosen the multireference version of the single and double configurations interaction method (MRCI(SD)) to calculate the correlated ground-state energy (2.51) and the matrix elements of the effective Hamiltonian (2.62) on both HF and correlation level. The size-consistency problem has been accounted for by the development of a special size-consistency correction (for details see Section 3.5).

Let us first consider the CI(SD) ansatz for correlated ground-state wavefunction Φ^{corr}. The HF ground-state wavefunction Φ is written as the Slater determinant composed from localized occupied spin orbitals. In general all singly- and doubly-excited configurations are provided to the CI(SD) expansion. However, one can further restrict the number of excited configurations by forbidding to take out an electron from some particular spin orbitals. For instance, we can "freeze" the artificial C–H bonds which are used to saturate the dangling bonds of the clusters. By this technique we exclude artificial contributions to the correlation energy associated with these C–H bonds. Also, we can freeze the majority of the bond orbitals of a molecule and allow excitations from a few particular bonds only. By this, we

can replace an expensive correlation calculation for a big molecule by a sequence of cheaper ones and sum up, in a proper way, the correlation contribution to the ground-state energy coming from the several parts of the molecule. This is the idea of the method of local increments introduced in [St92a] and [St92b] which we have adopted and which will be discussed in more details in Section 3.4.

Thus, the correlated ground-state wavefunction of a molecule with N electrons and n bonds (or $2n$ spin orbitals) open for constructing excited configurations is written as

$$\Phi^{\mathrm{corr}} = \Phi + \sum_{a=1}^{2n} \sum_{r} \alpha_a^r \Phi_a^r + \sum_{a,b=1}^{2n} \sum_{r,s} \alpha_{ab}^{rs} \Phi_{ab}^{rs}. \tag{2.68}$$

The coefficients α_a^r and α_{ab}^{rs} are determined by minimization of the ground-state energy of the system given by Eq. (2.51) where they play a role of variational parameters. The resulting eigenvalue problem can be obtained by multiplying the Schrödinger equation

$$H|\Phi^{\mathrm{corr}}\rangle = E_0^{\mathrm{corr}}|\Phi^{\mathrm{corr}}\rangle \tag{2.69}$$

successively by $\langle\Phi|$, $\langle\Phi_c^t|$ and $\langle\Phi_{cd}^{tu}|$ from the left:

$$\langle\Phi|H|\Phi\rangle + \sum_{a,r}\langle\Phi|H|\Phi_a^r\rangle\alpha_a^r + \sum_{a,b,r,s}\langle\Phi|H|\Phi_{ab}^{rs}\rangle\alpha_{ab}^{rs} = E_0^{\mathrm{corr}} \tag{2.70}$$

$$\langle\Phi_c^t|H|\Phi\rangle + \sum_{a,r}\langle\Phi_c^t|H|\Phi_a^r\rangle\alpha_a^r + \sum_{a,b,r,s}\langle\Phi_c^t|H|\Phi_{ab}^{rs}\rangle\alpha_{ab}^{rs} = E_0^{\mathrm{corr}}\alpha_c^t \tag{2.71}$$

$$\langle\Phi_{cd}^{tu}|H|\Phi\rangle + \sum_{a,r}\langle\Phi_{cd}^{tu}|H|\Phi_a^r\rangle\alpha_a^r + \sum_{a,b,r,s}\langle\Phi_{cd}^{tu}|H|\Phi_{ab}^{rs}\rangle\alpha_{ab}^{rs} = E_0^{\mathrm{corr}}\alpha_{cd}^{tu}. \tag{2.72}$$

This eigenvalue problem is too large to be solved directly and an iterative procedure (according to Davidson [D75]) is employed. The correlated ground-state energy can be obtained with any desired precision in this procedure. In our calculations the threshold for energy change form one iteration to the next is set to 10^{-7} eV. However, this does not mean that we get the full correlation energy with such an

accuracy. That would only be the case for a full CI calculation (with all possible excited configurations included). Rather it defines an upper bound for the exact correlation energy since truncated CI is a variational method.

Now we would like to show how the CI(SD) ansatz can be extended to get the matrix elements of the effective Hamiltonian (2.55). Suppose we want to get energies of n states with an electron removed from one of the n bonds of a molecule and also the hopping matrix elements between these bonds. As bonds are spatial orbitals containing two electrons with opposite spins per bond in the ground state, two spin-degenerate states are possible for a hole in some particular bond. To resolve the problem we consider only states of a particular spin symmetry, e.g. only one particle configurations obtained by annihilation of a *spin-up* electron. Then we have to provide n corresponding spin-adapted configurations Φ_i (i =1, 2, ..., n) into the model space. They define an $n \times n$ matrix $H_{ij} = \langle \Phi_i | H | \Phi_j \rangle$ on the HF level. The model wavefunctions Φ_j are first transformed to diagonalize this matrix:

$$\Psi_i = \sum_{j=1}^{n} (u^{-1})_{ji}\, \Phi_j = \sum_{j=1}^{n} u_{ij}\, \Phi_j, \qquad \langle \Psi_i | H | \Psi_j \rangle = E_i\, \delta_{ij}. \tag{2.73}$$

The configurations Ψ_i are called *reference configurations* or *reference states* and E_i are the energies of these states. In our calculations we get the SCF energies E_i and coefficients u_{ij} from a preliminary step of the MRCI calculations. Then the SCF matrix elements are obtained as

$$H_{ij} = \sum_{k=1}^{n} u_{ki} u_{kj} E_k \tag{2.74}$$

in close analogy to Eq. (2.62) for H_{ij}^{eff}.

To produce excited configurations for the CI expansion of the correlated wavefunctions Ψ_i^{corr}, pair excitation operators $c_a c_r^\dagger$ and $c_a c_b c_r^\dagger c_s^\dagger$ are applied to each of the reference states Ψ_i, yielding the following ansatz for the n correlated wavefunctions:

$$\Psi_i^{\text{corr}} = \sum_{j=1}^{n} \left(t_j(i) + {\sum_{a,r}}' t_{ja}^{\;\;r}(i) c_a c_r^\dagger + {\sum_{a,b,r,s}}' t_{jab}^{\;\;rs}(i) c_a c_b c_r^\dagger c_s^\dagger \right) \Psi_j \tag{2.75}$$

which (in case of an $(N-1)$-particle system) is equivalent to

$$\Psi_i^{\rm corr} = \sum_{j=1}^{n}\left(\alpha_j(i)\Phi_j + \sum_{a,r}{}'\alpha_{ja}^{\ r}(i)\Phi_{ja}^{\ r} + \sum_{a,b,r,s}{}'\alpha_{jab}^{\ rs}(i)\Phi_{jab}^{\ rs}\right) \tag{2.76}$$

since the n reference states Ψ_j and the n spin-adapted configurations Φ_j span the same (reference) space. In Eq. (2.76) prime over sums means that electrons are annihilated from the n active bonds and only the remaining spin-down electron can be removed from the localized orbital j. These n eigenfunctions (2.76) correspond to n eigenvalues of the full Hamiltonian:

$$H|\Psi_i^{\rm corr}\rangle = E_i^{\rm corr}|\Psi_i^{\rm corr}\rangle. \tag{2.77}$$

The amplitudes $t_j(i)$, $t_{ja}^{\ r}(i)$ and $t_{jab}^{\ rs}(i)$ or equivalently the coefficients $\alpha_j(i)$, $\alpha_{ja}^{\ r}(i)$ and $\alpha_{jab}^{\ rs}(i)$ are determined iteratively from a set of equations obtained by multiplying both sides of the n equations (2.77) successively by $\langle\Phi_j|$, $\langle\Phi_{jc}^{\ t}|$ and $\langle\Phi_{jcd}^{\ tu}|$ from the left. For details we refer to [WK88].

Once the iterations are converged the n correlated energies of $(N-1)$-electron system $E_i^{\rm corr}$ can be evaluated. Being used in (2.74) instead of the HF energies E_k they determine the matrix elements of the effective Hamiltonian $H_{ij}^{\rm eff}$ as have been discussed in the previous section (see Eq. (2.62)).

In the case of attached-electron states the wavefunctions Ψ_j in Eqs. (2.75) correspond to the m $(N+1)$-particle states given by linear combinations (2.73) of the local $(N+1)$-particle configurations Φ^l with an extra (spin-down) electron being added to one of the m localized virtual orbitals. The MRCI-ansatz for the m correlated wavefunctions is written in a form similar to Eq. (2.76):

$$\Psi_k^{\rm corr} = \sum_{l=1}^{m}\left(\alpha^l(k)\Phi^l + \sum_{a,r}{}'\alpha^{lr}{}_a(k)\Phi^{lr}{}_a + \sum_{a,b,r,s}{}'\alpha^{lrs}{}_{ab}(k)\Phi^{lrs}{}_{ab}\right) \tag{2.78}$$

and here primes mean that only spin-up electron can be put into a localized virtual orbital φ_l if it is already occupied by the attached spin-down electron. The obtained m correlated energies of the $(N+1)$-electron system $E_k^{\rm corr}$ can be used in Eq. (2.74)

instead of the corresponding m HF energies to calculate the matrix elements of the effective Hamiltonian H_{ij}^{eff} for the case of attached-electron states.

Thus, equations (2.73)–(2.78) define how the MRCI(SD) method is used to evaluate the matrix elements of the effective Hamiltonian in the case of both $(N-1)$- and $(N+1)$-particle states.

Chapter 3

Realization of the method

While we have outlined the general idea of our approach to the correlated band structures in the previous chapter we describe in detail the *actual* realization of this method here. The concepts we have developed to make such calculations possible are presented in the given chapter. We will refer to *trans*-polyacetylene (tPA) single chains as a test system. In section 3.1 the geometry and electronic properties of tPA on the HF level are described. In section 3.2 we show how to generate suitable localized occupied and virtual HF orbitals in the clusters. The corresponding HF local matrix elements are used to calculate the SCF band structure of tPA. In section 3.3 we discuss how to evaluate the correlation corrections to the LMEs by the MRCI(SD) method and the use of an approximate but well controlled scheme for this is presented in section 3.4. The possibility to reduce the size-extensivity error of the MRCI(SD) method is explored in section 3.5 and the analytic formula for the corresponding correction to the MRCI(SD) correlation energy is derived for open-shell systems. The occurrence of satellite states in cluster models and the handling of this problem by an appropriate construction of the model space in the MRCI calculation are discussed in section 3.6.

3.1 The investigated system

In Chapter 2 we have described the general idea of our wavefunction-based method for obtaining band structures of insulators and semiconductors with electron correlation effects being properly included. This approach was used in Ref. [GSF97] and [AFS00] to get the correlated valence bands of three structurally similar semiconductors (diamond, silicon and germanium). In the present work we make the first attempt to treat systematically not only the valence but also the conduction bands of a periodic system. For this purpose we introduce *localized* virtual HF orbitals which are, in contrast to localized occupied orbitals, usually extended over several unit cells of the crystal. Therefore, rather big clusters have to be used for a proper treatment of the $(N+1)$-electron states. Moreover, even larger clusters are needed to investigate the decay of the correlation effects with the distance from the localized extra charge. On the other hand, since rich basis sets are required to describe the anionic $(N+1)$-electron states properly and a powerful but rather expensive correlation method is employed, we reach the limits of our computational abilities when the size of the employed clusters reaches 30 atoms. In a bulk crystal a virtual WO extend in three dimensions and the number of atoms covered by the localized virtual orbital scales as r^3 with the size of the WO whereas in one-dimensional (1D) chains it only scales as r^1. Thus, for our test calculations, a linear system has been chosen.

3.1.1 Polyacetylene

A natural examples of 1D periodic systems are infinitely long linear polymers. One of the simplest among them is **polyacetylene** (PA). It is a plane periodic molecule which consists of repeating C_2H_2 units and exists in two basic conformations (Fig. 3.1). The first one exhibits a zigzag carbon chain with alternating single (or long) and double (or short) C–C bonds; the C–H bonds are pointing outwards this chain nearly perpendicular to the molecular axis. This is *trans*-polyacetylene

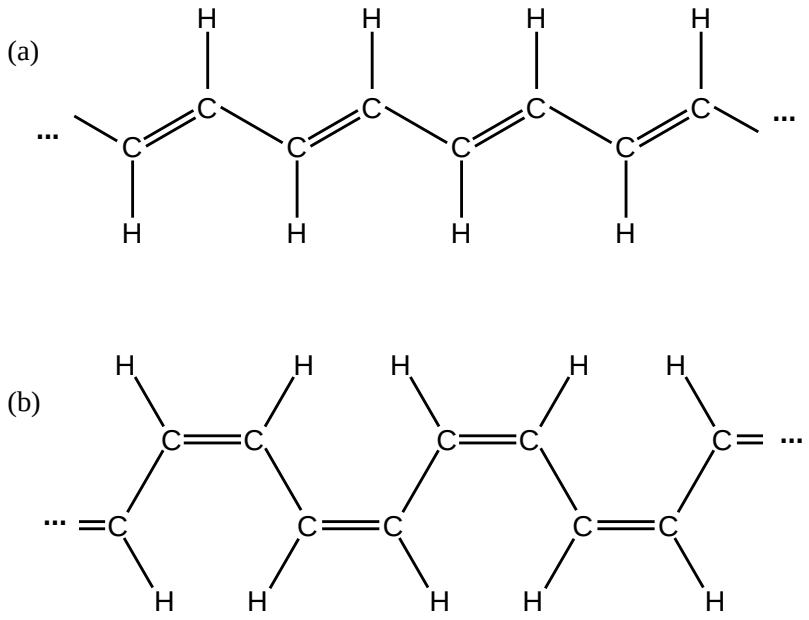

Figure 3.1: Two conformations of polyacetylene: (a) *trans*-PA and (b) *cis*-PA.

which is schematically shown on Fig. 3.1a. The second one is the *cis* conformation and one of its realization is drawn in Fig. 3.1b (another realization can be obtained by the interchange of single and double C–C bonds).

When a polyacetylene sample is synthesized it consists of finite molecules (oligomers) of both conformations (at room temperature). The *trans* conformation is thermodynamically more stable and the isomerisation of the sample is achieved by heating it to temperatures above 150 °C for a few minutes [SI79/80]. The *cis–trans* conversion of polyacetylene was rigorously studied in Ref. [RP+83] where the sample was annealed at 100 °C for more than 1 day. After 3 h it contained more than 50% of *trans* species and more than 80% after 1 day. The isomerization happened continuously during this time and homogeneously throughout the polymer rather than in isolated amorphous or crystalline regions. The crystallinity of these samples is estimated to about 90% and the amorphous content did not increase with isomerization.

There are two methods for the synthesis of crystalline polyacetylene. In the work of Sirakakawa and Ikeda [SI79/80] polyacetylene was grown in the form of randomly oriented fibrils. The corresponding electron micrograph is presented on Fig. 3.2a.

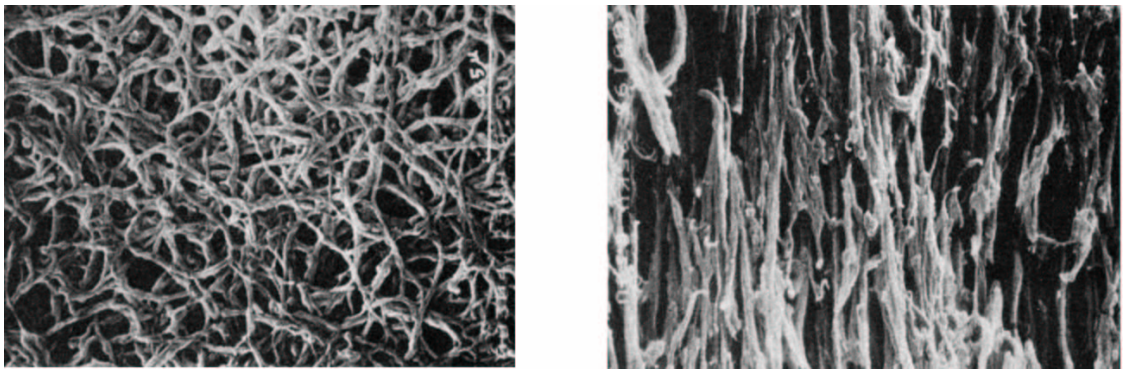

(a) (b)

Figure 3.2: Electron micrographs of *trans*-polyacetylene fibrils: (a) as-grown morphlogy and (b) fibrils are aligned by stretching (from [SI79/80]).

Inside a particular fibril the single chains of polyacetylene are directed along the axis of the fibril. In order to obtain a material with parallelly oriented chains of polyacetylene for further crystallographic and electronic structure studies the grown polymer is stretched along some direction. The corresponding micrograph is shown on Fig. 3.2b where all the fibrils are nearly aligned. The characteristic diameter of fibrils obtained by this method ranges from 200 Å to 500 Å. This technique was exploited in a number of experimental works on polyacetylene, e.g. [FO+79], [TG+80], [FC+82], [RP+83], [YC83] and [LS+93]. The disadvantages of samples produced this way are not perfectly aligned polyacetylene chains and even the presence of a certain amount of randomly oriented chains, and the fact that it is impossible to investigate the electronic properties of tPA in the direction perpendicular to the stretching due to the fibrillar morphology of the material.

The other method to produce crystalline tPA was developed at Durham University ([EF80] and [EFB84]) and provides true bulk polyacetylene. The synthesis utilizes a solution of a precursor polymer which is converted into polyacetylene. Under usual conditions, both conformations are present and the obtained polymer is amorphous. However, one can get samples with perfectly oriented chains of *trans*-polyacetylene by applying an appropriate stress at temperatures up to 120 °C.

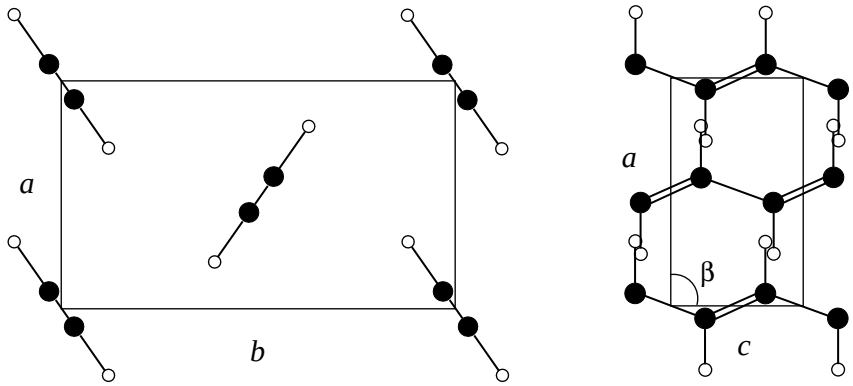

Figure 3.3: Two schematic projections of bulk *trans*-polyacetylene. $a = 4.24$ Å, $b = 7.32$ Å and $c = 2.46$ Å and $\beta = 91.5°$ (from [FC+82]).

Then, during the conversion, an elongation of the polymer film and simultaneous alignment of tPA chains take place. As the result highly anisotropic free-standing films of 100% *trans*-polyacetylene are obtained. This material exhibits a compact, non-fibrous morphology and smooth surfaces appropriate for further optical study ([FL86], [KLL87], [BF+87], [UTLK87] and [L88]).

Thus, when we refer to *trans*-polyacetylene as a bulk polymer we mean a crystal built by densely packed, flat and infinitely long tPA single chains all aligned in one direction. The crystalline structure of bulk tPA was studied in [FC+82] by x-ray scattering experiments and a fishbone-like packing of independent tPA chains was determined (Fig. 3.3). The space group of tPA crystals is $P2_1/n$ with a C_4H_4 unit cell consisting of two C_2H_2 units on neighboring tPA single chains. The parameters of the monoclinic structure are determined with a unique angle $\beta = 91.5°$ and lattice constants $a = 4.24$ Å, $b = 7.32$ Å and $c = 2.46$ Å. The angle between a chain plane and the b axis is 55°.

As one can see in Fig. 3.3, for any atom of the tPA crystal the first few closest atoms belong to the same tPA chain. Therefore, the crystal consists of weakly coupled chains with strong intrachain bonding. This is evident from the high anisotropy of the electronic properties of bulk tPA: SCF calculations give band widths between 5 and 10 eV for crystal-momentum vectors $\mathbf{k}$ parallel to the chains and less than

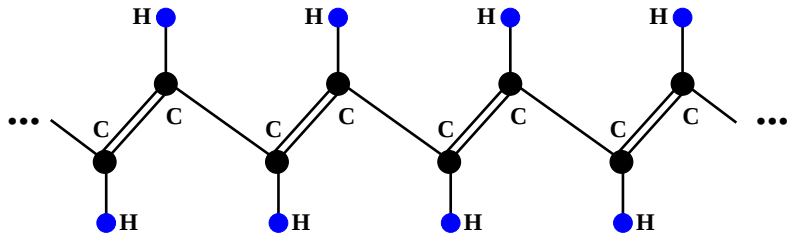

Figure 3.4: Investigated system: *trans*-polyacetylene single chains.

0.4 eV in perpendicular directions. These findings tell that the electrons in bulk tPA are delocalized exclusively along the polymer chain and thus each tPA single chain can indeed be considered as a quasi-one-dimensional crystal. Therefore, one can focus on the study of single 1D tPA chains to describe the electronic properties of *trans*-polyacetylene neglecting for a moment the weak interchain interactions.

3.1.2 Geometry of tPA single chain

A single tPA chain consists of repeating C_2H_2 units with alternating short and long C–C bonds (Fig. 3.4). The structure is produced by hybridization of the valence sp^2 electrons of carbon and the s^1 electron of hydrogen. Three out of four valence carbon electrons take part in this formation of σ bonds (with charge density maximum in the molecule plane), namely one long C–C bond, one (out of two) short C–C bond and one C–H bond. The fourth electron occupies the $2p_z$ atomic orbital, whose lobes lie out of the plane, and together with the $2p_z$ electron of the closest neighbor carbon atom form the second short C–C bond which is of π symmetry. The alternation in the C–C bond lengths emerges from the Peierls instability of 1D metals [P55]. If there would be no bond alternation (sometimes also called "dimerization") and all C–C bond were equal the unit cell would consist of just one CH unit with one unpaired electron on the $2p_z$ orbital per cell. In this case tPA would be a metal with a half-filled conduction band as can be seen from simple tight-binding-model considerations. However, such a 1D metal can reduce its energy by spontaneous breaking of the translational symmetry by moving two adjacent CH

groups towards each other and forming by this the short (or double) C–C bond. By this the system gains electronic energy whereas its elastic energy (i.e. the energy of the carbon skeleton) increases. The minimum of the system energy as a function of dimerization length defines the equilibrium C–C bond lengths in a $(C_2H_2)_x$ chain. The reduction of translation symmetry opens the band gap and tPA becomes a semiconductor with a completely filled upper valence band and with a band gap of the order of few electron-volts. The qualitative analysis of dimerization effect in *trans*-polyacetylene is comprehensively expounded in [F95], p. 179–183, where two original papers [SSH79] and [SSH80] are summarized.

To perform single-point *ab initio* calculations we need to know the positions of the atoms in the tPA chain. We take the relevant experimental data on the structure of the carbon skeleton of *trans*-polyacetylene from [KLL87]: the long C–C bond length is $r_1 = 1.45$ Å, the short C–C bond length is $r_2 = 1.36$ Å and the lattice constant is $a = 2.455$ Å. The angle γ between short and long bonds is measured to be 122°. The measured angle does not perfectly agree with measured lengths and we set this angle to 121.7421° (which is well within the experimental error bar).

The experimental data on the length and orientation of C–H bond of tPA are not available in the literature. Therefore, we have taken the C–H bond length from the paper [S92] where the geometry of tPA was optimized on both HF and MP2 level using different basis sets. The results for C–C bond lengths obtained on the MP2 level with the largest basis set (of double-zeta quality with polarization functions) agreed nicely with the experimental data mentioned above ($r_1 = 1.4450$ Å and $r_2 = 1.3634$ Å) however the angle between C–C bonds was somewhat different ($\gamma = 123.75°$). Therefore from [S92] we have taken only the value of the C–H bond length which is $r_3 = 1.0872$ Å.

The last undefined parameter of the geometry of tPA was the angle ϑ between short C–C bond and C–H bond. To determine this angle we used the geometry optimization option of the GAUSSIAN98 program package [G98]. We have optimized the angle ϑ in a hydrogen-terminated $C_{12}H_{14}$ cluster of *trans*-polyacetylene taking

$r_1 = 1.45$ Å, $r_2 = 1.36$ Å, $r_3 = 1.0872$ Å and $\gamma = 121.7421°$ as fixed parameters. The angle between the two cluster-saturating C–H bonds and adjacent short C–C bond was set to γ and kept fixed as well. Such an arrangement allows to reduce the influence of cluster edges on the optimized angle ϑ in the center of the cluster where its value is maximally close to that of the infinite chain. As follows from [S92], the value of the optimized angle ϑ does almost not depend on the method (HF or MP2) and the basis sets employed. Thus, we performed the optimization on the HF level with cc-pVDZ basis sets for both hydrogen and carbon atoms [D89]. We have tried several starting values ϑ_0 in the range from 118° to 122° and in all cases the optimized angle ϑ for the chosen fixed parameters was found to be 120.057°.

To summarize, our test system is a plane infinitely long single chain of *trans*-polyacetylene with alternating C–C bonds (Fig. 3.4). There are four σ bonds and one π bond (on the short C–C bond) per unit cell C_2H_2. The lengths of long C–C, short C–C and C–H bonds are 1.45 Å, 1.36 Å and 1.087 Å respectively. The angle between two neighbor C–C bonds is 121.742° and the angle between C–H bond and adjacent short C–C bond is 120.057°.

3.1.3 Basis sets

Throughout all our further HF and correlation calculations we use valence triple zeta (VTZ) atomic basis sets for carbon and hydrogen atoms [D89] (see Table 3.1). These Gaussian-type-orbital (GTO) basis sets are correlation consistent, have rather diffuse exponents to describe properly the decay of electron wavefunctions in the direction perpendicular to the chain, and are rich enough to provide reasonable results for correlation calculations in case of the anionic $(N+1)$-electron states.

The Gaussian-type orbitals (or more precisely Cartesian Gaussians) which were first proposed as an approximation to atomic orbitals in [B50] have the form

$$\chi_i(\mathbf{r}) = N_i x^l y^m z^n \mathrm{e}^{-\zeta_i r^2} \tag{3.1}$$

Table 3.1: Exponents and contraction coefficients of the cc-pVTZ basis sets for carbon and hydrogen atoms used in all our calculations.

atom	type	exponent	contraction coefficients			
			shell 1	shell 2	shell 3	shell 4
C						
	s	8236.0000	0.000531	-0.000878		
		1235.0000	0.004108	-0.000878		
		280.8000	0.021087	-0.004540		
		79.2700	0.081853	-0.018133		
		25.5900	0.234817	-0.055760		
		8.9970	0.434401	-0.126895		
		3.3190	0.346129	-0.170352		
		0.9059	0.039378	0.140382	1.0	
		0.3643	-0.008983	0.598684		
		0.1285	0.002385	0.395389		1.0
	p	18.7100		0.014031		
		4.1330		0.086866		
		1.2000		0.290216		
		0.3827		0.501008	1.0	
		0.1209		0.343406		1.0
	d	1.0970			1.0	
		0.3180				1.0
H						
	s	33.870000	0.006068			
		5.095000	0.045308			
		1.159000	0.202822			
		0.325800	0.503903	1.0		
		0.102700	0.383421		1.0	
	p	1.407000		1.0		
		0.388000			1.0	

where N_i a normalizing prefactor and l, m and n are integer numbers which are all zero for s-type orbitals, one of them is equal to 1 such that they sum up to 1 for p-type orbitals (e.g. for $2p_x$, $3p_x$, $4p_x$ *etc.* one has $l = 1$ and $m = n = 0$), they sum up to two (e.g. 110 or 200) for d-type orbitals and so on. To approximate better real atomic orbitals fixed linear combinations of Gaussians are used:

$$\chi_i(\mathbf{r}) = N_i x^l y^m z^n \left(\sum_{j=1}^{L_i} c_{ij} \mathrm{e}^{-\zeta_{ij} r^2} \right) \tag{3.2}$$

where c_{ij} are the so-called contraction coefficients, ζ_{ij} are the exponents of the so-called primitive Gaussians and L_i is the length of the contraction of the i-th atomic-like orbital. The exponents and contraction coefficients of the employed cc-pVTZ basis sets are listed in Table 3.1.

3.1.4 Band structure of tPA chain on the HF level

Now, that the geometry of our test system and the basis sets are assessed, we can start the investigation. At first, we would like to calculate the periodic HF solution for an infinite tPA single chain, mean the ground-state energy (per unit cell), Bloch orbitals and the corresponding orbital energies (the band structure). This can be done by the program package CRYSTAL [CRY98] which is able to perform HF calculations for periodic systems and uses Gaussian-type orbitals. However, due to the presence of rather diffuse Gaussians in the chosen basis set (with exponents less than 0.2) one faces the problem of "catastrophic" SCF results (non-converging SCF iterations) when default values of the ITOL parameters which control the accuracy of the calculation of the bielectronic Coulomb and exchange series (see [CRY98], p. 74 and 123-125) are used. The effect on these parameters on the convergence of SCF calculations in CRYSTAL is discussed in details in [PDR88], p. 79-85 and here we would only like to notice that in the case of *trans*-polyacetylene single chains and the chosen basis sets well-converged results are obtained with the ITOL parameters being set to 8 8 8 14 24 (the defaults are 6 6 6 6 12). The SCF ground-state energy

per unit cell is -3.53887 eV and the iteration is converged when the energy changes by less than 0.14 meV (5 μHartree) from one iteration step to the next.

The resulting orbital energies as a function of the one-dimensional crystal-momentum k (the band structure) are shown in Fig. 3.5. Blue lines correspond to Bloch states of π symmetry (single-electron wavefunction vanishes in the molecule plane) and the rest are of σ symmetry. Because of the different symmetry blue and black lines may cross.

From Fig. 3.5 one concludes that the ionization potential and the electron affinity of an infinite tPA chain are given by the top of π-type valence band and the bottom of π-type conduction band in the X point, respectively:

$$\mathrm{IP} = -\varepsilon_{\pi(\mathrm{val})}(k = \pi/a), \tag{3.3}$$

$$\mathrm{EA} = -\varepsilon_{\pi(\mathrm{cond})}(k = \pi/a) \tag{3.4}$$

On the HF level these quantities are IP= 5.90 eV and EA= -0.52 eV. The band gap, defined as the difference of these two values, is equal to 6.42 eV. However, from a number of experimental studies, *trans*-polyacetylene is known to have a positive electron affinity [KP+89] and a band gap of approximately 2 eV [FO+79], [TG+80], [L88]. Therefore, *trans*-polyacetylene is one of many systems for which the HF approximation fails to give both quantitatively and qualitatively correct results. By inclusion of electron correlation effects, following the scheme sketched in Chapter 2, we will approach the experimental data quite noticeably.

In our correlation calculations we focus our attention on the five valence bands and the three lowest conduction bands. Taking into account general considerations [F95] and earlier experience of the application of wavefunction-based correlation methods to covalent periodic systems [BF87], [GSF97] and [AFS00] we expect that the correlation effect will lead to an upward shift of the HF valence bands and a downward shift of the conduction bands and also to a flattening of the bands.

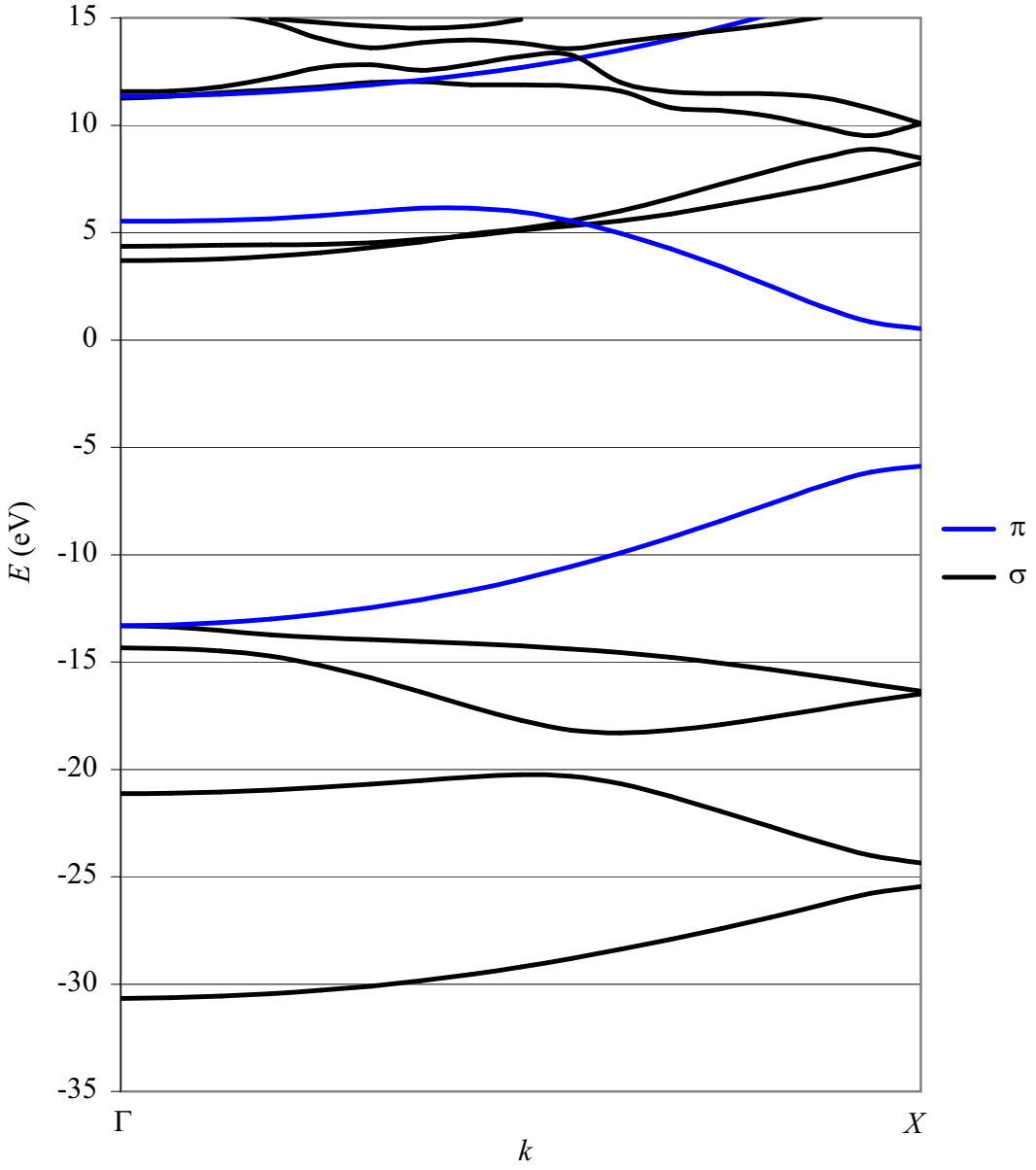

Figure 3.5: The HF band structure of *trans*-polyacetylene.

3.2 Localized orbitals

To set up the finite molecules for our correlation calculations we have chosen the following hydrogen-saturated clusters of *trans*-polyacetylene single chain: C_6H_8, C_8H_{10}, $C_{10}H_{12}$ and $C_{12}H_{14}$. All these clusters are terminated at single C–C bonds on both edges. There dangling C–C bonds are substituted by C–H bonds having the same angle γ with the adjacent double C–C bond and a characteristic C–H bond length of 1.087 Å. Such a termination on long C–C bond exclusively preserves the flat geometry of clusters and also minimizes the spurital impact of the saturating hydrogen atoms on the cojugated π system of tPA. Thus, we operate with closed-shell molecules which perfectly reproduce some finite part of our infinite system except for the two terminating C–H bonds. Therefore we expect that the localized single-particle wavefunctions (or molecular orbitals, LMOs) in these molecules are similar to those in the infinite system: in particular, in the central part of the molecule where an LMO has the same surrounding as in the infinite system they should coincides with the localized crystalline (Wannier) orbital (WO). On the edges of the cluster on one side there is only a terminating C–H bond which mimics the long C–C bond (and the remainder of the infinite chain). As LMOs centered on some bond always also have some small, but yet not negligible contribution of atomic orbitals of atoms in the neighborhood of the bond, WOs can not be reproduced correctly at the cluster edges. Thus, LMOs from edges of clusters will exhibit some deviations from the corresponding WOs (or equivalently from the corresponding LMOs in the central part of clusters). In accurate correlation calculations these edge LMOs are usually kept frozen or if not, the obtained results should be regarded as rough estimates only.

3.2.1 The case of occupied orbitals

To generate localized occupied spatial SCF orbitals (i.e. the bonding orbitals) on the clusters we use the Foster-Boys localization scheme [FB60] which is implemented

in MOLPRO [M2000]. The idea of this scheme is to find that unitary matrix u_{ij} in Eq. (2.26) which minimizes the sum of the spread of N_{orb} pre-selected spatial orbitals:

$$I = \sum_{i=1}^{N_{\text{orb}}} \sigma_i^2 \tag{3.5}$$

where the orbital spread is defined as

$$\sigma_i^2 = \int (\mathbf{r} - \mathbf{R}_i)^2 |\varphi_i(\mathbf{r})|^2 \mathrm{d}V, \tag{3.6}$$

and the center of i-th localized orbital φ_i as

$$\mathbf{R}_i = \int \mathbf{r} |\varphi_i(\mathbf{r})|^2 \mathrm{d}V \tag{3.7}$$

The question arises which canonical orbitals we have to provide for the localization to get properly localized occupied LMOs, which correspond to the individual bonds. We have count the valence electrons in the molecule (i.e. the electrons on the outer shells of each atoms which take part in the formation of bonds) and half of this number defines the number of the occupied canonical orbitals to be localized starting with the HOMO (highest occupied molecular orbital) and continuing with the successive energetically highest orbitals. All the other occupied orbitals are core orbitals which do not participate in bonding. In our case they are linear combinations of $1s$ orbitals of carbon atoms.

A special remark has to be made for flat molecules where orbitals of two different symmetries (σ and π) exist. Canonical orbitals of π type can be readily found in the set of SCF orbitals of a flat molecule as they have zero value in the molecule plane. Then the canonical σ and π orbitals can be localized separately and LMOs of σ and π symmetries are obtained. By doing so one reduces the number of LMEs to be treated on the correlation level as off-diagonal LMEs between σ and π orbitals are zeros and the effort for the correlation calculations, which are the most difficult and time consuming part of the whole approach, is reduced substentially.

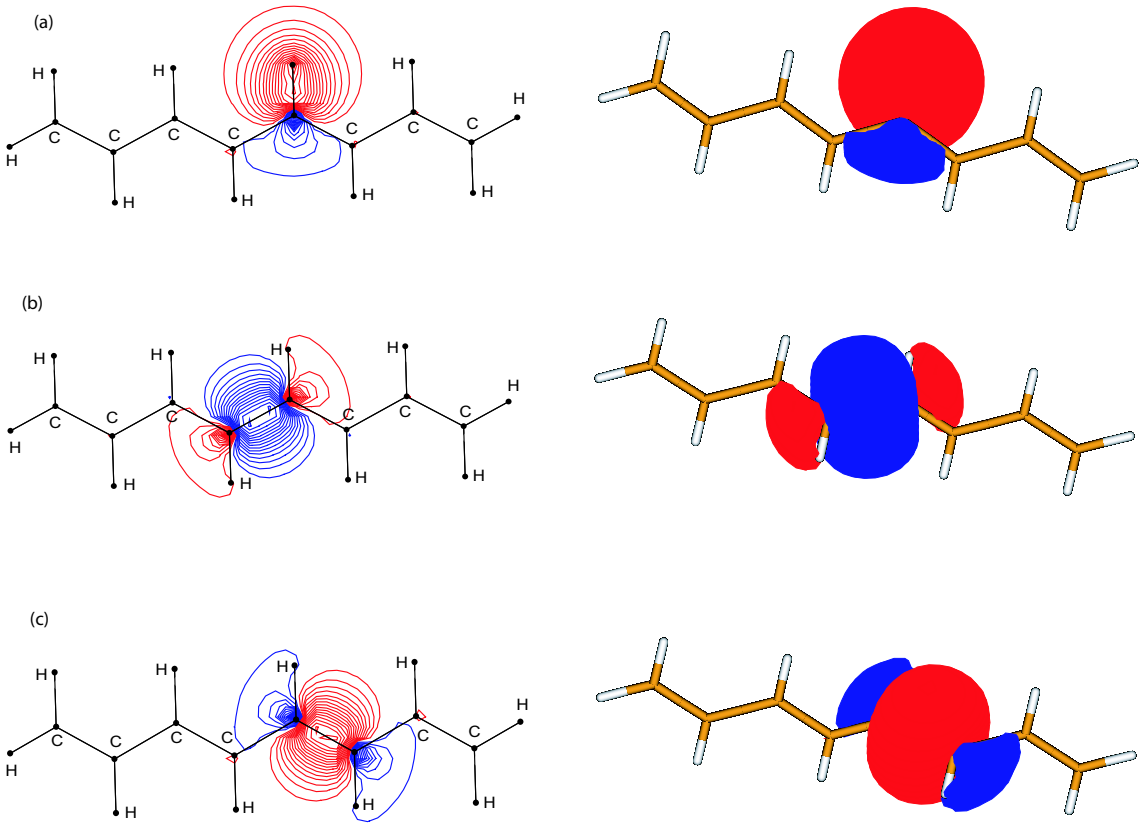

Figure 3.6: Three different σ bonds in *trans*-polyacetylene clusters: (a) C–H bond, (b) long C–C bond and (c) short C–C bond. Contours for different values of $\varphi_a(\mathbf{r})$ in the molecular plane are shown on the left, contoursurface plots for $|\varphi_a(\mathbf{r})| = 0.025$ a.u. on the right. The contour values increase in steps of 0.025 a.u.

In Fig. 3.6 contour plots (on the left) and contoursurface plots (on the right) of localized one-particle wavefunctions $\varphi_a(\mathbf{r})$ for three different σ bonds of a C_8H_{10} cluster are shown: (a) C–H bond, (b) long C–C bond and (c) short C–C bond. Red color denotes positive values of $\varphi_a(\mathbf{r})$ and blue color denotes negative ones.

In Fig. 3.7 a typical localized π orbital is shown. As it vanishes in the molecule plane ($\varphi(\mathbf{r})_{|z=0} = 0$) the plot plane for the contour plot is shifted to $z = 0.5$ Å. All plots in Figs. 3.6 and 3.7 are obtained by the MOLDEN program package [MOLDEN].

Comparing Fig. 3.6 and 3.7 we see that the π-bonds are more diffuse than

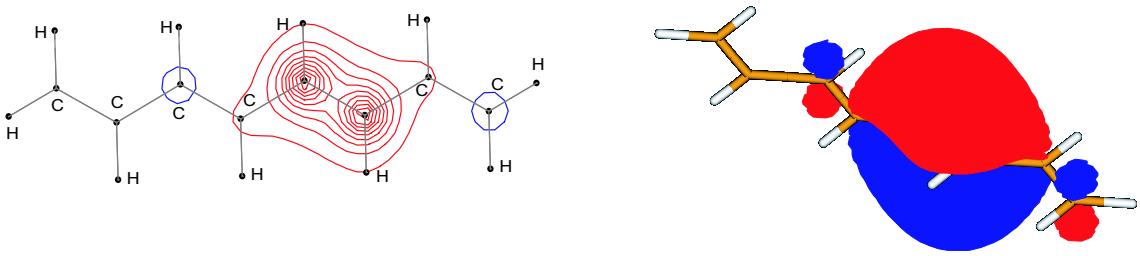

Figure 3.7: One of the π bonds of a C_8H_{10} cluster of tPA: a contour plot (left) and a contoursurface plot for $|\varphi_a(\mathbf{r})| = 0.025$ a.u. (right). The plot plane is parallel to the molecule plane at a hight of $z = 0.5$ Å.

the σ-bonds. The former have also a quite noticeable contribution of atomic basis functions from carbon atoms in the two nearest-neighbor unit cells. Therefore, for an accurate treatment of the correlation corrections to LMEs corresponding to π bonds substantially larger clusters are needed than for the case of σ bonds.

Having obtained the occupied LMOs we calculate the local SCF matrix elements IP_{ab} as defined in (2.46) and identify them with the corresponding crystalline local matrix elements $\mathrm{IP}_{R,nn'}$ which enter the truncated sum (2.32). The hopping matrix elements decay with the distance between two WOs. Setting some threshold for the absolute values of LMEs in (2.32) we define the two most distant WOs and by this the minimal size of the cluster in which the LMEs are calculated. Also, for choosing the proper cluster one takes into account that the LMOs on the edges of clusters can not reproduce the corresponding WOs correctly. Thus, the size of the cluster on which the LMEs are calculated is given by the two most distant WOs which give hopping matrix elements above the threshold plus one additional unit cell on both edges of the cluster. In the case of tPA the threshold is set to 1 mHartree (0.027 eV), and the minimal-sized saturated cluster arising from that is a $C_{10}H_{12}$ molecule.

This cluster is schematically shown in Fig. 3.8. For convenience we give names to the different bonds in the unit cell: on the double C–C bond we distinguish bonds of π and σ type and call them "pi" and "sig", respectively, the single C–C bond is called "CC" and the two C–H bonds are labelled "CH1" and "CH2". In the central

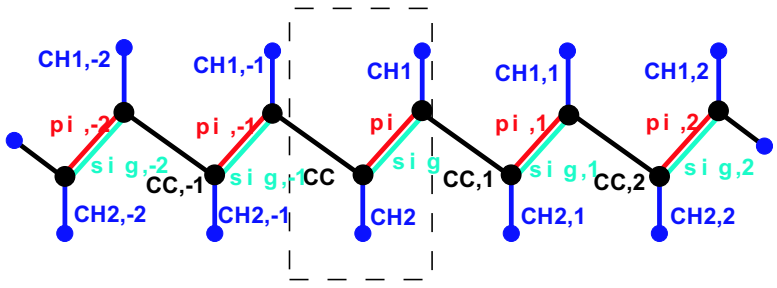

Figure 3.8: $C_{10}H_{12}$ cluster of tPA with the names given to each bond. The reference (central) unit cell is indicated by the dashed frame.

unit cell which is marked by dashed rectangle the bond names are taken as they are. Bonds in the other unit cells acquire an additional index which correspond to the ordering numbers n_c of the cell they are located in starting from the central (reference) cell and being negative on the left- and positive on the right-hand side. We build the finite matrix $\mathrm{IP}_{R,nn'}$ between the WOs φ_{0n} and $\varphi_{Rn'}$ defined in (2.30) with $R = n_c a_l$. The SCF values of $\mathrm{IP}_{R,nn'}$ matrix are summarized in Table 3.2 for σ-type WOs and in Table 3.3 for π-type WOs. The number of relevant non-equivalent entries in this matrix is finite since we omit hopping matrix elements which are below the threshold. The matrix $\mathrm{IP}_{R,nn'}$ is clearly diagonal dominant and the matrix elements nicely decay with increasing distance of the outers of the respective Wannier orbitals.

Let us emphasize that the matrix $\mathrm{IP}_{R,nn'}$ contains orbital energies and hopping matrix elements for an infinite tPA chain while its entries are calculated on the $C_{10}H_{12}$ molecule being IP_{ab}. To build the matrix $\mathrm{IP}_{R,nn'}$ correctly we use both, translation and inversion-center symmetry, of the infinite system and usually those matrix elements of IP_{ab} which correspond to bonds close to the center of the molecule. For example, all diagonal matrix elements IP_{0nn} are associated with IP_{aa} from the central unit cell. For off-diagonal elements we have $\mathrm{IP}^{\mathrm{chain}}_{2a,\mathrm{sig\ sig}} = \mathrm{IP}^{\mathrm{chain}}_{-2a,\mathrm{sig\ sig}} = \mathrm{IP}^{\mathrm{mol}}_{(\mathrm{sig},-1),\,(\mathrm{sig},1)}$ (use of translation symmetry) and $\mathrm{IP}^{\mathrm{chain}}_{0,\mathrm{CC\ CH2}} = \mathrm{IP}^{\mathrm{chain}}_{-a,\mathrm{CC\ CH1}} = \mathrm{IP}^{\mathrm{mol}}_{\mathrm{CC},\,\mathrm{CH2}}$ (use of inversion-center symmetry). Here, for the distinctness we temporarily use superscripts "chain" for LMEs from the infinite chain and "mol" for LMEs obtained from

Table 3.2: SCF values of the $\mathrm{IP}_{R,nn'}$ matrix for σ-type WOs (in eV).

n'	R	$\mathrm{IP}_{R,\mathrm{CH1}\ n'}$	$\mathrm{IP}_{R,\mathrm{sig}\ n'}$	$\mathrm{IP}_{R,\mathrm{CH2}\ n'}$	$\mathrm{IP}_{R,\mathrm{CC}\ n'}$
sig	$2a_l$		-0.049		
CC	$2a_l$	-0.153	0.202		
CH1	$1a_l$	0.338	-0.190		
sig	$1a_l$	0.634	-0.696	-0.190	0.202
CH2	$1a_l$	-0.803	0.634	0.338	-0.153
CC	$1a_l$	2.968	3.022	0.817	-0.767
CH1	0	18.904	3.022	-0.856	0.817
sig	0	3.022	22.396	3.022	3.022
CH2	0	-0.856	3.022	18.904	2.968
CC	0	0.817	3.022	2.968	21.230
CH1	$-1a_l$	0.338	0.634	-0.803	2.968
sig	$-1a_l$	-0.190	-0.696	0.634	3.022
CH2	$-1a_l$		-0.190	0.338	0.817
CC	$-1a_l$		0.202	-0.153	-0.767
sig	$-2a_l$		-0.049		0.202
CH1	$-2a_l$				-0.153

Table 3.3: SCF values of the $\mathrm{IP}_{R,nn'}$ matrix for π-type WOs (in eV).

$\mathrm{IP}_{0,\mathrm{pi\ pi}}$	$\mathrm{IP}_{\pm a,\mathrm{pi\ pi}}$	$\mathrm{IP}_{\pm 2a,\mathrm{pi\ pi}}$	$\mathrm{IP}_{\pm 3a,\mathrm{pi\ pi}}$	$\mathrm{IP}_{\pm 4a,\mathrm{pi\ pi}}$
10.526	1.683	-0.365	0.120	-0.047

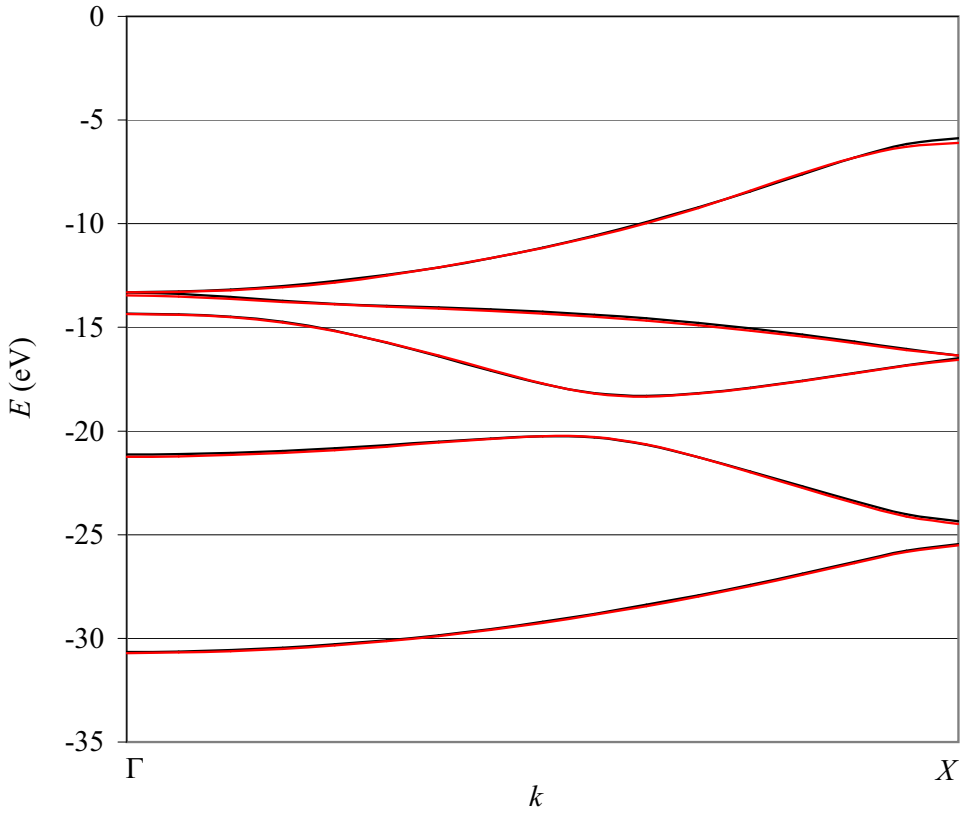

Figure 3.9: Valence bands of *trans*-polyacetylene obtained on the SCF level by LMEs calculated on clusters (red) and by a CRYSTAL calculation on an infinite tPA single chain (black).

SCF calculations of molecules.

Substituting the matrix elements from Tables 3.2 and 3.3 in the truncated sum (2.32) one obtains N_k matrices $\mathrm{IP}_{nn'}(k_i)$ on the chosen k-mesh of the Brillouin zone ($i = 1,\ 2, \ldots,\ N_k$). After diagonalization these matrices provide the positions of the bands at each point k_i. By choosing a rather dense grid one can easily produce a smooth band structure. In Fig. 3.9 the five valence bands of *trans*-polyacetylene obtained this way are presented and compared with the SCF bands of an infinite tPA single chain already shown in Fig. 3.5. Comparison reveals that the LMEs reproduce the SCF band structure very nicely and only small deviations (less than 0.2 eV) from the band structure by CRYSTAL appear due to the truncation in

Eq. (2.32). This demonstrates that LMEs obtained in molecules are practically equal to those comming directly for the infinite system using Wannier orbitals.

3.2.2 The case of virtual orbitals

The situation becomes more difficult when localized virtual orbitals have to be generated. In general, one can not simply use the same strategy as for the localization of the occupied orbitals. Occupied LMOs are obtained by applying e.g. the Foster-Boys localization scheme to the N_{bond} energetically highest occupied canonical spatial orbitals where N_{bond} is the number of bonds in the molecule. If one applies the localization procedure to the N_{bond} energetically lowest unoccupied canonical spatial orbitals one usually does *not* get any localized virtual orbitals (or antibonds) which can be regarded as the unoccupied WOs corresponding to the lowest few conduction bands. This difference in getting bonds but no antibonds lies in the fact that the valence bands are well-separated from the rest of the bandstructure by the band gap and that accordingly the occupied spectrum of the molecule representing a finite part of the crystal is clearly separated from the virtual spectrum by the HOMO–LUMO gap (see Fig. 3.10). In contrast, the lowest conduction bands are usually entangled with higher conduction bands and therefore the spectra of virtual states corresponding to lower and higher conduction bands overlap. For instance, in the band structure of tPA the five lowest conduction bands (which would correspond to the five antibonds per unit cell) are not separated from the other conduction bands. In this case one can not select in a simple and controlled way some suitable N_{bond} unoccupied canonical orbitals which could be converted to antibonds by the localization procedure. To illustrate this we show on Fig. 3.10 the spectrum of a C_6H_8 cluster together with the SCF band structure of tPA.

Alternatively, one could localize *all* virtual canonical orbitals of the molecule. However, even the energetically lowest localized virtual orbitals obtained this way have too high orbital energies since they contain contributions of both energetically low- and high-lying canonical orbitals. In this case non of the virtual LMOs can

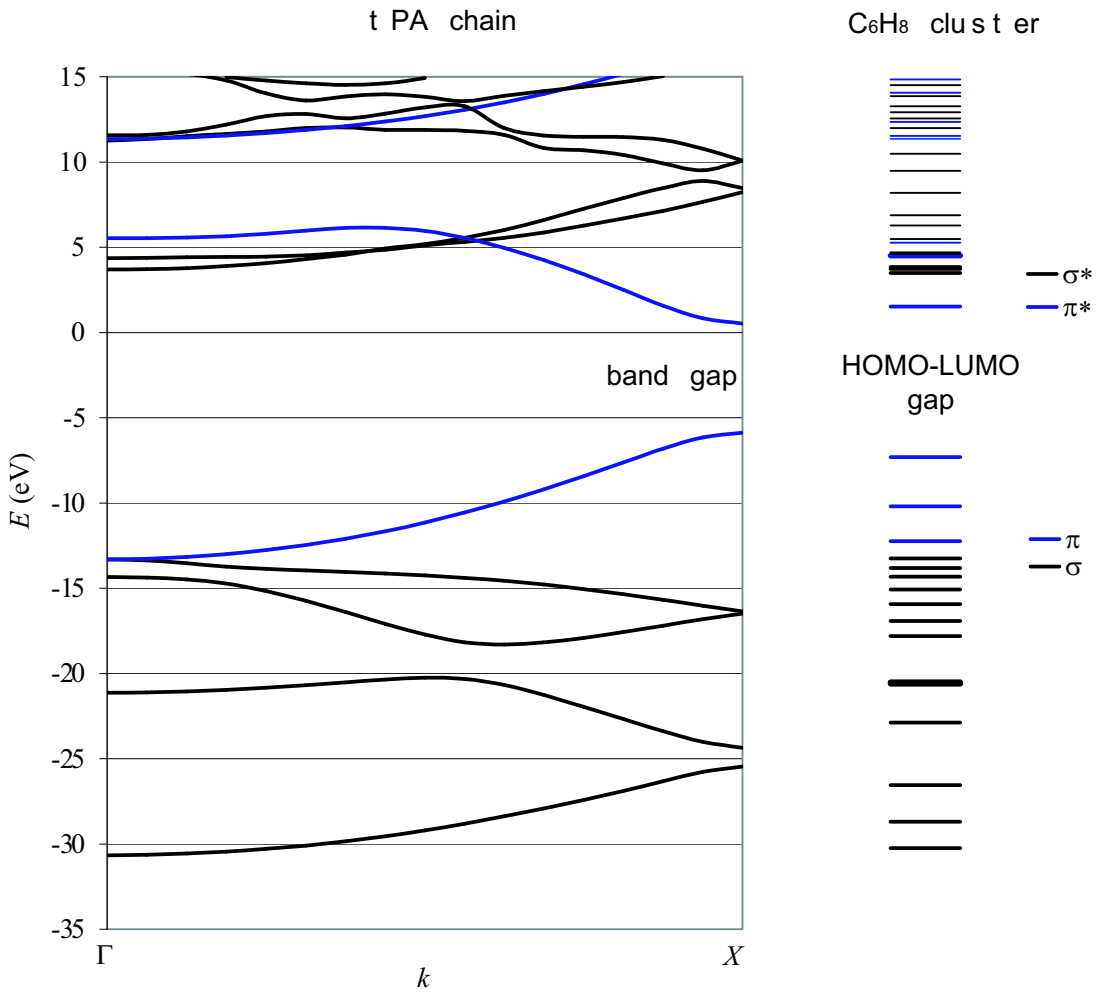

Figure 3.10: SCF band structure of tPA (on the left) and the one-particle spectrum of a C_6H_8 cluster (on the right).

be regarded as a WO corresponding to the lowest few conduction bands. Only the *whole* set of LMOs can be used to reproduce *all* conduction bands. Therefore LMOs obtained by localization of all virtual molecular orbitals can not be used in our approach for correlation correction to the *few* lowest conduction bands.

Thus, in general, antibonds can not be obtained on clusters by localization of some set of virtual canonical molecular orbitals (except of the cases of well separated conduction bands). Hence, we propose a completely different way of getting localized orbitals in clusters which can reproduce the bands of our interest: Wannier orbitals obtained in an infinite system are projected onto a cluster. If the Wannier orbital can be obtained as a linear combination of atomic orbitals with contributions of the latter rapidly decaying with the distance from the orbital center (see Fig. 3.11) such a WO can be represented on the cluster when the contributions from those atoms which are not present in the cluster are negligibly small such that they can be omitted. Then the projected WO can be used as the LMO. For instance, the WO shown schematically in Fig. 3.11 can reasonably be represented in a cluster consisting of five unit cells or more.

So, we have first to get well-localized Wannier orbitals in the infinite system which correspond to the conduction bands of interest. The concept of maximally localized Wannier orbitals was introduced for an isolated band or composite bands (an isolated group of bands) by Marzari and Vanderbilt [MV97]. There, the molecular localization criteria of Foster and Boys were applied to minimize the total spread of the WOs in the periodic system. In [MV97] Bloch functions $\psi_{n\mathbf{k}}(\mathbf{r})$ represented on a discrete mesh of k-points (n labels the band) are used and the Wannier orbital in cell $\mathbf{R}$ associated with band n is determined as $w_n(\mathbf{r}-\mathbf{R}) = 1/N_k \sum_k \mathrm{e}^{-i\mathbf{k}\cdot\mathbf{R}}\psi_{n\mathbf{k}}(\mathbf{r})$ (N_k is the number of considered k points in the Brillouin zone). The minimization of the total spread functional is carried out in the space of unitary matrices $U_{mn}^{(\mathbf{k})}$ describing the rotation among the Bloch functions at each k-point: $\psi'_{n\mathbf{k}} = \sum_m U_{mn}^{(\mathbf{k})}\psi_{m\mathbf{k}}$.

Later this idea was generalized in [SMV01] for the case of entangled bands to account for the case where no separate group of bands can be found. There, one speci-

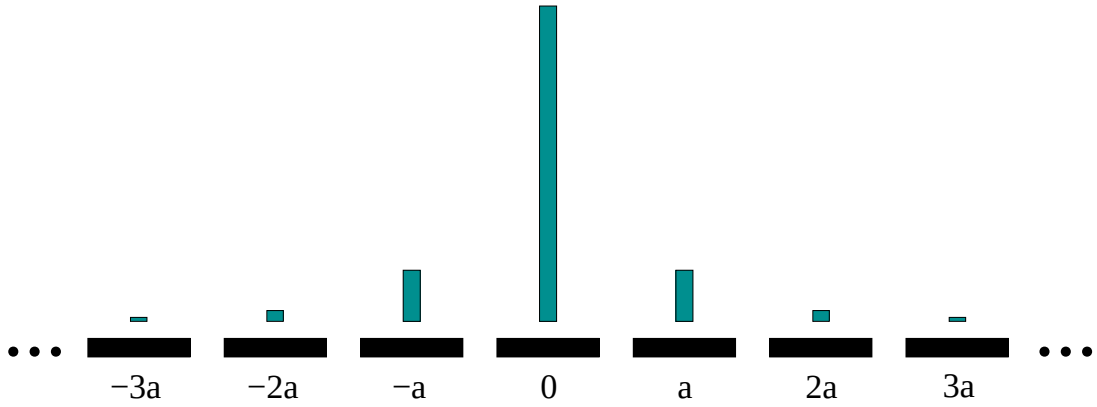

Figure 3.11: Schematic diagram showing the contributions of the atomic orbitals from different unit cells to a WO centered on the zero unit cell of a 1D crystal. Horizontal bars denote the unit cells and the hight of the vertical bars is proportional to the squared norm of the wavefunction contribution (or population) from the individual cells $R = 0, \pm a, \pm 2a, \ldots$.

fies an energy window with $N_{\mathrm{tot}}(\mathbf{k})$ bands with the N_b bands on interest being present together with higher or/and lower lying bands (at each k-point $N_{\mathrm{tot}}(\mathbf{k}) \geq N_b$). At k-points where $N_{\mathrm{tot}}(\mathbf{k}) > N_b$ an N_b-dimensional subspace of Bloch states which correspond to the bands of interest is first established (by minimization of some functional) and then the localization method from [MV97] is applied to the selected N_b states at each k-point. This way the maximally localized Wannier orbitals associated with selected bands are obtained.

A variant of the method of [MV97] for obtaining well-localized Wannier orbitals corresponding to composite bands was recently implemented in the CRYSTAL code ([BZ+01] and [ZWDS01]). The Bloch orbital for band n at point k is represented in CRYSTAL as the linear combination of atomic orbitals $\chi_\mu(\mathbf{r} - \mathbf{s}_\mu)$ (being contracted Gaussian-type function) centered at an atomic site $\mathbf{s}_\mu$

$$\psi_{n\mathbf{k}}(\mathbf{r}) = \sum_{\mu=1}^{M} \alpha_\mu^n(\mathbf{k}) \sum_{\mathbf{R}} \mathrm{e}^{i\mathbf{k}\cdot\mathbf{R}} \chi_\mu(\mathbf{r} - \mathbf{s}_\mu - \mathbf{R}) \tag{3.8}$$

where μ labels atomic orbitals centered in the reference cell and $\mathbf{R}$ denotes the lattice

vector. The N_b Wannier orbitals associated with the N_b composite bands at each unit cell are then obtained as linear combinations of atomic orbitals

$$w_n(\mathbf{r}-\mathbf{R}) = \sum_{\mu=1}^{M} \sum_{\mathbf{R}'} c_{\mu,\mathbf{R}'}^{n,\mathbf{R}} \chi_\mu(\mathbf{r}-\mathbf{s}_\mu-\mathbf{R}') \tag{3.9}$$

with the orthonormality condition being fulfilled $\langle w_n(\mathbf{r}-\mathbf{R})|w_{n'}(\mathbf{r}-\mathbf{R}')\rangle = \delta_{nn'}\delta_{\mathbf{R},\mathbf{R}'}$. This new feature of CRYSTAL was explicitely used in our work to get well-localized virtual WOs in *trans*-polyacetylene corresponding to the three lowest conduction bands since they can be regarded as composite bands being separated from other conduction bands by a gap in the whole Brillouin zone (see Fig. 3.5 or 3.10). However, at this point we would like to note that the idea of band disentanglement originally developed in [SMV01] was very recently implemented in the CRYSTAL program package by our work group and WOs corresponding to the lowest conduction bands of bulk diamond and silicon were obtained [IB]. Thus, the limitation of the method reported in [BZ+01] and [ZWDS01] for separated group of bands is removed and WOs for any bands of interest can now be obtained for the general case.

Having obtained well-localized virtual WOs in periodic system as linear combinations of atomic orbitals centered on atoms of a finite region of the crystal (usually some few unit cells close to the center of the WO) we need to project these orbitals onto the basis set of a finite molecule being a hydrogen-saturated cluster of the crystal. Then we could use them as virtual LMOs to get LMEs in our approach and also for further correlation calculations. For this purpose the program CRYREAD [CRYREAD] was recently designed in our group. It reads the WOs obtained in CRYSTAL as linear combinations of atomic functions and projects them onto the basis set of the user-specified cluster of the periodic system. The program takes all those WOs with norms exceeding a user-specified threshold after the coefficients $c_{\mu,\mathbf{R}'}^{n,\mathbf{R}}$ at atomic orbitals $\chi_\mu(\mathbf{r}-\mathbf{s}_\mu-\mathbf{R}')$ centered outside the cluster are set to zero, makes them othonormal and writes the corresponding matrix of coefficients $c_{\mu,\mathbf{R}'}^{n,\mathbf{R}}$ where

vectors $\mathbf{R}'$ and $\mathbf{R}$ are restricted to the specified cluster. After some further modification (contraction coefficients of atomic orbitals centered on cluster-saturating hydrogen atoms are added and set to zero) this matrix can be read by the program package MOLPRO and virtual localized molecular orbitals are obtained directly in the form of linear combinations of basis functions of the molecule. Virtual LMOs obtained this way perfectly represent WOs of the periodic system.

To be more precise, in the case of *trans*-polyacetylene we generate with CRYSTAL Wannier orbitals associated with core, valence and the first three conduction bands, performing three separate calculations for each subset of bands. The procedure for getting well-localized crystalline orbitals in CRYSTAL ([BZ+01] and [ZWDS01]) is an iterative one and requires (especially for virtual orbitals) an initial guess for the Wannier orbitals to start with. As discussed in [ZWDS01] the choice of the initial guess is critical for systems with fully covalent bonds (like diamond, silicon and also *trans*-polyacetylene). Therefore, we have to design good starting Wannier orbitals for each subset of bands. For core bands $1s$ atomic orbitals of carbon atoms are provided. In the case of valence bands we expect that the associated WOs are similar to the molecular bonds of hydrogen-saturated clusters. Therefore, we specify five bonding pairs of atomic orbitals per unit cell which correspond to the five bonds of the covalent system. The choice of the initial guess for three unoccupied WOs associated with the three lowest conduction bands of tPA is more subtle. We suppose that these three WOs correspond to three out of five antibonds per unit cell. As one of the conduction bands is formed by states of π symmetry the corresponding WO should be the π-antibond centered on the short C–C bond. For starting WOs associated with the two σ-bands the C–H antibonds are used. This choice is based on the fact that the C–H bonds in hydrogen-saturated clusters of tPA are energetically higher than the C–C σ bonds and therefore the C–H antibonds are expected to be energetically lower than the C–C σ antibonds. Since we already have occupied WOs $w_n(\mathbf{r})$ (or bonds) the antibonds of interest are obtained by a change of the sign of the coefficients $c_{\mu,0}^{n,0}$ from the atomic orbitals $\chi_\mu(\mathbf{r}-\mathbf{s}_\mu)$ centered

at one of two atoms of the corresponding bond. Providing antibonds constructed this way we were able to generate well-localized unoccupied WOs associated with three lowest conduction bands of tPA. The condition of orthonormality is fulfilled for all Wannier orbitals: $\langle w_i(\mathbf{r}-\mathbf{R})|w_j(\mathbf{r}-\mathbf{R}')\rangle = \delta_{ij}\delta_{\mathbf{R},\mathbf{R}'}$ (indices i and j running over core, valence and the first three conduction bands).

By the program CRYREAD we project the virtual WOs onto a $C_{12}H_{12}$ cluster (six unit cells, no saturating hydrogens) of the infinite tPA chain. Thus we obtain 18 (3×6) WOs centered on this cluster. The coefficient matrix produced by CRYREAD is enlarged to be consistent with the set of basis functions of an isolated $C_{12}H_{14}$ molecule (hydrogen-saturated). The enlarged matrix is read by the MOLPRO program where the SCF calculation on the $C_{12}H_{14}$ molecule has been performed and the set of one-particle SCF wavefunctions have been obtained. Then, the occupied and virtual spaces in $C_{12}H_{14}$ are constructed as follows. The occupied space $\{\psi_a\}$ is taken from the SCF calculation on $C_{12}H_{14}$ and is not changed. Next, the WOs $w_n(\mathbf{r}-\mathbf{R}) = \tilde{\varphi}_r(\mathbf{r})$ (obtained in the periodic system and projected onto the $C_{12}H_{12}$ cluster) are provided and are made orthogonal to the occupied space of the $C_{12}H_{14}$ molecule by Schmidt orthogonalization and re-orthonormalized thereafter by Löwdin (or symmetric) orthogonalization (see [SO96], p. 142-145). After this orthogonalization step the obtained virtual LMOs φ'_r may slightly differ from the projected WOs $\tilde{\varphi}_r$ as the occupied space of the $C_{12}H_{14}$ molecule differs from the one of the embedded $C_{12}H_{12}$ cluster. The space of the remaining virtual one-particle orbitals of $C_{12}H_{14}$ $\{\psi'_r\}$ is constructed to be orthogonal to the occupied space $\{\psi_a\}$ and the specified subspace of the 18 virtual LMOs $\{\varphi'_r\}$.

The 18 virtual LMOs constructed this way turned out to be 6 C–C antibonds of π type and 12 C–H antibonds of the $C_{12}H_{14}$ molecule. Two of these antibonds (one C–H and one C–C) from the central part of the molecule are presented in Fig. 3.12. Again as π orbitals have zero values in the molecule plane the plot plane in the contour plot in Fig. 3.12(b) is lifted by 0.5 Å. As one sees from these plots, the unoccupied LMOs are substantially more diffuse than the corresponding occupied

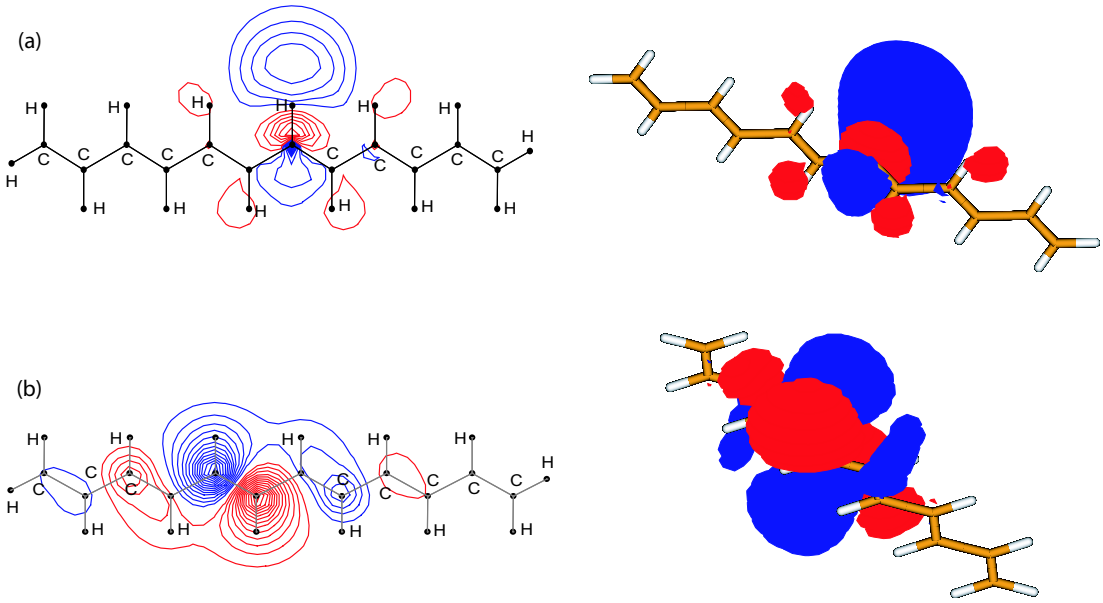

Figure 3.12: One C–H (a) and one C–C π (b) antibonds of a $C_{12}H_{14}$ cluster of tPA: the plane for the contour plot (left) of the C–H antibond lies in the molecular plane. That of the C–C π antibond is lifted upwards to $z = 0.5$ Å. Red lines correspond to positive and blue lines to negative vlues of $\varphi_r(\mathbf{r})$. The contour-surface plots (right) are drawn for $|\varphi_r(\mathbf{r})| = 0.025$ a.u. The contour values increase in step of 0.025 a.u.

ones (Fig. 3.6 and 3.7).

So, we got virtual LMOs of the molecule φ'_r in form of linear combinations of basis functions χ_μ centered on atoms of this molecule. The LMOs represent WOs and can be used to obtain LMEs on the SCF level and to reproduce the three conduction bands. However, at this point we would like to turn back to the question of getting virtual LMOs by applying the Foster–Boys localization scheme to virtual canonical orbitals ψ_r. The problem was that, in general, one can not simply select a subset of consecutive virtual canonical orbitals. Now with the LMOs at hand we can project the virtual LMOs onto the space of the virtual canonical orbitals $\{\psi_r\}$ of the $C_{12}H_{14}$ molecule (which altogether consists of 359 orbitals):

$$|\varphi'_s\rangle = \sum_{r=1}^{359} |\psi_r\rangle\langle\psi_r|\varphi'_s\rangle \tag{3.10}$$

and select the required subset for the localization by chosing those with the largest projection coefficients $\langle\psi_r|\varphi'_s\rangle$. This procedure is justified as long as all other coefficients are close to zero which was indeed the case for all our clusters. In case of the hydrogen-saturated $C_{12}H_{14}$ cluster of *trans*-polyacetylene the 20 energetically lowest virtual canonical orbitals were selected by the projection (3.10). After localization they give 6 C–C antibonds of π symmetry and 14 C–H antibonds including the two C–H antibonds with saturating hydrogen atoms which are not present in the crystal. (Again canonical orbitals of π and σ symmetry are localized separately from each other.) The LMOs obtained this way will be denoted by φ_r. We have to emphasize here that we could get these LMOs φ_r by Foster-Boys localization of suitably selected virtual canonical orbitals only because of two unique properties of *trans*-polyacetylene: i) it has three separated conduction bands (see Fig. 3.5) which correspond to the C–C π antibond and two C–H antibonds (note that no separated bands corresponding to two C–C σ antibonds can be found in the band structure of tPA) and ii) the two C–H bonds which connect two carbon atoms on the edges of the cluster with the saturating hydrogen atoms are similar to the characteristic C–H antibonds of the $(C_2H_2)_x$ 1D crystal and the energy of an electron in the artificial antibond is approximately the same as the one in the C–H antibond of the crystal. In general, localization of virtual canonical orbitals fails to produce proper antibonds. For instance, no suitable subset can be found in the virtual spectrum of hydrogen-saturated clusters of diamond (or silicon) to get the C–C (or Si–Si) antibonds by Foster–Boys localization. Thus, in general, one has to use projected WOs as LMOs. We decide to use the LMOs φ_r for *trans*-polyacetylene because they are easier to handle than the projected WOs φ'_r but we would like to analyze first the difference between φ_r and φ'_r.

For the C–C π antibonds there is no noticeable difference between the projected WOs and the LMOs obtained by localization of the first 6 virtual canonical π orbitals as there is no effect of the saturating C–H antibonds of σ symmetry on the C–C π antibonds. Therefore, the LMEs corresponding to states with an attached electron

Table 3.4: SCF values of the $EA_{R,mm'}$ matrix for π-type unoccupied WOs as obtained on a $C_{12}H_{14}$ cluster (in eV).

$EA_{0,pi^*\ pi^*}$	$EA_{\pm a,pi^*\ pi^*}$	$EA_{\pm 2a,pi^*\ pi^*}$	$EA_{\pm 3a,pi^*\ pi^*}$	$EA_{\pm 4a,pi^*\ pi^*}$
-4.497	-1.054	0.701	-0.146	0.025

in a projected virtual WOs and an LMOs of π symmetry are practically the same. In Table 3.4 we list the LMEs $EA_{R,mm'}$ defined in (2.31) for $(N+1)$-electron states where the additional electron is placed in a π antibonds as obtained by Foster-Boys localization. The names of antibonds coincide with those of the bonds but are marked with an asterisk. Again a rapid decay of the matrics elements with increasing bond distance is clearly discernable.

When C–H antibonds are obtained by localization of the 14 energetically lowest unoccupied canonical σ orbitals of $C_{12}H_{14}$ with the latter ones containing contibutions of the two C–H antibonds with the saturating hydrogen atoms. Since unoccupied LMOs are more diffuse than occupied ones (and spread over three unit cells of tPA as one sees in Fig. 3.12) the C–H antibonds obtained in the molecule are affected by the presence of the saturating atoms. As a consequence, the local SCF matrix elements for attached electron states $EA_{R,mm'}$ of σ type calculated in the $C_{12}H_{14}$ molecule by means of the projected WOs as localized virtual orbitals differ slightly from those calculated with the localized orbitals in the molecule. The two relevant matrices are listed in Table 3.5. The first two colunms of data show the values of the LMEs obtained when projected virtual WOs of σ type are used as C–H antibonds. The last two columns represent the same matrix elements obtained with localized virtual orbitals from a Foster-Boys localization of the canonical σ orbitals of $C_{12}H_{14}$. They differ by up to 0.12 eV which is small but not negligible for the calculation of the SCF bandstructure. The difference between the matrix elements $EA_{R,mm'}$ is caused by the presense of the two saturating hydrogen atoms in $C_{12}H_{14}$ molecule.

Table 3.5: SCF values of the $EA_{R,mm'}$ matrix for C–H antibonds in $C_{12}H_{14}$ cluster (in eV).

		Projected WOs		LMOs by FB localization	
m'	R	$EA_{R,CH1^* m'}$	$EA_{R,CH2^* m'}$	$EA_{R,CH1^* m'}$	$EA_{R,CH2^* m'}$
CH2*	$4a_l$	-0.063		-0.068	
CH1*	$3a_l$	0.120	-0.083	0.092	-0.054
CH2*	$3a_l$	0.097	0.120	0.107	0.092
CH1*	$2a_l$	-0.289	0.126	-0.244	0.078
CH2*	$2a_l$	-0.189	-0.289	-0.177	-0.244
CH1*	$1a_l$	1.012	-0.236	0.914	-0.194
CH2*	$1a_l$	-0.031	1.012	-0.025	0.914
CH1*	0	-5.603	-0.013	-5.487	-0.042
CH2*	0	-0.013	-5.603	-0.042	-5.487
CH1*	$-1a_l$	1.012	-0.031	0.914	-0.025
CH2*	$-1a_l$	-0.236	1.012	-0.194	0.914
CH1*	$-2a_l$	-0.289	-0.189	-0.244	-0.177
CH2*	$-2a_l$	0.126	-0.289	0.078	-0.244
CH1*	$-3a_l$	0.120	0.097	0.092	0.107
CH2*	$-3a_l$	-0.083	0.120	-0.054	0.092
CH1*	$-4a_l$		-0.063		-0.068

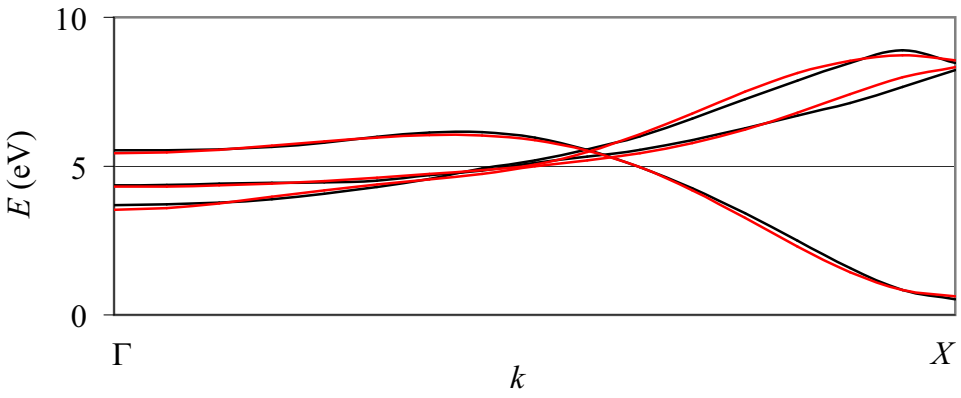

Figure 3.13: Conduction bands of *trans*-polyacetylene obtained on the SCF level by LMEs calculated in a $C_{12}H_{14}$ molecule with projected unoccupied Wannier orbitals (red) and by CRYSTAL calculation on the infinite tPA single chain (black).

To demostrate how the corresponding virtual LMEs reproduce the conduction bands we substitute the data from Table 3.4 and the first two columns of Table 3.5 into the truncated sum (2.33) and compare in Fig. 3.13 the bands obtained this way (red lines) with the three first conduction bands of infinite tPA chains as obtained by CRYSTAL (black lines). The deviation of bands by LMEs from those by CRYSTAL does not exceed 0.2 eV for all k-points like in the case of the valence bands and is mainly due to the truncation of the infinite summation (2.33).

It has to be noticed that one needs hopping matrix elements between more distant virtual LMOs (up to 4-th nearest neighbor cell) than in the case of the occupied LMOs to reproduce the σ conduction bands with the same accuracy as valence bands (where 2nd nearest neighbor cells were enough). Comparing Tables 3.5 and 3.2 we see that the decay of the SCF hopping matrix elements with the distance between the localized virtual orbitals is slower than in the case of the occupied orbitals since the former are more diffuse (cf. Fig. 3.6(a) and 3.12(a)). This implies that one needs larger clusters for getting the $\mathrm{EA}_{R,mm'}$ matrix elements than the $\mathrm{IP}_{R,nn'}$ matrix elements if the same value for the truncation threshold in (2.33) and (2.32) is used.

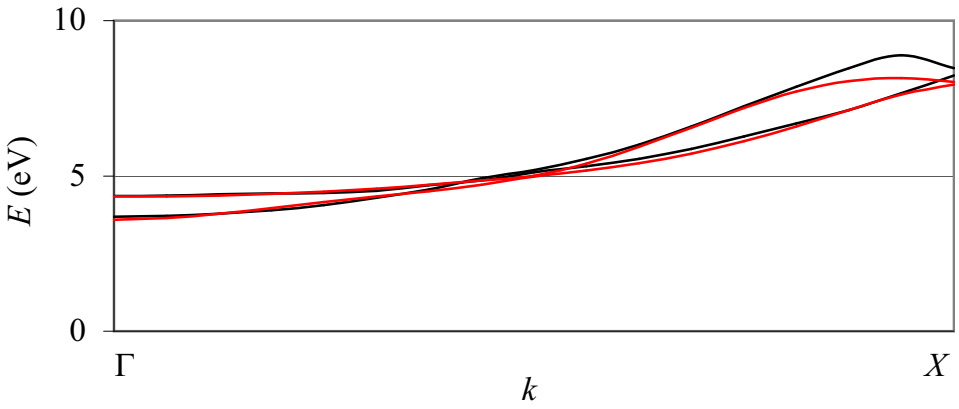

Figure 3.14: Two lowest conduction bands of σ-symmetry obtained on the SCF level by LMEs calculated fully in $C_{12}H_{14}$ molecule (red lines) as compared to σ bands from CRYSTAL calculation on the infinite tPA single chain (black lines).

In the case of *trans*-polyacetylene we have the unique possibility to compare the local matrix elements $\mathrm{EA}_{R,mm'}$ obtained with projected unoccupied Wannier orbitals φ'_r and antibonds φ_r obtained on a cluster by Foster-Boys localization of canonical virtual orbitals ψ_r of this cluster. If we also produce the lowest σ conduction bands by substitution the matrix elements from the two last columns of Table 3.5 into (2.33) and compare them to the corresponding σ bands obtained by CRYSTAL for the infinite tPA chain (see Fig. 3.14) we see rather big deviation for k-points close to the X point. This is most likely due to the onset of an avoided crossing in the upper σ conduction band close to the X point (see Fig. 3.5). Therefore, for the SCF values of the $\mathrm{EA}_{R,mm'}$ matrix elements we take those which are obtained with the projected unoccupied WOs.

3.3 Correlation corrections to the local matrix elements

The aim of our approach is to obtain the local matrix elements as defined in (2.63) and (2.64) with the correlation effects taken into account. This is equivalent to

finding corrections $\delta H_{ij}^{\text{corr}}$ and δE_0^{corr} to the matrix elements H_{ij} from Eq. (2.74) and the ground-state energy E_0 obtained in the framework of the HF approximation, respectively:

$$\delta H_{ij}^{\text{corr}} = H_{ij}^{\text{corr}} - H_{ij} \equiv H_{ij}^{\text{eff}} - H_{ij} \tag{3.11}$$

and

$$\delta E_0^{\text{corr}} = E_0^{\text{corr}} - E_0. \tag{3.12}$$

Then, the local matrix elements including the correction effects are obtained by adding these corrections to the corresponding SCF matrix elements as follows from Eqs. (2.63), (2.64), (3.11) and (3.12):

$$\text{IP}_{ab}^{\text{corr}} = \text{IP}_{ab} + \delta\text{IP}_{ab}^{\text{corr}} = H_{ab} + \delta H_{ab}^{\text{corr}} - \delta_{ab}(E_0 + \delta E_0^{\text{corr}}) \tag{3.13}$$

and

$$\text{EA}_{rs}^{\text{corr}} = \text{EA}_{rs} + \delta\text{EA}_{rs}^{\text{corr}} = -(H_{rs} + \delta H_{rs}^{\text{corr}}) + \delta_{rs}(E_0 + \delta E_0^{\text{corr}}) \tag{3.14}$$

The correlation corrections to the local SCF matrix elements

$$\delta\text{IP}_{ab}^{\text{corr}} = \delta H_{ab}^{\text{corr}} - \delta_{ab}\delta E_0^{\text{corr}} \tag{3.15}$$

and

$$\delta\text{EA}_{rs}^{\text{corr}} = -\delta H_{rs}^{\text{corr}} + \delta_{rs}\delta E_0^{\text{corr}} \tag{3.16}$$

appear as the consequence of electron correlation effects in the charged and the neutral system (which are two different effects as explained in chapter 2.4). Formally, $\delta\text{IP}_{ab}^{\text{corr}}$ and $\delta\text{EA}_{rs}^{\text{corr}}$ are non-zero because of the CI expansion of the wavefunctions

according to Eqs. (2.76) and (2.68). Without this expansion (i.e. when SCF many-particle wavefunctions are used) we get the SCF local matrix elements IP_{ab} and EA_{rs} which are listed in Tables 3.2–3.5.

In principle, correlation corrections to all matrix elements listed in these tables can be calculated. However, in order to get correlated band structure with sufficiant accuracy one needs to account for correlation effects only on the diagonal and the few largest off-diagonal matrix elements. As known from earlier works [GSF93], [GSF97], [ARM98] and [AFS00] (and as confirmed by the present work) the correlation corrections $\delta\mathrm{IP}_{ab}^{\mathrm{corr}}$ and $\delta\mathrm{EA}_{rs}^{\mathrm{corr}}$ are small fractions of the corresponding SCF matrix elements IP_{ab} and EA_{rs}. Also these corrections are obtained with final accuracy (10% say). Therefore one can conclude that for a given set of SCF local matrix elements reproducing some set of bands on the SCF level there is no sense to calculate correlation corrections to LMEs which are of the order of (or smaller than) 10% of the largest matrix element in the given set since the obtained correction to such small LMEs i) has no noticeable effect on the band structure and ii) themselves are of the order of the error bar for the largest matrix element. Thus we can restrict the number of matrix elements which need to be corrected to *all* diagonal elements and all those off-diagonal elements whose absolute values exceeds 10% of the largest diagonal matrix element in the given set (see Tables 3.2–3.5).

Practically, these off-diagonal elements are those where the two involved localized orbitals have the largest overlap. So, for π orbitals (occupied and virtual) the hopping matrix element for two π bonds (or antibonds) from two adjasent unit cells are considered. In the case of the occupied σ bonds we calculate correlation corrections to off-diagonal elements $\delta\mathrm{IP}_{ab}^{\mathrm{corr}}$ for all pairs of bonds sharing one atom. In tPA there are three such non-equivalent hopping matrix elements between adjacent σ bonds: $\mathrm{IP}_{\mathrm{CH2,sig}}$, $\mathrm{IP}_{\mathrm{CH2,CC}}$ and $\mathrm{IP}_{\mathrm{CC,sig}}$ (see Fig. 3.8). The C–H antibond is extended along the chain and therefore has the largest overlap with its translational copy from the nearest-neighbor unit cell (see Fig. 3.12a). Thus, taking into account the inversion and translation symmetry of tPA we only need to care for one off-diagonal

matrix element, $EA_{CH2^*,CH2,1^*}$, to correct the σ conduction bands.

As discussed in chapter 2.4, electron correlation is mainly a local effect. It takes into account the possibility of electrons in two neighbor localized orbitals to avoid each other and, by this, to reduce the energy of electron-electron repulsion. Also the rearrangement of electrons due to the presence of an extra charge happens mainly in the close vicinity of the charge. Therefore, the major contribution to the corrections δIP_{ab}^{corr} and δEA_{rs}^{corr} to the local SCF matrix elements IP_{ab} and EA_{rs} is produced by correlation of electrons in localized orbitals which are located in unit cells close to orbitals a and b (or r and s respectively). Thus, for each matrix element IP_{ab} (or EA_{rs}) one can explicitly define a cluster in which electron correlation gives the major contribution to δIP_{ab}^{corr} (δEA_{rs}^{corr}). For this cluster correlation should be treated with high accuracy (that is why the multireference CI method is used in our work).

To account for correlation effect on IP_{ab} matrix elements coming from electrons in σ bonds a C_6H_8 cluster is enough. However, in order to treat accurately correlation between electrons in π bonds one needs C_8H_{10} and $C_{10}H_{12}$ molecules because the occupied π bonds are more diffuse than the σ bonds. As unoccupied localized orbitals are even more diffuse than the occupied ones, correlation calculations in $C_{12}H_{14}$ molecule have to be performed to properly account for corrections to the EA_{rs} matrix elements. The details of the application of the multireference single and double configuration interaction method to get the corrections δIP_{ab}^{corr} and δEA_{rs}^{corr} are outlined in the next section.

3.4 The method of local increments

Having chosen the molecule (a hydrogen-saturated cluster of the crystal) for explicit correlation calculations we have to treat all electrons of the $(N-1)$, N or $(N+1)$-electron system on the correlation level except of the electrons in the core orbitals and in the bonds with the saturating hydrogen atoms. Let us say that in some cluster we have to handle electrons from n_{occ} occupied bonds. Then, to get the correlation

correction to the ground-state energy all singly and doubly excited configurations with electrons removed from these $n_{\rm occ}$ bonds are included into the expansion (2.68). For hole states, $n_{\rm occ}$ reference configurations $\Psi_i^{\rm corr}$ are formed as linear combinations of $n_{\rm occ}$ one-particle configurations Φ_a with the hole in one of the $n_{\rm occ}$ bonds. Then, excited configurations are produced by taking one or two out of $(2\,n_{\rm occ}-1)$ electrons from the occupied bonds and placing them into some virtual orbitals as defined in Eq. (2.76), and the energies of $n_{\rm occ}$ hole states have to be calculated. In the case of an attached electron in $n_{\rm virt}$ antibonds of the cluster we have $n_{\rm virt}$ reference states with the extra electron being delocalized over these antibonds. Due to the presence of the extra electron the electrons in the $n_{\rm occ}$ occupied bonds rearrange and in order to account for the correlation effect in this case all excited configurations with one or two electrons removed from either one of the $n_{\rm occ}$ occupied or virtual orbital which carries the extra electron and placed in some free virtual orbitals have to be taken into account in Eq. (2.76). Then, the energies of $n_{\rm virt}$ states are calculated. In all these three cases the number of excited configurations which are taken into account is huge even for small molecules and robust CI calculations as described above are not feasible (an enormous number of coefficients α from Eqs. (2.68) or (2.76) have to be optimized simultaneously). To proceed one needs an approximate scheme which consists of a series of calculations with the number of excited configurations being drastically reduced but which still accounts for electron correlation in the cluster with the desired accuracy.

3.4.1 Formulation in terms of bonds

A simple but powerful scheme to estimate correlation correction to SCF ground-state energy of clusters and solids was proposed by Stoll in Ref. [St92a] and [St92b]. This scheme is based on a clear physical idea and systematically sums contributions to $\delta E_0^{\rm corr}$ where each term accounts for correlation of a very limited number of electrons in localized orbitals. The method is as follows. First, corrections to the ground-state energy from electrons in each bond a individually are calculated: $\epsilon_a =$

$E_0^{\rm corr}(a) - E_0$, the energy $E_0^{\rm corr}(a)$ is obtained from Eq. (2.51) where in the CI expansion for the correlated wavefunction (2.68) *only* electrons in bond a are used to construct the excited configurations Φ_a^r and $\Phi_{a\bar{a}}^{rs}$. Here $\bar{a}$ stands for a spin orbital with the same spatial orbital as a but with opposite spin-orientation with respect to the spin orbital a. Let us notice here that a drastic reduction of the number of excited configurations in (2.68) takes place when excitations of two electrons only are considered. Summing up the contributions ϵ_a from all bonds one gets a first estimate $\delta E_0^{(1)}$ for the correction to the HF ground-state energy. To account for the non-additive corrections $\epsilon_{a,b} = E_0^{\rm corr}(a,b) - (\epsilon_a + \epsilon_b) - E_0$, correlation calculations with only the pair (a,b) of bonds being open for producing excited configurations are performed. Adding all pair corrections $\epsilon_{a,b}$ to $\delta E_0^{(1)}$ we reach the next order of approximation $\delta E_0^{(2)}$. The third order is obtained when we account for correlation corrections of electrons in bond triples (a,b,c) in the cluster: $\delta E_0^{(3)} = \delta E_0^{(2)} + \sum_{a<b<c} \epsilon_{a,b,c}$; the non-additivity corrections to the second-order approximation are $\epsilon_{a,b,c} = E_0^{\rm corr}(a,b,c) - (\epsilon_a + \epsilon_b + \epsilon_c) - (\epsilon_{a,b} + \epsilon_{a,c} + \epsilon_{b,c}) - E_0$. Continuing this way one builds order by order a converging series

$$\delta E_0^{\rm corr} = \sum_a \epsilon_a + \sum_{a<b} \epsilon_{a,b} + \sum_{a<b<c} \epsilon_{a,b,c} + \sum_{a<b<c<d} \epsilon_{a,b,c,d} + \ldots \qquad (3.17)$$

which in its limit gives the exact value of $\delta E_0^{\rm corr}$. However, as was discussed in a number of papers (e.g. in Ref. [St92a], [St92b], [PFS95], [PFS96], [KPFS97], [DDFS97] and [F02]) one obtains a very accurate estimate of $\delta E_0^{\rm corr}$ when the series (3.17) is truncated after the third term. Thus, in each separate correlation calculation at most six electrons are treated simultaneously. Moreover, as correlation effect decays rapidly with the distance between localized orbitals, the two- and three-bond increments $\epsilon_{a,b}$ and $\epsilon_{a,b,c}$ involving distant bonds can be neglected and therefore the effort for evaluating the correlation correction to the ground-state energy of a big molecules is substantially reduced. In fact, in the case of a periodic system only a finite number of energy increments has to be considered.

An extension of this approach to the correlation corrections to local SCF matrix

elements of *hole* states was proposed in the paper [GSF93] and developed further in [GSF97], [AFS00] and [AF02]. It was shown that the corrections to the matrix elements $\delta\mathrm{IP}_{ab}^{\mathrm{corr}}$ given by Eq. (3.15) can be also obtained with any desired accuracy by means of local increments. In Eq. (3.15) the term $\delta H_{ab}^{\mathrm{corr}}$ accounts for correlation in the $(N-1)$-electron system where electrons react on the presence of the hole while $\delta E_0^{\mathrm{corr}}$ accounts for electron correlation in the neutral system. As the difference of these two quantities define $\delta\mathrm{IP}_{ab}^{\mathrm{corr}}$ they must be evaluated consistently in the incremental scheme.

By analogy to Eq. (3.17) for the correlation correction to the ground-state energy the incremental approach to $\delta\mathrm{IP}_{ab}^{\mathrm{corr}}$ can be written as

$$\delta\mathrm{IP}_{ab}^{\mathrm{corr}} = \Delta\mathrm{IP}_{ab}^{\mathrm{corr}}() + \sum_{c\neq a,b} \Delta\mathrm{IP}_{ab}^{\mathrm{corr}}(c) + \sum_{c<d\neq a,b} \Delta\mathrm{IP}_{ab}^{\mathrm{corr}}(c,d) + \ldots \tag{3.18}$$

where in parentheses we denote those additional bonds which are "open" for correlation together with the matrix element defining bonds a and b. Below we explain the performance of the approach separately for diagonal and off-diagonal elements.

The first order of approximation to the diagonal element $\delta\mathrm{IP}_{aa}^{\mathrm{corr}}$ is obtained when only bond a is open for correlation. This means that in the $(N-1)$-electron system one electron in bond a is destroyed and the second electron from this bond can be excited to the virtual orbitals thus forming singly excited configurations in the expansion (2.76) of the reference wavefunction:

$$\Psi_a^{\mathrm{corr}} = \alpha_a(a)\Phi_a + \sum_r \alpha_{a\bar{a}}^{\ r}(a)\Phi_{a\bar{a}}^{\ r} \tag{3.19}$$

with energy E_a^{corr}. In this case the effective Hamiltonian is a 1×1 matrix whose element is equal to E_a^{corr}. The corresponding energy of the neutral (i.e. N-electron) system is $E_0^{\mathrm{corr}}(a)$. The first-order approximation to $\delta\mathrm{IP}_{aa}^{\mathrm{corr}}$ thus is

$$\Delta\mathrm{IP}_{aa}^{\mathrm{corr}}() = \delta\mathrm{IP}_{aa}^{\mathrm{corr}}() = H_{aa}^{\mathrm{eff}}() - H_{aa} - \left[E_0^{\mathrm{corr}}(a) - E_0\right] = \mathrm{IP}_{aa}^{\mathrm{corr}}() - \mathrm{IP}_{aa}. \tag{3.20}$$

The second-order approximation is obtained when the contributions to $\delta\mathrm{IP}_{aa}^{\mathrm{corr}}$ from each of the remaining $(n_{\mathrm{occ}}-1)$ bonds individually are summed up, where the corrections are defined relative to $\Delta\mathrm{IP}_{aa}^{\mathrm{corr}}()$,

$$\Delta\mathrm{IP}_{aa}^{\mathrm{corr}}(c) = \delta\mathrm{IP}_{aa}^{\mathrm{corr}}(c) - \Delta\mathrm{IP}_{aa}^{\mathrm{corr}}() \tag{3.21}$$

The first term in the right-hand side of Eq. (3.21) is

$$\delta\mathrm{IP}_{aa}^{\mathrm{corr}}(c) = H_{aa}^{\mathrm{eff}}(c) - H_{aa} - \left[E_0^{\mathrm{corr}}(a,c) - E_0\right] = \mathrm{IP}_{aa}^{\mathrm{corr}}(c) - \mathrm{IP}_{aa}. \tag{3.22}$$

In Eq. (3.22) the effective Hamiltonian element $H_{aa}^{\mathrm{eff}}(c)$ stems from a 2×2 matrix defined in the configurations Φ_a and Φ_c. At this point we would like to notice that due to the decay of the correlation effect with the distance between the correlated electrons one finds a rapid decrease of the increments $\Delta\mathrm{IP}_{aa}^{\mathrm{corr}}(c)$ when the distance between the orbitals a and c increases. This ensures that one can indeed use finite clusters to evaluate the correlation corrections to the local matrix elements defined in a crystal.

It is obvious that summing over all second-order increments does not yet give a correct estimate of $\delta\mathrm{IP}_{aa}^{\mathrm{corr}}$ as correlation between electrons in different additional bonds (c and d) is missing. The next order of approximation is obtained when we account for the corresponding non-additivity corrections

$$\Delta\mathrm{IP}_{aa}^{\mathrm{corr}}(c,d) = \delta\mathrm{IP}_{aa}^{\mathrm{corr}}(c,d) - \Delta\mathrm{IP}_{aa}^{\mathrm{corr}}() - \left[\Delta\mathrm{IP}_{aa}^{\mathrm{corr}}(c) + \Delta\mathrm{IP}_{aa}^{\mathrm{corr}}(d)\right]. \tag{3.23}$$

Here the correlation correction $\delta\mathrm{IP}_{aa}^{\mathrm{corr}}(c,d)$ to the diagonal matrix element IP_{aa} is calculated with three bonds (a, c and d) being open:

$$\delta\mathrm{IP}_{aa}^{\mathrm{corr}}(c,d) = H_{aa}^{\mathrm{eff}}(c,d) - H_{aa} - \left[E_0^{\mathrm{corr}}(a,c,d) - E_0\right] = \mathrm{IP}_{aa}^{\mathrm{corr}}(c,d) - \mathrm{IP}_{aa}. \tag{3.24}$$

The hole is delocalized within these three bonds and thus three correlated $(N-1)$-electron states are obtained. This procedure can be continued further order by order.

However, as increments are expected to decrease rapidly with increasing order (see Ref. [GSF97], [AFS00] and [AF02]), the series (3.18) can be truncated after the third term.

The correlation corrections to off-diagonal (or hopping) matrix elements $\mathrm{IP}_{ab}^{\mathrm{corr}}$ are evaluated the same way, however, the procedure is started with the two bond a and b and no ground-state energies are present:

$$\Delta\mathrm{IP}_{ab}^{\mathrm{corr}}() = \delta\mathrm{IP}_{ab}() = H_{ab}^{\mathrm{eff}}() - H_{ab} = \mathrm{IP}_{ab}^{\mathrm{corr}}() - \mathrm{IP}_{ab}. \tag{3.25}$$

Here the starting effective Hamiltonian matrix elements $H_{ab}^{\mathrm{eff}}()$ already originate from a 2×2 matrix defined in configurations Φ_a and Φ_b. Next we compute the correlation contribution of an individual additional orbital:

$$\Delta\mathrm{IP}_{ab}^{\mathrm{corr}}(c) = \delta\mathrm{IP}_{ab}^{\mathrm{corr}}(c) - \Delta\mathrm{IP}_{ab}^{\mathrm{corr}}() \tag{3.26}$$

where

$$\delta\mathrm{IP}_{ab}^{\mathrm{corr}}(c) = H_{ab}^{\mathrm{eff}}(c) - H_{ab} = \mathrm{IP}_{ab}^{\mathrm{corr}}(c) - \mathrm{IP}_{ab}. \tag{3.27}$$

In this case the hole is delocalized over a triple of bonds (a, b and c). Summing over c we get the second term in the series (3.18). The third-order increments are

$$\Delta\mathrm{IP}_{ab}^{\mathrm{corr}}(c,d) = \delta\mathrm{IP}_{ab}^{\mathrm{corr}}(c,d) - \Delta\mathrm{IP}_{ab}^{\mathrm{corr}}() - \left[\Delta\mathrm{IP}_{ab}^{\mathrm{corr}}(c) + \Delta\mathrm{IP}_{ab}^{\mathrm{corr}}(d)\right] \tag{3.28}$$

where correlated matrix elements $\delta\mathrm{IP}_{ab}^{\mathrm{corr}}(c,d)$ are obtained when four bonds are open for correlations always including the bonds a and b:

$$\delta\mathrm{IP}_{ab}^{\mathrm{corr}}(c,d) = H_{ab}^{\mathrm{eff}}(c,d) - H_{ab} = \mathrm{IP}_{ab}^{\mathrm{corr}}(c,d) - \mathrm{IP}_{ab}. \tag{3.29}$$

Again, the series (3.18) can be truncated after the third term.

In the present work this approach is used to obtain good estimates for the correlation corrections of the local matrix elements IP_{ab}. For the σ bonds a C_6H_8 molecule

is used. Due to the truncation of the series (3.18) in each CI calculation we have at most four bonds open for correlation which keeps the calculations reasonably cheap. However, even in such a small molecule as C_6H_8 the number of all third-order increments is 78 (all pair combinations among 13 bonds) for the diagonal elements IP_{aa} and 66 for the off-diagonal elements (2 out of 12 combinations). Dozens of input files have to be prepared for the correlation calculations and the results of these calculations have to be gathered and summed up properly. As discussed in the section 3.3 we need much larger molecules to account for the correlation corrections to local matrix elements IP_{ab} with a and b being π bonds and also for selected EA_{rs} matrix elements. The number of increments increases quadratically with the size of the cluster (i.e. with the number of bonds). Therefore, the incremental scheme introduced above in terms of bond contributions becomes unfeasible because of the huge number of increments though each increment individually can be evaluated by the CI method at low cost.

3.4.2 Formulation in terms of bond groups

To proceed in the case of big clusters we propose to reformulate the incremental scheme in terms of *groups* of orbitals. In this approach to the correlation corrections of the matrix element IP_{ab} we subdivide all bonds except of a and b in groups g_1, g_2, ... consisting of a couple of bonds each ($n_{g_i} \geq 1$, n_{g_i} being the number of bonds in the i-th group g_i). It is natural that the bonds in a particular group g_i belong to the same unit cell (or two adjacent unit cells) and that the groups do not overlap. Then, in Eq. (3.18) we replace the single orbitals c and d in parentheses by entire orbital groups g_i and g_j and sum over group indices i and j:

$$\delta IP_{ab}^{corr} = \Delta IP_{ab}^{corr}() + \sum_i \Delta IP_{ab}^{corr}(g_i) + \sum_{i<j} \Delta IP_{ab}^{corr}(g_i, g_j) + \ldots \tag{3.30}$$

In the case of a diagonal element, IP_{aa} say, the other orbital b forms its own group and has to be included in the summation over the groups g_i in Eq. (3.30). Consequently,

we replace the bonds c and d in Eqs. (3.21)–(3.24) and (3.26)–(3.29) by groups g_i and g_j. Thus, the increments in the series (3.30) become

$$\Delta \mathrm{IP}_{ab}^{\mathrm{corr}}(g_i) = \delta \mathrm{IP}_{ab}^{\mathrm{corr}}(g_i) - \Delta \mathrm{IP}_{ab}^{\mathrm{corr}}() \tag{3.31}$$

and

$$\Delta \mathrm{IP}_{ab}^{\mathrm{corr}}(g_i, g_j) = \delta \mathrm{IP}_{ab}^{\mathrm{corr}}(g_i, g_j) - \Delta \mathrm{IP}_{ab}^{\mathrm{corr}}() - \left[\Delta \mathrm{IP}_{ab}^{\mathrm{corr}}(g_i) + \Delta \mathrm{IP}_{ab}^{\mathrm{corr}}(g_j)\right] \tag{3.32}$$

The substitution of a group g_i instead of a single bond c in (3.21) physically means that we account for all the contribution to the correlation correction $\delta \mathrm{IP}_{ab}^{\mathrm{corr}}$ which are associated with electrons from the *whole* group of bonds g_i instead of a single electron from bond c:

$$\delta \mathrm{IP}_{ab}^{\mathrm{corr}}(g_i) = H_{ab}^{\mathrm{eff}}(g_i) - H_{ab} - \delta_{ab}\left[E_0^{\mathrm{corr}}(a, g_i) - E_0\right] = \mathrm{IP}_{ab}^{\mathrm{corr}}(g_i) - \mathrm{IP}_{ab}. \tag{3.33}$$

To get the matrix element $H_{ab}^{\mathrm{eff}}(g_i)$ of the effective Hamiltonian, $(n_{g_i} + 2 - \delta_{ab})$ correlated hole states have to be calculated explicitly. Also for diagonal elements the correlation correction to the ground-state energy is obtained when all bonds of the group g_i together with the bond a are open for correlation simultaneously and the rest of the bonds of the cluster are frozen. Summing up the correlation contributions associated with the individual *groups* one gets a first estimate of the response of the cluster to the presence of a hole. Note that this first-order estimate $\delta \mathrm{IP}_{ab}^{(1)}$ contains much more correlation contributions than the sum over all *single bond* increments because intragroup correlation is fully included. This result is improved when the non-additivity corrections $\Delta \mathrm{IP}_{ab}^{\mathrm{corr}}(g_i, g_j)$ for all *pairs of groups* are summed up. The scheme can be continued by adding increments of higher orders. However, as group increments also decrease rapidly with the order, the series (3.30) can be terminated after the third term to get rather accurate estimate for the correlation correction to the LME IP_{ab}. The incremental scheme in terms of bond groups, as it is introduced

in this subsection, was used in our approach to evaluate the correlation correction to the matrix element $\mathrm{IP}_{\pm a,\mathrm{pi\,pi}}$ from Table 3.3. In that case groups of σ bonds were composed. The corresponding data on the increments are given in chapter 4.1.

Grouping the bonds substantially reduces the numbers of increments in (3.30) as compared to (3.18) however to the price of more expensive CI calculations for each increment in (3.30). In the latter case up to $(n_{g_i} + n_{g_j} + 2)$ bonds can be open for correlation simultaneously and the same number of hole states have to be calculated to get the matrix element $H^{\mathrm{eff}}_{ab}(g_i, g_j)$ for a particular increment $\Delta\mathrm{IP}^{\mathrm{corr}}_{ab}(g_i, g_j)$.

3.4.3 Incremental scheme for attached-electron states

The method of local increments can be also used for the evaluation of the correlation corrections to the matrix elements EA_{rs}. In this case $(2n_{\mathrm{bond}} + 1)$ electrons have to be correlated and the additional electron is delocalized over all antibonds of the chosen molecule. To reduce the computational efforts for the MRCI calculations, one can additionally freeze the majority of antibonds when calculating a particular increment forbidding electrons to occupy the frozen antibonds. This way one reduces i) the number of calculated $(N+1)$-electron states and ii) the external space. At the same time only electrons from the bonds belonging to one or two groups are open for correlation simultaneously. (Here we need to group the bonds again, because large clusters are required to account for correlation effects in the $(N + 1)$-electron systems.) In the incremental scheme the extension of the external space (i.e. the opening of antibonds) and the opening of the bonds must be done consistently. Otherwise the increment series will converge poorly. Thus, we find it reasonable to group the virtual localized orbitals centered on one bond together with the occupied orbitals from this bond (or adjacent bonds). The general formula for correlation correction to matrix element EA_{rs} by means of local increments is analogous to

Eq. (3.30):

$$\delta\mathrm{EA}_{rs}^{\mathrm{corr}} = \Delta\mathrm{EA}_{rs}^{\mathrm{corr}}() + \sum_i \Delta\mathrm{EA}_{rs}^{\mathrm{corr}}(g_i) + \sum_{i<j} \Delta\mathrm{EA}_{rs}^{\mathrm{corr}}(g_i, g_j) + \ldots \tag{3.34}$$

where

$$\Delta\mathrm{EA}_{rs}^{\mathrm{corr}}(g_i) = \delta\mathrm{EA}_{rs}^{\mathrm{corr}}(g_i) - \Delta\mathrm{EA}_{rs}^{\mathrm{corr}}() \tag{3.35}$$

and

$$\Delta\mathrm{EA}_{rs}^{\mathrm{corr}}(g_i, g_j) = \delta\mathrm{EA}_{rs}^{\mathrm{corr}}(g_i, g_j) - \Delta\mathrm{EA}_{rs}^{\mathrm{corr}}() - \left[\Delta\mathrm{EA}_{rs}^{\mathrm{corr}}(g_i) + \Delta\mathrm{EA}_{rs}^{\mathrm{corr}}(g_j)\right]. \tag{3.36}$$

Here indices r and s denote two groups g_r and g_s each containing the relevant antibond plus corresponding bond (or few adjacent bonds). Again for the diagonal element, EA_{rr} say, the summation over the groups in Eq. (3.34) includes the group g_s of the other antibond.

The first-order increment

$$\Delta\mathrm{EA}_{rs}^{\mathrm{corr}}() = -\left[H_{rs}^{\mathrm{eff}}() - H_{rs}\right] + \delta_{rs}\left[E_0^{\mathrm{corr}}(g_r) - E_0\right] = \mathrm{EA}_{rs}^{\mathrm{corr}}() - \mathrm{EA}_{rs} \tag{3.37}$$

contains the effective Hamiltonian defined in configurations Φ_r and Φ_s, all occupied orbitals from the groups g_r and g_s are open for constructing the excited configurations in the MRCI ansatz for the correlated wavefunctions (2.78) and all antibonds except of r and s are forbidden for the excited electrons. For the diagonal element ($s = r$) only one group is considered in Eq. (3.37). The correlated energy of the N-electron state $E_0^{\mathrm{corr}}(g_r)$ is calculated with only bonds of the group g_r being open.

When we add individual groups for the second-order increments and pairs of groups for the third-order increment we simultaneously open antibonds and the corresponding bonds for correlation. This way we approach in a systematic way the value of $\delta\mathrm{EA}_{rs}^{\mathrm{corr}}$ for *all* bonds and *all* antibonds being open simultaneously, however,

in each separate MRCI calculation the number of configurations (and the number of coefficients α in Eq. (2.68) and (2.78) to be optimized) is considerably restricted.

3.4.4 Additional features of the incremental scheme

The incremental scheme described above has five important additional features. The calculation of individual second-order increments $\Delta\mathrm{IP}_{ab}^{\mathrm{corr}}(g_i)$ and $\Delta\mathrm{EA}_{rs}^{\mathrm{corr}}(g_i)$ gives information on the decay of the correlation effect with the distance between the bonds of a group g_i and the localized charge in bonds a and b (or antibonds r and s). This information allows one to estimate whether a chosen cluster is big enough to account for the dominant part of the correlation corrections.

The second feature is that one uses the symmetry of the crystal to reduce the number of increments which have to be calculated: the contribution of symmetry-equivalent increments to the correlation correction is the value of one of them times the number of such equivalent increments. This reduces the computational efforts and works especially well for highly symmetric crystals with simple unit cells like diamond, silicon and germanium (see Ref. [GSF93], [GSF97], [AFS00] and [AF02]).

The third feature: the main computational effort is directed to get the effective Hamiltonian from which we only need one of its matrix element for a particular increment. However, it is easy to see that some other matrix elements of a given effective Hamiltonian can be used for other increments without any extra cost. For instance, the diagonal element $H_{aa}^{\mathrm{eff}}(b,c)$ and the off-diagonal element $H_{ab}^{\mathrm{eff}}(c)$ are obtained from one and the same MRCI calculation with Φ_a, Φ_b and Φ_c being the model configurations.

The fourth feature is the possibility to use the translational symmetry of the crystal and reduce the so-called *cluster-edge* error by this. Such errors arise when one of the bonds open for correlation is close to the edge of a cluster and this localized orbital is affected by the lack of supporting atoms (i.e. the energy of the electron in this orbital differs noticeably from the energy of the electron in a translation-equivalent orbital in the central part of the cluster). Then, for the evaluation of this

particular increment one can open a translational-equivalent set of orbital groups for correlation which does not contain orbitals at the edge of the cluster if the size of the cluster allows one to do so. Let's say that we want to get the contribution to the correlation correction to the diagonal matrix element $\mathrm{IP}_{\mathrm{pi,pi}}$ associated with the additional bond "pi,-2" in the molecule $C_{10}H_{12}$ which is shown in Fig. 3.8. We know that orbital "pi,-2" is not equivalent to orbital "pi,-1" as one more unit cell from the left side is needed to reproduce properly the occupied Wannier π orbital centered on the bond "pi,-2" (see Fig. 3.7). Also we expect that the increment $\Delta\mathrm{IP}^{\mathrm{corr}}_{\mathrm{pi,pi}}(\mathrm{pi},-2)$ is still relatively large as orbitals "pi" and "pi,-2" overlap as can be understood from Fig. 3.7. Therefore, this increment has to be evaluated when two equivalent bonds with proper crystalline surrounding are open for correlations and in the series (3.18) we substitute it by the translation-equivalent increment $\Delta\mathrm{IP}^{\mathrm{corr}}_{\mathrm{pi1,pi1}}(\mathrm{pi},-1)$. This way we reduce the influence of the edge of the cluster on the correlation corrections to the local matrix elements defined for the periodic infinite systems.

The fifth feature becomes important when one uses a correlation method which suffers from size-consistency problems. This is particularly the case when truncated CI methods are used. When the second- and third-order increments are calculated, correlation corrections obtained with different numbers of open bonds are subtracted from each other. The difference itself may easily be of the order of the size-consistency error (better to say size-extensivity error) for each term entering this difference. Then, by the incremental scheme, we would sum up these errors which would accumulate and finally lead to wrong results. Therefore, one needs an accurate correction to minimize the size-extensivity error when the MRCI(SD) method is used for the evaluation of the increments. Such a correction is the topic of the next section.

3.5 Size-extensivity correction

The occurrence of a size-extensivity error in truncated CI calculations can easily be understood from the example of two H_2 molecules at large distance from each other. Each molecule has one bond (an orbital obtained in the Hartree–Fock approximation) occupied by two electrons. Let us evaluate the correlation correction $\delta E_0^{\rm corr}(2H_2)$ to the HF ground-state energy $E_0(2H_2)$ of this system by the single and double configuration interaction method (for shortness we will call here this correction as *correlation energy*). We can do this in two ways. Firstly, we can calculate the correlation energies for each H_2 molecule separately, $\delta E_0^{\rm corr}(H_2)$, and add them. This approximation gives exact result since on big distances between the H_2 molecules excited configurations with electrons being destroyed in the bond of one molecule and created in some virtual orbital of the second H_2 molecule give no contribution to the correlation energy (dissociation limit). Alternatively, we can directly calculate the correlation energy of the whole system of two H_2 molecules. Due to the truncation of the CI expansion (2.52) we have more configurations in the first case than in the second one: for instance, double excitations on both molecules simultaneously are neglected in the second case while they are taken into account in the first case. Therefore, the correlation energy obtained in the whole system $\delta E_0^{\rm corr}(2H_2)$ is higher than the sum of the two correlation energies of the separate H_2 molecule $2\delta E_0^{\rm corr}(H_2)$. The error in the CI(SD) correlation energy of the system consisting of n H_2 molecules increases with increasing n (see the third column in Table 3.6). Thus, when one investigates correlation energy of systems with different number of bonds open for the correlation one has to correct for the size-extensivity error.

Explicitly this situation arises when one uses the incremental scheme to evaluate correlation energies. There, correlation energies of the system with different numbers of correlated bonds are subtracted from each other. Therefore, all the energy values defining a particular increment must be consistent.

The general strategy to obtain size-extensive correlation energy is to estimate the value $n \times \delta E_0^{\rm corr}(H_2)$ by means of information on the wavefunction and the correlation energy $\delta E_0^{\rm corr}(nH_2)$ of the whole system. There exist two well-known size-extensivity corrections to the correlation energy of the ground state calculated by the CI method which are widely used in quantum chemistry.

The first is the Davidson correction [LD74] which is the simplest estimate of the size-extensivity error in CI(SD) calculations:

$$\Delta E_{\rm D}^{\rm SE} = \delta E_0^{\rm corr}(1 - \alpha_0^2). \tag{3.38}$$

Here α_0 is the coefficient of the SCF ground-state configuration Φ in (2.68) when the correlated wavefunction $\Phi^{\rm corr}$ is *normalized*. The Davidson correction does not depend explicitly on the number of correlated bonds. It gives a rather accurate estimate of correlation energy for n ranging from 4 to 10 (the residual error is within 1% as pointed out in [SO96], p.268) however the error is larger for $n = 2$ or 3 (see Table 3.6) and it diverges for large numbers of open bonds. Since in our incremental calculations we have dozens of increments the error may accumulate up to 100% of the correlation energy. Thus, for our purposes we need a more accurate size-extensivity correction.

The Pople correction [PSK77] estimates the size-extensivity error much better than the Davidson correction (see Table 3.6) giving perfect size-extensive correlation energy in the case of any number of equivalent non-interacting two-level systems:

$$\Delta E_{\rm P}^{\rm SE} = \delta E_0^{\rm corr}\left(\frac{\sqrt{n^2 + n\tan^2 2\theta} - n}{\sec 2\theta - 1} - 1\right) \tag{3.39}$$

where $\theta = \arccos \alpha_0$.

We have investigated the reduction of the size-extensivity error of the CI(SD) method in evaluating the correlation correction to the ground-state energy when the two error corrections are used. As a test system we have chosen four H_2 molecules in the arrangement shown in Fig. 3.15. In the dissociation limit the distance between

Figure 3.15: Four H_2 molecules at large distances. The contour plot of the bonding HF orbital of one H_2 molecule is shown.

Table 3.6: Comparison of the size-extensivity errors of the CI(SD) method with and without error corrections. The correct size-extensive correlation energy for different numbers n of correlated H_2 molecules is presented in the second column (in eV). The correlation energy of three different methods (pure CI(SD), CI(SD) with Davidson correction and CI(SD) with Pople correction) are presented in the three next columns as deviation from the correct correlation energy.

n	$n\,\delta E_0^{\mathrm{corr}}(\mathrm{H_2})$	$\delta E_0^{\mathrm{corr}}(n\mathrm{H_2})$	$\delta E_0^{\mathrm{corr}}(n\mathrm{H_2}) + \Delta E_{\mathrm{D}}^{\mathrm{SE}}$	$\delta E_0^{\mathrm{corr}}(n\mathrm{H_2}) + \Delta E_{\mathrm{P}}^{\mathrm{SE}}$
2	-2.063	1.721%	-1.706%	0.008%
3	-3.094	3.318%	-1.533%	0.031%
4	-4.126	4.806%	-1.318%	0.064%

nearest-neighbor molecules (20 Å) is much larger than the distance between the two H atoms in a molecule (the characteristic bond length in H_2 molecule is 0.7414 Å which is taken from Ref. [HW76], p. 52). The basis set for hydrogen used here is the same as in Table 3.1. The correlation energy of the system with n correlated H_2 molecules ($n = 2$, 3 and 4) obtained by the CI(SD) method is compared in Table 3.6 to the size-extensive one which is equal to n times the correlation energy of a single H_2 molecule.

The Pople correction reduces the size-extensivity error in average by two order of magnitudes as compared to pure CI(SD) or Davidson corrected CI(SD) which both yield error of more than 1% (see Table 3.6). Thus, we use the Pople correction to CI(SD) correlation energies to get size-extensive results for the neutral closed-

shell systems. (More detailed study of the performance of these two corrections for different systems can be found in e.g. Ref. [PSK77], [LBT87], [GA88] and [DD94]). Unfortunately, being applied to the correlation energies of open-shell systems (as the $(N-1)$- and $(N+1)$-particle systems we need to consider) the two size-extensivity corrections do not yield satisfactorily accurate results (see Table 3.7) to be used in the method of local increments. Therefore, we need a size-extensivity error correction which gives accurate estimates of the correlation energy in the case of open-shell systems (systems with a hole or with captured electron) like the Pople correction does for closed-shell systems.

Let us consider again the system consisting of n equivalent H_2 molecules at large distances and let us consider a $(2\,n-1)$-electron state with one electron annihilated at some molecule a. We can get the correlation energy of this state on the MRCI(SD) level but we would like to approach the correct size-extensive correlation energy

$$\delta E_a^{\mathrm{SE}} = (n-1)\;\delta E_0^{\mathrm{corr}}(\mathrm{H_2}) + \delta E_a^{\mathrm{corr}}(\mathrm{H_2^+}) \tag{3.40}$$

having information on the correlation energy and the wavefunction from the MRCI(SD) calculation of the whole system. In Eq. (3.40) $\delta E_0^{\mathrm{corr}}(\mathrm{H_2})$ denote the correlation energy of a neutral H_2 molecule and $\delta E_a^{\mathrm{corr}}(\mathrm{H_2^+})$ the one of the molecule carrying the hole. The latter is in fact just the orbital relaxation energy.

Like in the derivation of the Pople correction [PSK77] we switch to a minimal basis description such that the H_2 molecule becomes a two-level system. The spin-adapted reference configurations for the MRCI ansatz for our system consists of all hole configurations $\{\Phi_a\}_{a=1,\ldots,n}$ with $a = 1,\ldots,n$ being the occupied spin-down orbitals on the different H_2 molecules. In the dissociation limit the only 2-hole 1-particle configurations $\Phi_{bc}^{\ r}$ which couple to a given model configuration Φ_a, i.e. for which the CI matrix element $\langle\Phi_a|H|\Phi_{bc}^{\ r}\rangle$ is non-zero, are the "vertical" single excitations $\Phi_{ab}^{\ b^*}$ where b^* labels the unoccupied counter part of the spin orbital φ_b. Because of Brillouin's theorem $\langle\Phi_a|H|\Phi_{ab}^{\ b^*}\rangle$ vanishes if the spin orbital φ_b is located on a different molecule than a. Hence, only the configuration $\Phi_{aa}^{\ a^*}$ couples to Φ_a.

Similarly, the only 3-hole 2-particle configurations $\Phi_{b\,cd}^{\,rs}$ which couple to a given model configuration Φ_a are the "vertical" double excitations $\Phi_{a\,b\bar{b}}^{\,b^*\bar{b}^*}$ on sites different than the one of the spin orbital φ_a. Furthermore, the configuration space $\{\Phi_a\}_{a=1,\ldots,n} \oplus \{\Phi_{a\,a\bar{a}}^{\,\bar{a}^*}\}_{a=1,\ldots,n} \oplus \{\Phi_{a\,b\bar{b}}^{\,b^*\bar{b}^*}\}_{a\neq b=1,\ldots,n}$ is closed in the sense that *no* other 2-hole 1-particle or 3-hole 2-particle configuration couple to any of the configurations in that space. Hence, (in the dissociation limit) we can write the MRCI wavefunction of our system as

$$\Psi_i^{\mathrm{corr}} = \sum_{a=1}^{n} \alpha_a(i)\Phi_a + \sum_{a=1}^{n} \alpha_{a\,a\bar{a}}^{\,\bar{a}^*}(i)\Phi_{a\,a\bar{a}}^{\,\bar{a}^*}(i) + \sum_{a\neq b=1}^{n} \alpha_{a\,b\bar{b}}^{\,b^*\bar{b}^*}(i)\Phi_{a\,b\bar{b}}^{\,b^*\bar{b}^*}(i). \tag{3.41}$$

For the sake of simplicity let us denote Φ_a by Φ_a^0, $\Phi_{a\,a\bar{a}}^{\,\bar{a}^*}$ by Φ_a^1, $\Phi_{a\,b\bar{b}}^{\,b^*\bar{b}^*}$ by $\Phi_a^2, \ldots$. Then, the CI matrix elements for the MRCI ansatz (3.41) can be written as

$$C_{ab}^{xy} = \langle \Phi_a^x | H | \Phi_b^y \rangle. \tag{3.42}$$

In the dissociation limit the CI matrix becomes block-diagonal, i.e.

$$C_{ab}^{xy} = \delta_{ab} C_{aa}^{xy}$$

with all subblocks $\{C_{aa}^{xy}\}_{x,y=0,\ldots,n}$ being of the form

$$\begin{pmatrix} E_{1h} & \beta & \gamma & \cdots & \gamma \\ \beta & E_{2h} & 0 & \cdots & 0 \\ \gamma & 0 & E_{3h} & \cdots & 0 \\ \vdots & \vdots & \vdots & \ddots & \vdots \\ \gamma & 0 & 0 & \cdots & E_{3h} \end{pmatrix}. \tag{3.43}$$

The entries E_{1h}, E_{2h}, E_{3h}, β and γ do not depend on the position of the hole in the H_2 chain which implies that our $(2n-1)$-electron system of nH_2 molecule has n degenerate lowest hole states each of them residing on one of the H_2 molecules. Delocalization of the hole over the chain does not lead to a gain in energy.

The matrix elements $\gamma = \langle \Phi_a | H | \Phi_{a\, b\bar{b}}^{\;\; b^*\bar{b}^*} \rangle = \langle \varphi_b \bar{\varphi}_b | v_{12} | \varphi_b^* \bar{\varphi}_b^* \rangle$ are identical for all $b \neq a$ since all the neutral H_2 molecules are equivalent (in the dissociation limit). For that reason the CI coefficients $\alpha_{a\, b\bar{b}}^{\;\; b^*\bar{b}^*}(i)$ must all be equal, and the wavefunction for a hole state on the a-th H_2 molecule (with energy $E_a^{\rm corr}$) can be written as

$$\Psi_a^{\rm corr} = \Phi_a + c_1 \Phi_a^1 + c_2 \sum_{x=2}^{n} \Phi_b^x. \tag{3.44}$$

As a consequence the secular equation to determine the coefficients c_1 and c_2 reduces to

$$\begin{pmatrix} 0 & \beta & (n-1)\gamma \\ \beta & 2\Delta_1 & 0 \\ \gamma & 0 & 2\Delta_2 \end{pmatrix} \begin{pmatrix} 1 \\ c_1 \\ c_2 \end{pmatrix} = \delta E_a^{\rm corr} \begin{pmatrix} 1 \\ c_1 \\ c_2 \end{pmatrix} \tag{3.45}$$

where $\delta E_a^{\rm corr} = E_a^{\rm corr} - E_a$ is the correlation energy, and $2\Delta_1 = E_{2h} - E_a$ and $2\Delta_2 = E_{3h} - E_a$ are the energies of the 2-hole 1-particle and the 3-hole 2-particle configurations $\Phi_{a\bar{a}}^{\;\; \bar{a}^*}$ and $\Phi_{a\, b\bar{b}}^{\;\; b^*\bar{b}^*}$, respectively, relative to the Hartree–Fock energy $E_{1h} \equiv E_a$ of the model configuration Φ_a. From the first row one concludes that the correlation energy consists of two parts: $\delta E_a^{\rm corr} = c_1\beta + (n-1)c_2\gamma = E_s + E_d$ where the part E_s (E_d) is associated with singly (doubly) excited configurations only. The quantities E_s and E_d (and also $c_s \equiv c_1$ and $c_d \equiv \sqrt{n-1}\, c_2$) can be obtained from the output of an MRCI(SD) calculation with the MOLPRO program packadge [M2000], [WK88], [KW88], [KW92] and our aim is to express the size-extensive correlation energy in terms of these parameters.

As can be seen from Eq. (3.40) the size-extensive correlation energy of the considered system is equal to the correlation energy the of charged H_2^+ molecule plus $(n-1)$ times the correlation energy of a separated neutral H_2 molecule. To find the required energies $\delta E_a^{\rm corr}(H_2^+)$ and $\delta E_0^{\rm corr}(H_2)$ of the two isolated molecules (charged and neutral) we note, that one gets the following CI matrices when the isolated

molecules are treated analogously to the whole system:

$$\begin{pmatrix} 0 & \beta \\ \beta & 2\Delta_1 \end{pmatrix} \begin{pmatrix} 1 \\ c_1' \end{pmatrix} = \delta E_a^{\mathrm{corr}}(\mathrm{H}_2^+) \begin{pmatrix} 1 \\ c_1' \end{pmatrix} \tag{3.46}$$

and

$$\begin{pmatrix} 0 & \gamma \\ \gamma & 2\Delta_2 \end{pmatrix} \begin{pmatrix} 1 \\ c_2' \end{pmatrix} = \delta E_0^{\mathrm{corr}}(\mathrm{H}_2) \begin{pmatrix} 1 \\ c_2' \end{pmatrix} \tag{3.47}$$

with the entries β, Δ_1, γ and Δ_2 being the *same* as in Eq. (3.45). From these two equations the correlation energies of the charged and neutral H_2 molecules can easily be derived yielding:

$$\delta E_a^{\mathrm{corr}}(\mathrm{H}_2^+) = \Delta_1 - \sqrt{\Delta_1^2 + \beta^2} \tag{3.48}$$

and

$$\delta E_0^{\mathrm{corr}}(\mathrm{H}_2) = \Delta_2 - \sqrt{\Delta_2^2 + \gamma^2}. \tag{3.49}$$

Substitution of (3.48) and (3.49) into Eq. (3.40) gives the size-extensive correlation energy of the lowest n hole states in our system of n H_2 molecules in terms of the parameters entering the secular equation (3.45):

$$\delta E_a^{\mathrm{SE}} = \Delta_1 - \sqrt{\Delta_1^2 + \beta^2} + (n-1)\left(\Delta_2 - \sqrt{\Delta_2^2 + \gamma^2}\right). \tag{3.50}$$

With the help of Eq. (3.45) the parameters β, γ, Δ_1 and Δ_2 can be linked to the output quantities $\delta E_a^{\mathrm{corr}}$, E_s, E_d, c_s and c_d which are available from the MRCI(SD) calculations for the $n \times H_2$ molecules as a whole:

$$\begin{aligned} \beta &= E_s/c_s\,, & 2\Delta_1 &= \delta E_a^{\mathrm{corr}} - E_s/c_s^2 \\ \gamma &= E_d/\sqrt{n-1}\,c_s\,, & 2\Delta_2 &= \delta E_a^{\mathrm{corr}} - E_d/c_d^2\,. \end{aligned} \tag{3.51}$$

Then, the final formula for the size-extensive energy of the hole state reads

$$\delta E_a^{\rm SE} = \frac{1}{2}\Bigg[n\,\delta E_a^{\rm corr} - \frac{E_s}{c_s^2} - (n-1)\frac{E_d}{c_d^2} - \sqrt{\left(\delta E_a^{\rm corr} - \frac{E_s}{c_s^2}\right)^2 + 4\frac{E_s^2}{c_s^2}} - (n-1)\sqrt{\left(\delta E_a^{\rm corr} - \frac{E_d}{c_d^2}\right)^2 + 4\frac{E_d^2}{(n-1)c_d^2}}\ \Bigg]. \tag{3.52}$$

This correlation energy effectively takes into account the missing configurations in the truncated CI expansion of the wavefunction of an open-shell system as a function of the number of bonds open for correlation. For a system more complicated than a chain of isolated two-level systems the quantities E_s (E_d) and c_s (c_d) are associated with the contribution from all single (double) excitations to the correlation energy $E_i^{\rm corr}$ and the squared norm of the (normalized) wavefunction $\Psi_i^{\rm corr}$, respectively, as is also done usually for the Davidson and Pople corrections to the MRCI correlation energies in quantum chemistry.

To test this new size-extensivity correction for the MRCI(SD) method we perform correlation calculations for the hole states in our $4\times H_2$ system. The correlation energies of this system size-corrected by different methods (Davidson and Pople correction as realized in MOLPRO [M2000], [WK88], [KW88], [KW92] and $\delta E_a^{\rm SE}$ from Eq. (3.52)) are compared to the correct size-extensive correlation energy computed for a separate charged H_2^+ molecule and $(n-1)$ neutral H_2 molecules (denoted as $\delta E_a^{\rm exact}$ for shortness). They are presented in Table 3.7 for different number of open bonds (n = 2, 3 and 4). The distance between nearest-neighbor H_2 molecules in these calculations is set to 50 Å to reach the dissociation limit in our charged system.

From Table 3.7 one concludes that the new size-extensivity correction for open-shell systems proposed in this section gives results which are by several orders of magnitude more accurate than the convensional corrections to the MRCI(SD) method. The accuracy obtained with our size-extensivity correction is the same as that of the Pople correction to correlation energy of a neutral closed-shell system. The use of these two corrections in all our calculations for individual increments (the first one for open-shell and the second for closed-shell calculations) finally allowed us to re-

Table 3.7: Comparison of the size-extensivity errors of the CI(SD) method with and without error correction (three different methods) for a hole states. The correct size-extensive correlation energy for different numbers n of correlated H_2 molecules is presented in the second column (in eV). The relative deviation of the correlation energy of four different methods (the same as in Table 3.6 plus our own correction $\delta E_a^{\rm SE}$) are presented in the four next columns.

n	$\delta E_a^{\rm exact}$	$\delta E_a^{\rm corr}(n{\rm H}_2)$	$\delta E_a^{\rm corr}(n{\rm H}_2) + \Delta E_{\rm D}^{\rm SE}$	$\delta E_a^{\rm corr}(n{\rm H}_2) + \Delta E_{\rm P}^{\rm SE}$	$\delta E_a^{\rm SE}$
2	-1.857	2.342%	-2.176%	2.342%	0.002%
3	-2.888	4.050%	-1.749%	1.153%	0.017%
4	-3.919	5.553%	-1.400%	0.807%	0.045%

duce the estimated error for the correlation corrections to the local matrix elements (the target quantities of our approach) down to a few percents of their values.

3.6 Satellite states problem

In the last section of this chapter we would like to draw our attantion to the problem of satellite states which may ruin the convergence of the MRCI calculations. This problem appears when one (or more) of model configurations Φ_i which define the effective Hamiltonian $H_{ij}^{\rm eff}$ for some particular increment has an energy higher than the energy E_{jk}^r of a single excitation Φ_{jk}^r of another model configuration Φ_j. This situation may happen in systems with relatively broad bands and a narrow band gap. For instance, in the case of *trans*-polyacetylene the HF energies of hole states range from approximately -31 to -6 eV and the band gap is 6.42 eV. The position and dispersion of the lowest valence band of tPA (see Fig. 3.5) is mainly defined by states with a hole in the carbon sceleton. In a C_6H_8 molecule the lowest localized valence orbital is a short C–C σ bond and the energy of taking out an electron from this bond is 22.3 eV. The position and the dispersion of the highest valence band

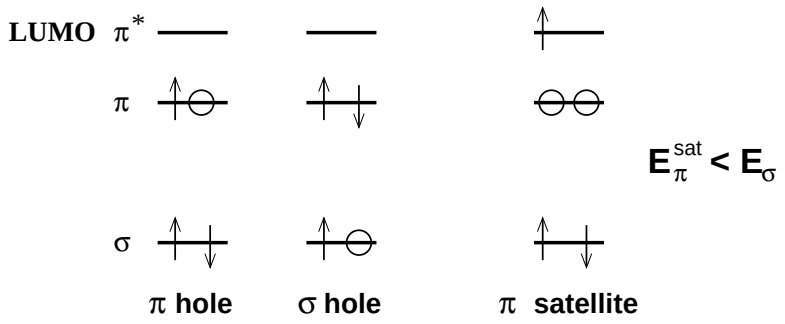

Figure 3.16: Three possible configurations for an $(N-1)$-electron states of tPA: single hole in iether a π or a σ bonds and a satellite state of π symmetry.

(a π band) in turn is determined by states with a hole in the π system of tPA. In the C_6H_8 molecule the highest localized valence orbital is a π bond with an orbital energy of 10.4 eV. The energy of a state with two electrons destroyed in that π bond and one electron created in the lowest unoccupied molecular orbitals (LUMO) is found to be 19.8 eV in a C_6H_8 molecule, and is lower than the energy of the σ hole. A schematic sketch of this three configurations is shown in Fig. 3.16.

If in such a case we would perform MRCI(SD) calculations to determine the correlation contributions to a matrix element $\mathrm{IP}_{\sigma\sigma}(\pi)$, say, we would construct the model space of two one-particle configurations Φ_π and Φ_σ and calculate the two lowest correlated $(N-1)$-electron states with wavefunctions defined by Eq. (2.76). During the CI iteration a decrease of the CI coefficient $\alpha_\sigma(2)$ for the model configuration Φ_σ and an increase of the CI coefficient $\alpha_{\pi\bar{\pi}^*}(2)$ for the satellite configuration $\Phi_{\pi\bar{\pi}^*}$ (which is present in the CI expansion (2.76)) would lead to a gain in energy and after few iterations we would arrive at a state which is dominated by the satellite configuration $\Phi_{\pi\bar{\pi}^*}$ instead of the model configuration Φ_σ. The obtained correlated wavefunction does not obey the requirement of the MRCI approximation that reference configurations (the model configurations here) must be dominant in the CI expansion of the wavefunctions. At this point the program stops the iteration with an error message and no data for the two correlated states are obtained. To proceed in this situation we include the satellite configuration in the reference space

Table 3.8: Correlation data for two hole and one satellite state in a C_6H_8 molecule. Correlation energies are given with respect to the HF ground-state energy of the molecule.

state	$\|\Psi_i\|^2$ projected	E_i^{corr} (eV)
π hole	0.96	8.63
π satellite	0.00	16.15
σ hole	0.86	18.54

and calculate the first *three* correlated states. Two hole and one satellite state will emerge from this calculation.

The hole states can easily be separated from the satellite state by checking the square of the norms $(\alpha_a(i))^2$ of their projection onto the subspace spanned by the one-particle model configurations. In all our calculations where satellite states show up the squares of the norms of the projected σ hole states are higher than 0.70 such that the distinction between satellite states and single hole states is clear. Thus, the requirement that we have to find those wavefunctions Ψ_i^{corr} which are dominated by model configurations is fulfilled.

In Table 3.8 we present the correlation data corresponding to the case described above. In the second column the squares of the norm of the correlated wavefunctions projected onto the subspace spanned by model configurations Φ_π and Φ_σ are shown. The wavefunction of the satellite state has essentially zero projection and is clearly more stable than the deep-lying σ hole state.

In the present case, the inclusion of singly excited configurations into the reference space helps to solve the problem of competing states in MRCI calculations and allows us to get the desired target matrix elements of the effective Hamiltonian. However, this approach has limitations. When many one-particle configurations with relatively large energy dispersion are included in the model space or bigger clusters are considered (which implies more low-lying unoccupied orbitals) there

may be a lot of satellite states competing energetically with the one-particle states. Therefore, many states have to be optimized simultaneously in the MRCI iterations and such calculations may become quite expensive (or even unfeasible). To proceed in this case one needs an improved version of the MRCI program which could sort out the relevant states at each step of the iteration (again by the norm of the projection) and converge only states with a dominant contribution of one-particle configurations in the CI wavefunctions. Such a treatment would completely solve the problem of satellite states in the MRCI method as long as the satellites do not strongly mix with the single hole states.

Chapter 4

Results for *trans*–polyacetylene

In this chapter we present and discuss the numerical results for *trans*–polyacetylene. In section 4.1 the individual increments obtained in clusters are given and the convergence and accuracy of the incremental scheme is explored. The correlation corrections to the local matrix elements are obtained and the change of the LMEs due to electron correlation is discussed. In the next section we present the *correlated* band structure of *trans*–polyacetylene and compare it to that on the HF level. In section 4.3 we estimate the error for the individual local matrix elements, the band gap and the band widths. In section 4.4 we discuss how results obtained for the one-dimensional system can be compared to experimental data on bulk *trans*–polyacetylene.

4.1 From single increments to final local matrix elements

We start the discussion of the numerical results with the correlation corrections to the local matrix elements associated with a hole in σ bonds. In this case, the convergence of the correlation effect with the distance from the localized hole is most rapid as σ bonds are the most compact localized orbitals. Therefore, we only

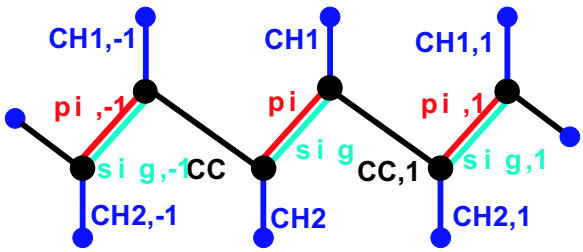

Figure 4.1: C_6H_8 cluster of tPA with bond labels.

need a relatively small C_6H_8 cluster to account for the correlation effects.

First, we would like to discuss the effect of truncating the incremental scheme after the third order. For this purpose we perform a correlation calculation for nine hole states when the most inner nine bonds of C_6H_8 are open simultaneously ("CH1,-1", "CC", "CH2", "sig", "CH1", "CC,1", "CH2,1", "sig,1" and "CH1,1"). The names of the bonds are indicated in Fig. 4.1. We do not include π bonds here to avoid the appearance of satellite states. From this calculation we get the correlation corrections to the local matrix elements which are associated with these nine bonds (e.g. one diagonal element $\delta' \mathrm{IP}^{\mathrm{corr}}_{\mathrm{CH1,CH1}} = -1.077$ eV and one off-diagonal element $\delta' \mathrm{IP}^{\mathrm{corr}}_{\mathrm{CH1,CC,1}} = -0.407$ eV).

We can get the same corrections by the method of local increments. The corresponding data on the individual increments are presented in Tables 4.1 and 4.2 where increments of different orders are placed in different columns. Numbers at the bottom of these tables are the sums over all increments $\Delta \mathrm{IP}^{(n)}_{ab}$ of the given order n. These numbers demonstrate the convergence of the incremental scheme with the order of increments: the third term in Eq. (3.18) drops with respect to the second one by more than an order of magnitude that insures the possibility to truncate the series (3.18) after the third term. Actually, non of the third-order increments of the *off-diagonal* metrix elements is larger than 5 meV, so that these contributions might be neglected as well. Summing up the increments of 1st, 2nd and 3rd order one gets the correlation correction estimated by the incremental scheme: $\delta'' \mathrm{IP}^{\mathrm{corr}}_{\mathrm{CH1,CH1}} = -1.149$ eV and $\delta'' \mathrm{IP}^{\mathrm{corr}}_{\mathrm{CH1,CC,1}} = -0.389$ eV. The differences between

Table 4.1: Increments for the correlation correction to the diagonal matrix element $IP_{CH1,CH1}$ of a C_6H_8 molecule (in eV) when only the σ bonds are open for correlation. The reference value $\delta' IP^{corr}_{CH1,CH1}$ where the electrons from all nine σ bonds are correlated is given as well.

$\Delta IP^{corr}_{CH1,CH1}()$	$\Delta IP^{corr}_{CH1,CH1}(c)$		$\Delta IP^{corr}_{CH1,CH1}(c,d)$		
	c	ΔIP	c	d	ΔIP
0.188	sig	-0.336	sig	CC,1	0.013
	CC,1	-0.393	CH2	sig	-0.064
	CH1,-1	-0.069	CC	sig	-0.012
	CH1,1	-0.073	CH1,-l	sig	-0.000
	CH2	-0.123	CC,1	CH2,1	-0.070
	CH2,1	-0.114	CC,1	sig,1	-0.015
	CC	-0.092	CC,1	CH1,1	0.003
	sig,1	-0.080	CH2	CC,1	0.013
			CC	CC,1	0.008
			CH1,-1	CC,1	0.009
			CH1,-1	CC	0.003
			CH1,-1	CH2	0.003
			CH1,-1	CH2,1	0.006
			CH1,-1	sig,1	0.003
			CH1,-1	CH1,1	0.005
			CC	CH2	-0.017
			CC	CH2,1	0.007
			CC	sig,1	0.003
			CC	CH1,1	0.005
			CH2	CH2,1	0.011
			CH2	sig,1	0.006
			CH2	CH1,1	0.006
			sig	sig,1	0.005
			sig	CH2,1	0.008
			sig	CH1,1	0.006
			CH2,1	sig,1	-0.010
			CH2,1	CH1,1	0.002
			sig,1	CH1,1	0.007
0.188		**-1.280**			**-0.057**
$\sum_{i=1}^{3} \Delta IP^{(i)}_{CH1,CH1}$					**-1.149**
$\delta' IP^{corr}_{CH1,CH1}$					**-1.077**

Table 4.2: Increments for the correlation correction to the off-diagonal matrix element $\mathrm{IP}_{\mathrm{CH1,CC,1}}$ of a C_6H_8 molecule (in eV) when only the σ bonds are open for correlation. The reference value $\delta'\mathrm{IP}^{\mathrm{corr}}_{\mathrm{CH1,CC,1}}$ where the electrons from all nine σ bonds are correlated is given as well.

$\Delta\mathrm{IP}^{\mathrm{corr}}_{\mathrm{CH1,CC,1}}()$	$\Delta\mathrm{IP}^{\mathrm{corr}}_{\mathrm{CH1,CC,1}}(c)$		$\Delta\mathrm{IP}^{\mathrm{corr}}_{\mathrm{CH1,CC,1}}(c,d)$		
	c	ΔIP	c	d	ΔIP
-0.213	sig	-0.118	sig	CH1,-1	0.001
	CH2,1	-0.029	sig	CC	0.004
	sig,1	-0.024	sig	CH2	0.004
	CH1,1	-0.014	sig	CH2,1	-0.001
	CH2	-0.002	sig	sig,1	0.001
	CH1,-1	0.001	sig	CH1,1	0.004
	CC	0.000	CH1,-1	CC	-0.002
			CH1,-1	CH2	0.000
			CH1,-1	CH2,1	0.000
			CH1,-1	sig,1	0.003
			CH1,-1	CH1,1	0.001
			CC	CH2	0.000
			CC	CH2,1	0.003
			CC	sig,1	0.001
			CC	CH1,1	0.001
			CH2	CH2,1	0.002
			CH2	sig,1	0.002
			CH2	CH1,1	0.000
			CH2,1	sig,1	-0.004
			CH2,1	CH1,1	-0.003
			sig,1	CH1,1	-0.005
-0.213		**-0.186**			**0.010**
$\sum_{i=1}^{3}\Delta\mathrm{IP}^{(i)}_{\mathrm{CH1,CC,1}}$					**-0.389**
$\delta'\mathrm{IP}^{\mathrm{corr}}_{\mathrm{CH1,CC,1}}$					**-0.407**

Table 4.3: Convergence of the second-order increments of the matrix elements $IP_{CC,CC}$ and $IP_{CC,sig}$ with the distance to the added σ bond (in eV).

c	$\Delta IP^{corr}_{CC,CC}(c)$	c	$\Delta IP^{corr}_{CC,sig}(c)$
CH2	-0.576	CH2	-0.129
sig	-0.380	CH1	-0.064
CH1	-0.132	CC,1	-0.031
CH2,1	-0.025	CH2,1	-0.007
sig,1	-0.022	sig,1	-0.003

the exact and the estimated values of correlation corrections are -72 meV (or 6.3%) and -18 meV (or 4.6%) for the diagonal and off-diagonal matrix elements, respectively. Thus, we can argue that the incremental scheme estimates the correlation corrections with an error of a few percent.

From Tables 4.1 and 4.2 one also nicely sees the convergence of the second-order increments with the distance to the added σ bond c. To study this decay of correlation effect with the distance from the localized extra charge more extensively we provide the second-order increments of the matrix elements $IP_{CC,CC}$ (diagonal) and $IP_{CC,sig}$ (off-diagonal) in Table 4.3 ordered by the distance of the added bond from the reference bonds. The largest value occur for the added bond adjacent to the one of reference bonds (or even to both in the case of off-diagonal matrix elements). Values of increments drop by more than an order of magnitude when the added bond is moved outwards by one unit cell. The contribution to the correlation correction coming from farther bonds is negligibly small and will not be treated explicitly by our correlation calculations. Rather the infinite-size extrapolation of the correlation correction obtained in a cluster can be estimated in a continuum approximation (see section 4.3). The data presented in Table 4.3 justifies the use of the C_6H_8 molecule as the smallest cluster of *trans*-polyacetylene to calculate the correlation corrections to all local matrix elements corresponding to σ hole states.

Table 4.4: Correlation corrections to local matrix elements corresponding to σ bonds (in eV). The last column gives the total sum of the incremental contributions.

matrix element	$\Delta\mathrm{IP}^{\mathrm{corr}}_{\mathrm{a,b}}()$	$\sum_c \Delta\mathrm{IP}^{\mathrm{corr}}_{\mathrm{a,b}}(c)$	$\sum_{c<d} \Delta\mathrm{IP}^{\mathrm{corr}}_{\mathrm{a,b}}(c,d)$	$\delta\mathrm{IP}^{\mathrm{corr}}_{\mathrm{a,b}}$
$\mathrm{IP}_{\mathrm{CH1,CH1}}$	0.188	-3.274	0.468	**-2.804**
$\mathrm{IP}_{\mathrm{CC,CC}}$	0.166	-5.422	1.554	**-3.702**
$\mathrm{IP}_{\mathrm{sig,sig}}$	0.064	-3.834	-0.098	**-3.867**
$\mathrm{IP}_{\mathrm{CH1,CC,1}}$	-0.213	-0.514	0.011	**-0.718**
$\mathrm{IP}_{\mathrm{CH1,sig}}$	-0.210	-0.816	-0.014	**-1.040**
$\mathrm{IP}_{\mathrm{CC,sig}}$	-0.165	-0.756	-0.014	**-0.936**

Of course, the π orbitals also contribute to the correlation corrections of the local matrix elements of σ-type. Together with the pure σ- and mixed π-σ-type contributions they sum up to the total correlation corrections summarized in Table 4.4 where the results for all diagonal and first-nearest-neighbor off-diagonal matrix elements are given. They are obtained by the incremental scheme when electrons from *all* bonds of the C_6H_8 molecule are correlated: the σ bonds discussed above but also the π bonds. Only the bonds with saturating hydrogen atoms are excluded. To show the convergence of the incremental scheme we provide the data for each increment order of the series (3.18) in different columns of this table. As a rule, the major contributions are coming from the second-order increments $\Delta\mathrm{IP}^{\mathrm{corr}}_{ab}(c)$. The third-order increments $\Delta\mathrm{IP}^{\mathrm{corr}}_{ab}(c,d)$ are usually more than an order of magnitude smaller than the second-order ones, and even in the worst case ($\mathrm{IP}_{\mathrm{CC,CC}}$) they are by a factor of 4 smaller.

The same cluster is used to estimate the contribution from the σ bonds to the correlation correction of the diagonal matrix element $\mathrm{IP}^{\mathrm{corr}}_{\mathrm{pi,pi}}$. However, one needs C_8H_{10} molecule to get useful values for the correlation correction to the *off-diagonal* matrix element $\mathrm{IP}^{\mathrm{corr}}_{\mathrm{pi,pi,1}}$ as the two π bonds of *trans*-polyacetylene are spread over four unit cells. In this case the adjacent σ bonds were grouped in pairs as indicated

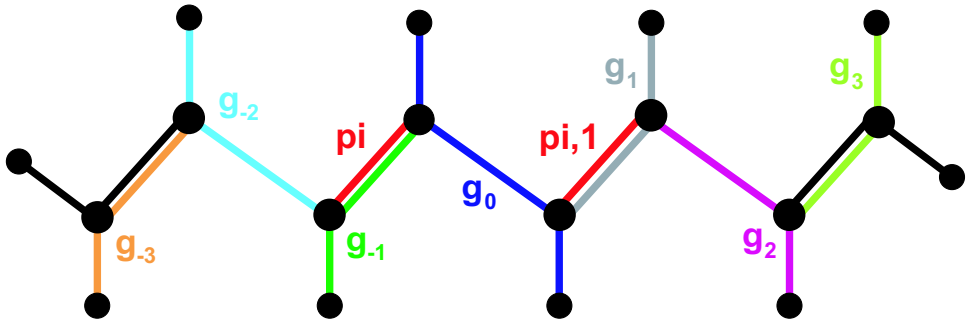

Figure 4.2: Grouping of σ bonds in the C_8H_{10} cluster of tPA for the calculation of the correlation correction of $IP_{pi,pi,1}$ matrix element.

in Fig. 4.2.

Nevertheless even this cluster turned out to be not big enough for the evaluation of the contributions from the π bonds of tPA to $\delta IP^{corr}_{pi,pi}$ and $\delta IP^{corr}_{pi,pi,1}$. The localized π orbitals are more diffuse than the σ ones (see Fig. 3.7) and therefore the correlation effects decay noticeably slowler with the distance from the π hole. Hence, the calculation of the increments with added π bonds is performed in a $C_{10}H_{12}$ cluster which contains five bonds of π symmetry (see Fig 3.8).

We are going to show again the accuracy of the incremental scheme in the case of π bonds by first calculating the correlation corrections to the matrix elements $IP^{corr}_{pi,pi}$ and $IP^{corr}_{pi,pi,1}$ when all five π bonds of $C_{10}H_{12}$ are correlated simultaneously ($\delta' IP^{corr}_{pi,pi} = -1.145$ eV and $\delta' IP^{corr}_{pi,pi,1} = -0.573$ eV) and comparing them to the values obtained by the incremental scheme. The data on the increments are presented in Tables 4.5 and 4.6. The convergence of the incremental scheme with the order is clearly discernable. Yet, there are also some third-order contributions which are still in the order of the second-order terms ($\sim$0.3 eV). Those are *not* increments $\Delta IP_{pi,pi}(c,d)$ with the orbitals c and d being arranged symmetrically around the reference π bond (as one would intuitively expect) but a linear configuration of the three bonds with the two added bonds c and d on the *same* side, i.e. $\Delta IP_{pi,pi}(pi,1;pi,2)$. Summing up the individual contributions in each table one gets the total correlation corrections for the five π-bonds as estimated by the incre-

Table 4.5: Increments for the correlation correction to the diagonal matrix element $IP_{pi,pi}$ of a $C_{10}H_{12}$ molecule (in eV) when only the π bonds are open for correlation. The reference value $\delta' IP^{corr}_{pi,pi}$ where the electrons from all five π bonds are correlated is given as well.

$\Delta IP^{corr}_{pi,pi}()$	$\Delta IP^{corr}_{pi,pi}(c)$		$\Delta IP^{corr}_{pi,pi}(c,d)$		
	c	ΔIP	c	d	ΔIP
0.445	pi,1	-0.604	pi,2	pi,1	-0.291
	pi,2	-0.162	pi,-2	pi,-1	-0.291
	pi,-1	-0.604	pi,-2	pi,1	0.061
	pi,-2	-0.162	pi,2	pi,-1	0.061
			pi,2	pi,-2	0.036
			pi,1	pi,-1	0.154
0.445		**-1.532**			**-0.271**
$\sum_{i=1}^{3} \Delta IP^{(i)}_{pi,pi}$					**-1.358**
$\delta' IP^{corr}_{pi,pi}$					**-1.145**

Table 4.6: Individual increments for the correlation correction to the off-diagonal matrix element $IP_{pi,pi,1}$ of a $C_{10}H_{12}$ molecule (in eV) obtained when only the π bonds are open for correlation.

$\Delta IP^{corr}_{pi,pi,1}()$	$\Delta IP^{corr}_{pi,pi,1}(c)$		$\Delta IP^{corr}_{pi,pi,1}(c,d)$		
	c	ΔIP	c	d	ΔIP
-0.460	pi,2	-0.082	pi,-1	pi,-2	-0.043
	pi,-1	-0.079	pi,-1	pi,2	0.031
	pi,-2	-0.005	pi,-2	pi,2	0.015
-0.460		**-0.157**			**0.003**
$\sum_{i=1}^{3} \Delta IP^{(i)}_{pi,pi,1}$					**-0.614**
$\delta' IP^{corr}_{pi,pi,1}$					**-0.573**

mental scheme: $\delta'' IP^{corr}_{pi,pi} = -1.358$ eV and $\delta'' IP^{corr}_{pi,pi,1} = -0.615$ eV. The differences between the exact and the estimated values of correlation corrections are 213 meV (or 15.7%) and 42 meV (or 6.8%) for the diagonal and off-diagonal matrix elements, respectively. We see that the performance of the incremental scheme is still good even in the case of rather diffuse orbitals and in the worst case it produces an error of approximately 0.2 eV.

To illustrate the decay of the correlation effects with the distance from the localized π hole a representavive selection of the second-order increments obtained in the $C_{10}H_{12}$ molecule when only π bonds are added are given in Table 4.7. The values of the increments of the diagonal matrix element drop by an order of magnitude when distance of the added bond increases by two lattice constants. The decay of the increments for the off-diagonal matrix element is even more rapid. The dash in Table 4.7 (and also in Table 4.9) means that the absolute value of the corresponding increment is below the estimated size-extensivity error for this increment.

The increments for the correlation corrections to the matrix elements $IP^{corr}_{pi,pi}$

Table 4.7: Convergence of the diagonal (left) and first nearest-neighbor off-diagonal increments $\Delta\mathrm{IP}^{\mathrm{corr}}_{b,a}(c)$ with the distance between the additionally correlated bond (in eV). The dash means that the increment is too small to be reliable due to size-extensivity problem of MRCI.

a,a	c	ΔIP	a,b	c	ΔIP
pi,pi	pi,-1	-0.604	pi,pi,1	pi,-1	-0.079
pi,pi	pi,-2	-0.162	pi,pi,1	pi,-2	-0.005
pi,1,pi,1	pi,-2	-0.053	pi,1,pi,2	pi,-2	—
pi,2,pi,2	pi,-2	-0.015			

Table 4.8: Correlation corrections to the local matrix elements $\mathrm{IP}^{\mathrm{corr}}_{\mathrm{pi,pi}}$ and $\mathrm{IP}^{\mathrm{corr}}_{\mathrm{pi,pi,1}}$ (in eV). The total values are presented in the last column.

matrix element	$\Delta\mathrm{IP}^{\mathrm{corr}}_{\mathrm{a,b}}()$	$\sum_c \Delta\mathrm{IP}^{\mathrm{corr}}_{\mathrm{a,b}}(c)$	$\sum_{c<d} \Delta\mathrm{IP}^{\mathrm{corr}}_{\mathrm{a,b}}(c,d)$	$\delta\mathrm{IP}^{\mathrm{corr}}_{\mathrm{a,b}}$
$\mathrm{IP}_{\mathrm{pi,pi}}$	0.445	-2.006	-0.446	**-2.007**
$\mathrm{IP}_{\mathrm{pi,pi,1}}$	-0.460	0.087	0.057	**-0.316**

and $\mathrm{IP}^{\mathrm{corr}}_{\mathrm{pi,pi,1}}$ obtained on the C_6H_8 and $C_{10}H_{12}$ clusters are summed up for both, σ and π orbitals, and presented in Table 4.8. The contribution of the part of the crystal outside the $C_{10}H_{12}$ cluster will be estimated in section 4.3 using the data from Table 4.7. There we show that even in the case of the rather slow decay of the correlation effect with the distance the polarization of the remaining part of the infinite one-dimensional crystal outside the $C_{10}H_{12}$ cluster amounts to 1% of the correlation correction $\delta\mathrm{IP}^{\mathrm{corr}}_{\mathrm{pi,pi}}$ only that is well-below the error bar of the incremental scheme itself.

Let us turn to the electron affinities now. To calculate the correlation corrections to the matrix elements corresponding to attached-electron states we proceed as described in section 3.4.3. In the case of the diagonal matrix elements $\mathrm{EA}^{\mathrm{corr}}_{\mathrm{pi^*,pi^*}}$ and $\mathrm{EA}^{\mathrm{corr}}_{\mathrm{CH2^*,CH2^*}}$ the molecule $C_{10}H_{12}$ may serve as a minimal-size cluster for the

Table 4.9: Convergence of increments with the distance between correlated bonds (in eV). Dashes mean that the increments are too small to be reliable due to size-extensivity problem of MRCI.

$\Delta\mathrm{EA}^{\mathrm{corr}}_{\mathrm{CH2^*,CH2^*}}(\mathrm{pi^*})$	0.181	$\Delta\mathrm{EA}^{\mathrm{corr}}_{\mathrm{pi^*,pi^*}}(\mathrm{pi^*},-1)$	0.314
$\Delta\mathrm{EA}^{\mathrm{corr}}_{\mathrm{CH2^*,CH2^*}}(\mathrm{pi^*},-1)$	0.034	$\Delta\mathrm{EA}^{\mathrm{corr}}_{\mathrm{pi^*,pi^*}}(\mathrm{pi^*},-2)$	0.088
$\Delta\mathrm{EA}^{\mathrm{corr}}_{\mathrm{CH2^*,CH2^*}}(\mathrm{pi^*},-2)$	—	$\Delta\mathrm{EA}^{\mathrm{corr}}_{\mathrm{pi^*,1,pi^*,1}}(\mathrm{pi^*},-2)$	—

Table 4.10: Correlation corrections to diagonal local matrix elements corresponding to antibonds obtained in the cluster $C_{10}H_{12}$ (in eV).

matrix element	$\Delta\mathrm{EA}^{\mathrm{corr}}_{\mathrm{a,b}}()$	$\sum_c \Delta\mathrm{EA}^{\mathrm{corr}}_{\mathrm{a,b}}(c)$	$\sum_{c<d} \Delta\mathrm{EA}^{\mathrm{corr}}_{\mathrm{a,b}}(c,d)$	$\delta\mathrm{EA}^{\mathrm{corr}}_{\mathrm{a,b}}$
$\mathrm{EA}_{\mathrm{CH2^*,CH2^*}}$	0.191	0.816	-0.161	**0.846**
$\mathrm{EA}_{\mathrm{pi^*,pi^*}}$	0.237	1.815	-0.430	**1.623**

correlation calculations. The decay of the second-order increments with the distance to the added π bond-antibond pair of π symmetry (the most diffuse ones, referred to by the π^* orbital only for simplicity) is presented for both matrix elements in Table 4.9. The convergence with the distance looks even better than in the case of π hole states, however, that is most probably simply because only a limited number of the antibonds are open for excitations from the occupied bonds in the incremental scheme for attached electrons which leads to a partial reduction of the virtual space, the effect which is more pronounced for increments $\Delta\mathrm{EA}_{rs}(t)$ with separated bond groups r, s and t.

The convergence of incremental series (3.34) with order is shown in Table 4.10; the *total* values of the correlation corrections to the diagonal matrix elements are presented in the last column of this Table. As in the case of the hole states the major contribution to the local matrix elements EA_{rs} comes from the second-order increments $\Delta\mathrm{EA}_{rs}(t)$ while the third-order contributions $\Delta\mathrm{EA}_{rs}(t,u)$ are at least by a factor of 4 smaller than the second-order terms.

Table 4.11: Change of the local matrix elements $IP_{R,nn'}$ and $EA_{R,mm'}$ of the periodic system due to correlation effects.

matrix element	$IP_{0,\text{pi pi}}$	$IP_{0,\text{CH1 CH1}}$	$IP_{0,\text{CC CC}}$	$IP_{0,\text{sig sig}}$
SCF value	10.526 eV	18.904 eV	21.230 eV	22.396 eV
reduction	-2.007 eV	-2.804 eV	-3.702 eV	-3.867 eV
	19.1 %	14.8 %	17.4 %	17.2 %
total value	8.519 eV	16.100 eV	17.528 eV	18.529 eV

matrix element	$IP_{\pm a,\text{pi pi}}$	$IP_{a,\text{CC CH1}}$	$IP_{0,\text{CH1 sig}}$	$IP_{0,\text{CC sig}}$
SCF value	1.683 eV	2.968 eV	3.022 eV	3.022 eV
reduction	-0.316 eV	-0.718 eV	-1.040 eV	-0.936 eV
	18.7 %	24.2 %	34.4 %	31.0 %
total value	1.367 eV	2.250 eV	1.982 eV	2.087 eV

matrix element	$EA_{0,\text{pi}^* \text{ pi}^*}$	$EA_{0,\text{CH1}^* \text{ CH1}^*}$	$EA_{\pm a,\text{pi}^* \text{ pi}^*}$	$EA_{\pm a,\text{CH1}^* \text{ CH1}^*}$
SCF value	-4.497 eV	-5.603 eV	-1.054 eV	1.012 eV
reduction	1.623 eV	0.846 eV	0.365 eV	-0.035 eV
	36.1%	15.1 %	34.6 %	3.5 %
total value	-2.941 eV	-4.764 eV	-0.689 eV	0.976 eV

To evaluate the correlation corrections to the off-diagonal matrix elements $\mathrm{IP}^{\mathrm{corr}}_{\mathrm{pi}^*,\mathrm{pi}^*,1}$ and $\mathrm{EA}^{\mathrm{corr}}_{\mathrm{CH2}^*,\mathrm{CH2}^*,1}$ we had to use even larger, the $C_{12}H_{14}$ molecule. The convergence of the increments with the order and the distance between the correlated electrons was checked and turned out to be satisfactory. Summing up these increments we get the following values for the corrections: $\delta\mathrm{EA}^{\mathrm{corr}}_{\mathrm{CH2}^*,\mathrm{CH2}^*,1} = -0.035$ eV and $\delta\mathrm{EA}^{\mathrm{corr}}_{\mathrm{pi}^*,\mathrm{pi}^*,1} = 0.365$ eV.

To summarize our results on the correlation corrections to the local matrix elements we present in Table 4.11 the SCF matrix elements together with the absolute corrections (and their percentage relative the SCF value) and the *total correlated* matrix elements $\mathrm{IP}^{\mathrm{corr}}$ and $\mathrm{EA}^{\mathrm{corr}}$. Note that we also switched back to the notation for the matrix elements in the infinite periodic system as done in Tables 3.2–3.5. though the correlation contributions are actually calculated in molecules representing finite parts of the crystal. In the one-dimensional crystal the polarization outside the specified clusters only gives negligibly small effect as compared to the correlation effect in the close vicinity of the localized extra charge (see section 4.3) and therefore the correlation correction to a local matrix element obtained in the molecules are equal to the corresponding one in the crystal within the accuracy of the incremental scheme.

From Table 4.11 one can see that the change of the SCF matrix elements due to correlation effects is quite pronounced, ranging from 15% to 30%. One also sees that in all cases the absolute values of the SCF matrix elements are reduced, i.e. overall the ionization potentials decrease while the electron affinities increase. This indicates that the reduction of the total energy due to electron correlation is always stronger in the charged systems than in the neutral one.

4.2 Correlated band structure of *trans*-polyacetylene

Having obtained the local matrix elements including all correlation effects (the "total values" in Table 4.11) we are able to compile the band structure of *trans*-

polyacetylene which takes into account electron correlation, the ultimate goal of our approach. For this purpose we replace the LMEs in the truncated series (2.32) and (2.33) obtained on the SCF level by the correlated ones and diagonalize the obtained matrices at each k-point analogously to the case of the SCF bands. The new band structure (we call it *correlated* band structure) will exhibit small deviations from the one obtained by an infinite summation in Eqs. (2.32) and (2.33) like the SCF band structure (see Figs. 3.9 and 3.13). To correct for this (minor) deficiency we simply add at each k-point the difference between the band energies obtained by the local SCF matrix elements and those obtained by the CRYSTAL code for an infinite periodic tPA single chain. The resulting correlated band structure of *trans*-polyacetylene is presented in Fig. 4.3 (red lines) and compared to the SCF band structure by the CRYSTAL code (black lines).

From this Figure we see that the band structure changes dramatically when electron correlation is taken into account. Two effects are clearly seen: i) a shift of the "center-of-mass" positions of all bands (valence bands are shifted upwards and conduction bands downwards) and ii) a flattening of all bands (significantly more pronounced for the valence bands). These effects lead to a narrowing of the band gap, a change of the sign of the electron affinity of *trans*-polyacetylene and an overall reduction of the band widths. But there are also some more subtle changes like the narrowing of the avoided crossing of the 2nd and 3rd lowest valence bands close to the X point or the lifting of the accidental degeneracy of the highest two valence bands at the Γ point.

The value of the band gap of the infinite tPA single chain is reduced by 2.31 eV from 6.42 eV (on the SCF level) down to 4.11 eV when electron correlation is included, a 36.0% reduction. Similar values of the reduction of the SCF band gap, 2.35 and 2.38, are reported in two recent independent MP2 studies, [SB96] and [AKS01], respectively, on the π bands of isolated tPA chains.

The corrected values of the lowest ionization potential and the highest electron affinity of *trans*-polyacetylene are 4.58 eV and 0.47 eV, respectively. The posi-

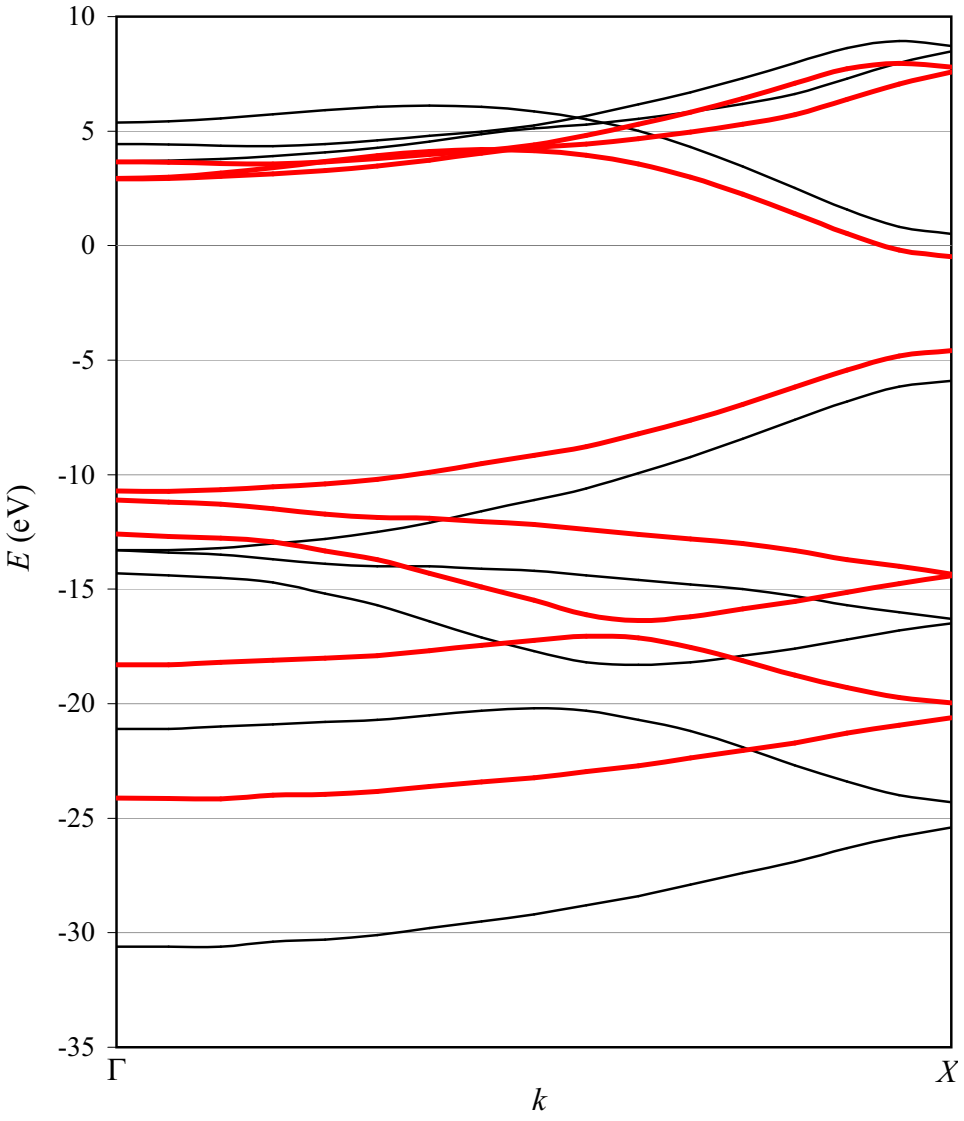

Figure 4.3: Correlated band structure of the infinite *trans*-polyacetylene single chain (red lines) compared to the SCF one (black lines).

Table 4.12: Change of the band widths due to the correlation effects (in eV).

			reduction	
bands	SCF width	correlated width	absolute	relative
σ valence	17.30	13.01	4.29	24.8 %
π valence	7.40	6.14	1.26	17.0 %
π conduction	4.86	4.67	0.19	3.9 %
σ conduction	5.25	5.05	0.20	3.9 %

tive sign of the electron affinity (after inclusion of electron correlation) tells that *trans*-polyacetylene is able to retain an extra electron as is known from experiments [KP+89].

The changes of the band widths are summarized in Table 4.12. There, the σ valence band width refer to the width of all four σ valence bands while the σ conduction band width is that of the two σ conduction bands only. One sees that the relative reduction of the conduction bands widths is much smaller than that of the valence bands. Since the dispersion of the bands is mainly determined by the hopping matrix element between nearest-neighbor sites (especially in 1D systems) one can conclude that the hopping of holes is much stronger affected by electron correlation than hopping of extra electrons.

4.3 Accuracy of the method

Now that we have obtained numerical results for some physical quantities which are characteristic for the investigated system the question arises how accurate these results are and whether we are able to estimate the accuracy of our method. In this section we show that we can indeed provide some estimated error bars for the calculated quantities.

As the correlation corrections to the local matrix elements (the key quantities

of our method) are composed of dozens of increments we first estimate the error for the individual increments. As can be seen from equations (3.15) and (3.20)–(3.24) each individual increment is defined as the difference of several correlation energies (correlation corrections to the total energies of various states under various conditions which are calculated to evaluate a particular increment). The uncertainty in the evaluation of these individual increments essentially arises from the size-extensivity error of the CI(SD) method. As shown in section 3.5 we are able to reduce this error to about 10^{-4} of the value of the correlation energy (see last columns in Tables 3.6 and 3.7). In all our calculations these correlation energies are of the order of a few electron-volts. Therefore, we estimate the error for a single increment being a few meV. That is why in our calculations we simply omit all increments whose absolute values are smaller than 1 meV (see Tables 4.7 and 4.9).

The possible accumulated size-extensivity errors in the correlation correction to some particular local matrix element are expected to be not higher than the error for a single increment times the number of increments entering the series. Usually this amounts to few dozens of meV.

Another kind of error in the correlation corrections to LMEs emerges from the truncation of the incremental series after some order (after the third order in our case). In section 4.1 we have explored the accuracy of the truncated incremental scheme in detail. In the case of the most compact localized orbitals (σ bonds) the error produced by the incremental scheme is of the same order as the accumulated size-extensivity error (4–7% of the total value of correlation correction to a LME, see the discussion of Tables 4.1 and 4.2). However, in the case of the more diffuse π orbitals the error due to the truncation of the series ($\sim$15%, see the discussion of Table 4.5) is higher than the estimated size-extensivity error for diagonal matrix element ($\sim$2%). This indicates that for more diffuse orbitals the fourth term of the incremental series (3.18) may give noticeable contribution. Unfortunately, we can not calculate this term explicitly as individual increments of the fourth order are usually smaller than their size-extensivity error. Thus, we agree that the er-

ror for correlation corrections to the diagonal matrix elements $IP_{pi,pi}$, EA_{pi^*,pi^*} and $EA_{CH1^*,CH1^*}$ are not more than 15% and those for all the other matrix elements not more than 10% of absolute values of the corrections.

Another question which we would like to discuss here concerns the effect of polarization of infinite insulator due to the presence of an uncompensated charge. The polarization of the infinite crystal outside the explored cluster may also contribute to correlation corrections. We can estimate such a contribution by a continuum approximation as already done earlier by other authors, e.g. in [HHF84], [GSF97] and [AFS00].

In this approximation far-range contributions to the reduction of the SCF energy of the $(N-1)$- or $(N+1)$-electron system are attributed to the polarization energy of an insulator in an electric field. This energy is equal to

$$\delta E_i^{\mathrm{pol}} = \frac{1}{2} \int \mathbf{P}\,\mathbf{E}\,\mathrm{d}V \tag{4.1}$$

where $\mathbf{E}$ is the electric field, $\mathbf{P} = \frac{(\epsilon-1)}{4\pi}\mathbf{E}$ is the polarization response and ϵ is the dielectric constant of the crystal. The subscript i in Eq. (4.1) denotes that this energy corresponds to the charged system with a hole (an extra electron) being in the bond (antibond) i. In other words, we are estimating the polarization effects on diagonal matrix elements here.

Let us say that starting with a distance r_1 from the center of a localized orbital we can treat the electron in this orbital as a point charge. Then the integration in Eq. (4.1) can be divided in two parts:

$$\delta E_i^{\mathrm{pol}} \;=\; \delta E_i(r_1) + \int_{r_1}^{\infty} \mathrm{d}r\; \frac{(\epsilon-1)}{4\pi} \left(\frac{e}{\epsilon r^2}\right)^2 \;=\; \delta E_i(r_1) + C\, r_1^{-3}. \tag{4.2}$$

Here we performed the integration for the case of one-dimensional system, $\delta E_i(r_1)$ is the change of the energy due to electron correlation for distances less than r_1 from the localized charge (this value we calculate explicitly by the incremental scheme) and C is a constant characteristic for the given material. Knowing two $\delta E_i(r)$ values

$\delta E_i(r_1)$ and $\delta E_i(r_2)$ for two different cut-off radii r_1 and r_2 ($r_2 > r_1$) we can extract the tail correction Cr_1^{-3} and by this estimate change of the energy of the *whole* charged system

$$\delta E_i(\infty) = \frac{\delta E_i(r_2)(r_2/r_1)^3 - \delta E_i(r_1)}{(r_2/r_1)^3 - 1}. \tag{4.3}$$

Note the different power (r^3) which enter this relation compared to the corresponding relation for a bulk crystal [AFS00] r^1.

Thus, the correlation correction to diagonal matrix elements with the polarization of the infinite crystal taken into account is

$$\delta\mathrm{IP}_{aa}^{\mathrm{corr}}(\infty) = \frac{\delta\mathrm{IP}_{aa}^{\mathrm{corr}}(r_2)(r_2/r_1)^3 - \delta\mathrm{IP}_{aa}^{\mathrm{corr}}(r_1)}{(r_2/r_1)^3 - 1} \tag{4.4}$$

where $\delta\mathrm{IP}_{aa}^{\mathrm{corr}}(r_i)$, i=1, 2 are the correlation correction to the matrix element IP_{aa} when all bonds up to distances r_i from the bond a are correlated. An analogous formula holds for $\delta\mathrm{EA}_{rr}^{\mathrm{corr}}(\infty)$.

The hopping matrix element IP_{ab} is one-half of the difference between energies of the states $(\Phi_a + \Phi_b)/\sqrt{2}$ and $(\Phi_a - \Phi_b)/\sqrt{2}$ which are two states with holes of two different shapes delocalized within two bonds a and b. Therefore, the change of the hopping matrix element in continuum approximation emerges due to the polarization of the insulator in the electric field of a dipole. Substitution of the field of a point charge in Eq. (4.2) by that of a dipole leads to the approximate formula for the correlation correction to the off-diagonal matrix elements with the polarization of the entire crystal taken into account:

$$\delta\mathrm{IP}_{ab}^{\mathrm{corr}}(\infty) = \frac{\delta\mathrm{IP}_{ab}^{\mathrm{corr}}(r_2)(r_2/r_1)^5 - \delta\mathrm{IP}_{ab}^{\mathrm{corr}}(r_1)}{(r_2/r_1)^5 - 1}. \tag{4.5}$$

Let us calculate explicitly the missing polarization effect in the correlation correction $\delta\mathrm{IP}_{\mathrm{pi,pi}}^{\mathrm{corr}}$ caused by adding farther π bonds using the data on the decay of the second-order increments in Table 4.7. The total value of the correlation correction in a cluster $C_{18}H_{20}$ (four unit cells on both sides from the central one) as obtained by

the incremental scheme effectively is 2.007 eV and the cut-off radius $r_2 = 4a$. As the correlation effect associated with the σ bonds decay much faster than those arising from the π bonds, the change of the correlation correction when the effective cluster increases from $C_{10}H_{12}$ to $C_{18}H_{20}$ is mainly due to correlation of the electrons in π bonds. Thus, the value $\delta IP^{corr}_{pi,pi}(2a)$ is equal to -1.871 eV. Using Eq. (4.4) we obtain the value of the correlation correction in the infinite system $\delta IP^{corr}_{pi,pi}(\infty) = 2.026$ eV compared to $\delta IP^{corr}_{pi,pi}(4a) = 2.007$ eV. Therefore, the polarization of the outer part of the crystal leads to less than 1% change of the correlation correction which can be neglected within the error bar of the incremental scheme.

The continuum correction in the case of the off-diagonal matrix elements is expected to be even less as the decay of correlation effect with the distance is more rapid than for diagonal ones (see Eqs. 4.3 and 4.4). In fact for an effective $C_{16}H_{18}$ cluster (with $r = 3.5\,a$) $\delta IP^{corr}_{pi,pi,1}(3.5\,a) = -0.316$ eV while for the smaller effective C_8H_{10} cluster (with $r = 1.5a$) $\delta IP^{corr}_{pi,pi,1}(1.5a) = -0.148$ eV. The resulting continuum correction is -0.002 eV leading to $\delta IP^{corr}_{pi,pi,1}(\infty) = -0.318$ eV. Thus, we conclude that the effect of polarization of the infinite one-dimensional crystal outside the treated cluster is negligibly small.

Now we can estimate the accuracy of our method for the ultimate physical quantities characterizing the investigated material. The shift of the ionization potential due to electron correlation is governed by two corrections: $\delta IP^{corr} = \delta IP^{corr}_{0,pi,pi} - 2\delta IP^{corr}_{1,pi,pi}$. This is easy to realize in terms of a Hückel (or tight-binding) model where only diagonal matrix element and the hopping between nearest-neighbor sites are considered. Then, energy of the valence π band as a function of crystal-momentum k is $\varepsilon_\pi(k) = -IP^{corr}_{0,pi,pi} - 2IP^{corr}_{1,pi,pi}\cos(ak)$. The top of this band is at the X point ($k = \pi/a$) and therefore the ionization potential is given by $IP = IP^{corr}_{0,pi,pi} - 2IP^{corr}_{1,pi,pi}$. We have estimated the error for the correction $\delta IP^{corr}_{0,pi,pi}$ being equal to 15% of its value (-2.0 eV) which is 0.3 eV. The error for the correction $\delta IP^{corr}_{0,pi,pi}$ is smaller by one order of magnitude and is omitted. Thus, we consider the ionization potential of tPA single chain to be $IP = 4.6 \pm 0.3$ eV. Approximately the same error bar is

obtained for the electron affinity: EA $= 0.5 \pm 0.3$ eV. Consequently, the error for the band gap is at most 0.6 eV that is 15% of its value. However, we have to emphasize that the estimated error of 0.3 eV is an upper bound for the energy of any band at any k-point which is in the order of 1% of the total range of band energies only.

As one can conclude, the two main reasons, which lead to the error bar for correlation corrections up to 15% of their values, are i) the error due to truncation of the incremental scheme after the third order and ii) the size-extensivity error of the CI(SD) method for evaluation of correlation energies of $(N \pm 1)$- and N-electron states. The truncation error of the incremental scheme can not be reduced by taking into account the next order because the values of the increments of the fourth order are below the estimated size-extensivity error for the entering correlation energies. Therefore, namely the latter error controls the accuracy of our whole approach. To improve the accuracy further one first needs a true size-extensive multireference correlation method that could be multireference coupled-cluster which is at the stage of development at the present moment.

4.4 Comparison to experimental data

In this section we would like to compare our result for the band gap to experimental data. One has to emphasize that there are, of course, no experimental data on *trans*-polyacetylene *single* chains and all data available correspond to bulk *trans*-polyacetylene and we have to compare properties of a bulk system with calculated results for the linear one.

One attempt to estimate the effect of the interchain coupling on the band gap of tPA single chains was made by Ayala *et al.* [AKS01]. They have compared the band gap of an isolated single chain with the band gap of a system consisting of two chains one precisely on the top of another at a distance of 3.335 Å. In this particular arrangement of the two chains the intermolecular overlap of the π orbitals (which define the gap) is maximal. The chosen distance corresponds to the minimum of

the interaction energy of the two stacked chains on the MP2 level of approximation. The reduction of the band gap due to interchain coupling was found to be 1.22 eV on the HF level and further a 0.22 eV reduction (1/6 of the HF value) was obtained when electron correlation was taken into account (the Møller–Plesset perturbation method to second order was used for this purpose). Thus, one can conclude that the main reduction of the band gap due to the interchain interaction already emerges on the HF level.

We investigate this reduction for the true fishbone-like packing of tPA chains in the bulk material as shown in Fig. 3.3 which was found experimentally [FC+82]. The unit cell of bulk tPA consists of two C_2H_2 units of linear tPA (one on each non-equivalent chain). The interchain interaction leads to the splitting of the otherwise two-fold degenerate bands of single tPA chain. This splitting at the X point amounts to a 0.6 eV reduction of the band gap of the bulk system as compared to that of a single chain. Further reduction of the band gap due to electron correlation in each of the four nearest-neighbor chains is not expected to be noticeable because in the experimentally-found packing of the chains the overlap of the π orbitals between neighbor chains is actually minimal. Thus, based on the MP2 data presented in [AKS01] we estimate it to be less than 1/6 of the HF reduction for each of the four chains leading at most to a further 0.2 eV narrowing of the band gap. Therefore, the account for the interchain splitting reduces the calculated band gap of the bulk tPA down to 3.3 eV.

Two other effects should also be mentioned which can lead to a reduction of the calculated band gap of tPA. Firstly, though our basis set (VTZ) is already rather flexible we have not yet reached the basis set limit. A more rich basis set will affect the correlation corrections of the LMEs as a larger variational space will be provided to the MRCI calculations. Secondly, the long-ranged polarization of the infinite *bulk* system has to be considered. There, one expects a more pronounced effect than in the case of a one-dimensional system. A discussion of the polarization effect on local matrix elements of different bulk systems can be found in [GSF97]

and [AFS00]. However, both effects mentioned here are small compared to the calculated electron correlation effects and each of them can lead to a few tenth of an electron-volt reduction of the band gap only.

Next, we would like to address the experimental value of 2 eV for the tPA band gap obtained from absorption spectra of bulk *trans*-polyacetylene [FO+79], [TG+80] and [L88]. There is no clear indication in these publications that the observed maximum of the absorbtion coefficient at approximately 2 eV can really be assigned to the interband transition rather than to an excitonic state. A theoretical investigation of such gap states showed [RL99] that the energy of these excitons in tPA show up approximately 0.4 eV below the band gap. Therefore, the fundamental band gap of bulk *trans*-polyacetylene is expected to be 2.4 eV.

Thus, taking into account the bulk effects in tPA which all lead to a reduction of the band gap with respect to the one in a 1D single chain and also the estimated error of our method the calculated gap reaches the experimental value.

Chapter 5

Excitons

In this Chapter we would like to show how our approach to correlated band structures can be extended to the study of the electron correlation effects of *neutral* excitations in periodic systems, namely excitons, such that standard quantum-chemical methods can be used. We refer here to the process of the absorption of a light quantum by the electrons of an extended non-conducting system in its ground state i.e. the process of generating an excited state of the same *neutral* system. In this case no electron leaves the system (in contrast to the photoionization process which we refer to when describing the valence bands).

In frames of the most simple model one can say that an electron from the valence band ν and with band energy $\varepsilon_{k\nu}$ is excited to the conduction band μ where it occupies the virtual Bloch orbital $\psi_{k'\mu}$ with energy $\varepsilon_{k'\mu}$. The wavefunction of such a state can be obtained by applying the two operators $c_{k\nu}$ and $c^{\dagger}_{k'\mu}$ entering the equations (2.22) and (2.23) to the ground-state wavefunction (2.21) of the closed-shell system (we omit here the spin indices as we suppose that the electron does not change its spin during such a process). The operator $c_{k\nu}$ produces a hole in the valence band ν and the operator $c^{\dagger}_{k'\mu}$ creates an electron in the conduction band μ. If we neglect the electron-hole interaction, the energy to produce shuch an excited state is equal to $\varepsilon_{k'\mu} - \varepsilon_{k\nu}$. This way we describe a pure interband transition and the threshold energy for such processes is equal to the fundamental gap of the non-

conducting system.

However, if we take into account the interaction between the electron in the conduction band and the hole in the valence band, the system may gain energy from the electron-hole interaction when a bound electron-hole pair is formed. In other words, in the extended system there exist *gap* states which correspond to excitons (bound electron-hole pairs) travelling through the crystal. Such gap states were found experimentally in many semiconductors and insulators, in particular in *trans*-polyacetylene [LE+81], [OB82] and [SY+82], the system which we refer to here. These states form bands and we would like to use our approach to calculate these excitonic bands. This means, we want to construct a set of localized model electron-hole pair wavefunctions (forming our excitonic model space) which can be represented in finite clusters, and calculate the corresponding local matrix elements (diagonal and off-diagonal) in sufficiently large clusters of the crystal. These *excitonic* LMEs are essentially the matrix elements of an effective Hamiltonian obtained from an equation similar to Eq. (2.62), and we will get the excitonic bands by the use of a (back) transformation analogous to Eqs. (2.32) and (2.33).

We exclusively refer here to bound excitons which carry a single crystal momentum (associated with the center of mass motion) and are otherwise regarded as a fixed entity. The appealing aspect of this approach is that in quantum chemistry which deals with finite systems an exciton is just an eigenstate of the given system like the ground state, but different from it, and the same CI ansatz and methodology as used for the correlated ground-state wavefunction can be used. In fact, the CI equations are the same and one is just looking at another root of these equations.

To describe a bound electron-hole pair of a crystal in real space it is convenient to use local Wannier orbitals (both occupied and virtual ones) to construct the *local* excited configurations. Let as consider one such configuration $\Phi_{\mathbf{Rn}}^{\mathbf{R'm}}$ where an electron is removed from the occupied Wannier orbital $\varphi_{\mathbf{Rn}}$ centered at the unit cell with lattice vector $\mathbf{R}$ and put into the virtual orbital $\varphi_{\mathbf{R'm}}$ centered at the unit cell with lattice vector $\mathbf{R'}$ while the rest of the system remains unchanged (i.e. we

start again from the frozen orbital approximation). Taking into account Eqs. (2.15)–(2.19) one can readily show that the energy to produce an excited state with this configuration is equal to

$$\begin{aligned} E^{\mathrm{exc}} &= \langle \Phi^{\mathbf{R'm}}_{\mathbf{Rn}} \mid H \mid \Phi^{\mathbf{R'm}}_{\mathbf{Rn}} \rangle - E_0 \\ &= \varepsilon_m - \varepsilon_n - \big(\langle \mathbf{R}'m\, \mathbf{R}n \mid \mathbf{R}'m\, \mathbf{R}n \rangle - \langle \mathbf{R}'m\, \mathbf{R}n \mid \mathbf{R}n\, \mathbf{R}'m \rangle \big) \\ &= -\mathrm{EA}_m + \mathrm{IP}_n - \big(\langle \mathbf{R}'m\, \mathbf{R}n \mid \mathbf{R}'m\, \mathbf{R}n \rangle - \langle \mathbf{R}'m\, \mathbf{R}n \mid \mathbf{R}n\, \mathbf{R}'m \rangle \big) \quad (5.1) \end{aligned}$$

where we have used $\mid \mathbf{R}n \rangle$ instead of $\mid \varphi_{\mathbf{R}n} \rangle$, and ε_m and ε_n are the energies of the Wannier orbitals (associated with the bands μ and ν, respectively) which are independent of the vectors of lattice translation $\mathbf{R}'$ and $\mathbf{R}$. The energy E^{exc} is not equal to the difference of the ionization potential IP_n and the electron affinity EA_m which defines the interband transition but differs from it by the term $\langle \mathbf{R}'m\, \mathbf{R}n \mid \mathbf{R}'m\, \mathbf{R}n \rangle - \langle \mathbf{R}'m\, \mathbf{R}n \mid \mathbf{R}n\, \mathbf{R}'m \rangle$. This term decays with increasing distance between the centers of the Wannier orbitals $\varphi_{\mathbf{Rn}}$ and $\varphi_{\mathbf{R'm}}$ (as follows from Eq. (2.6)) and is the interaction energy between the electron and the hole. Such terms will be responsible for the formation of bound electron-hole pairs when we describe excited states of crystals (or big clusters) as linear combinations of local configurations like $\Phi^{\mathbf{R'm}}_{\mathbf{Rn}}$. The energies of such states can be substantially reduced compared to the energy of the interband transitions and thus the gap states of semiconductors and insulators may emerge.

Below, for the sake of simplicity, we consider a single valence and conduction band only that yields one occupied and one unoccupied Wannie orbital per unit cell. Such a simplification is justified for *trans*-polyacetylene, when excitations of the valence π electrons to the lowest conduction band of π symmetry are considered. We then can omit the band indices n and m baring in mind that subscripts (superscripts) in $\Phi^{\mathbf{R'm}}_{\mathbf{Rn}}$ correspond to the hole (electron) orbitals. Also, again we will refer to a one-dimensional system as the excitons in the conjugated π system of polymers are essentially confined to a single polymer chain [FG+99].

Let us start to describe a bound electron-hole pair by writing an excitonic wavefunction in the form of a linear combination of local configurations $\Phi_R^{R'}$:

$$\Psi^{\text{exc}} = \sum_{RR'} \alpha_R(R')\Phi_R^{R'} = \sum_R \sum_d \alpha_R(d)\Phi_R^{R+d} \tag{5.2}$$

where we introduced the relative distance d of the centers of the Wannier orbitals φ_R and $\varphi_{R'}$: $d = R' - R$. Here we have to make a few remarks. Let us focus for a moment on a wavefunction where the hole is pinned to a certain unit cell, R, say. Then the CI ansatz (5.2) for the exciton is reduced to

$$\Psi_R^{\text{exc}} = \sum_d \alpha_R(d)\Phi_R^{R+d} \tag{5.3}$$

Firstly, if we set all coefficients $\alpha_R(d \neq 0)$ to zero and $\alpha_R(0) = 1$ we get a so-called Frenkel exciton [Fr31] where the excitation is restricted to one unit cell. Yet, we use the ansatz (5.3) which allows us to describe excitons in the general case when the atomic structure of the given crystal is explicitly taken into account. Secondly, it is possible to produce N^{virt} excitonic states using the ansatz (5.3) where N^{virt} is the number of virtual WOs in the system. However, we focus our attention on the energetically lowest excited state which corresponds to the gap state and is usually well separated from the other excitonic states by some energy. Thirdly, doubly excited configurations like $\Phi_{R,R'}^{R+d,R+d'}$ may, of course, also contribute to the wavefunction of the excited state but here we aim to construct our model space, which is built up by singly excited configurations which describe the electron-hole pair as being a two-particle object. The effect of doubly (and higher) excited configurations on the energy of excited states can be taken into account later by the MRCI procedure.

The representation of the exciton-state wavefunction given by the right-hand-side expression in Eq. (5.3) suggests to plot the distribution of the electrons relative to the fixed hole. As the electron-hole interaction energy (the two last terms in Eq. (5.1)) contained in each configuration decays with the distance between the electron and the hole orbital, one expects configurations with small distances d to

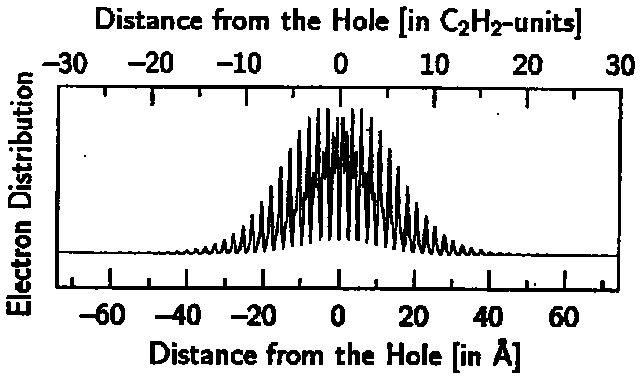

Figure 5.1: Electron-hole wavefunction of the exciton state of a tPA single chain showing the distribution of the electron relative to the hole which is fixed at some arbitrary position on the chain (at 0 Å). The figure is taken from Ref. [RL99] where the calculations were done within the *GW* approximation and using the Bethe–Salpeter equation.

dominate the wavefunction (5.3). This expectation is based on the fact that the electron tries to stay as close as possible to the hole.

An investigation of such electron-hole pairs in a *trans*-polyacetylene single chain was presented in Ref. [RL99] which was done in the framework of a different (recently developed) approach based on solving the Bethe–Salpeter equation of the two-particle Green's function and using the *GW* approximation for the self-energy operator. That approach allowed the authors to visualize the distribution of the electron relative to the hole fixed somewhere in real space (see Fig. 5.1). From this Figure one concludes that such localized objects can indeed be found in periodic non-conducting systems and the probability to find the electron of this pair at some place decays with the distance from the fixed hole. Hence, a finite cluster can be used to represent this localized excitonic state.

As follows from Fig. 5.1, the dimension of a single electron-hole pair in a tPA chain is approximately 30 unit cells that implies that a $C_{60}H_{60}$ cluster is required to properly describe such an exciton within our cluster approach. Presently we can not stand calculations for such big clusters of *trans*-polyacetylene with reasonable

Table 5.1: Sqares of coefficients $\alpha_5(d)$ of the configurations Φ_5^{5+d} entering the local excitonic wavefunction (5.3) in a $9 \times H_2$ cluster of an $(H_2)_x$ chain with the hole being fixed at the central (5-th) H_2 molecule.

d	0	$\pm a$	$\pm 2a$	$\pm 3a$	$\pm 4a$
$(\alpha_5(d))^2$	0.951	0.024	1.54×10^{-4}	5.84×10^{-7}	1.79×10^{-9}

basis sets. Therefore, all our calculations presented in this Chapter are done for a much simpler system consisting of 9 H_2 molecules which are arranged analogously to the system of 4 H_2 molecules considered in section 3.5 (see Fig. 3.15) but with the distance of 3 Å between neighbor H_2 molecules to allow the exciton to travel along the chain. This system represents a 9-unit-cell cluster of an infinite $(H_2)_x$ chain which can be considered as a simple model for the π system of a tPA chain. In our $9 \times H_2$ cluster we first generate localized occupied and virtual molecular orbitals (in fact, bonding and anti-bonding orbitals of the H_2 molecules) and then compute the energetically lowest excited state when only the configurations Φ_5^{5+d} with the hole fixed at the central molecule H_2 (the 5-th one) and the electron in any of anti-bonding orbitals in the 9 H_2 chain are used (by a reference space only CI-calculation using the MOLPRO program package [M2000], [WK88], [KW88], [KW92]). The squares of the coefficients $\alpha_5(d)$ of these configurations, being the probabilities to find an electron in the localized virtual orbital centered in the unit cell $R' = 5 + d$, are presented in Table 5.1. We find the same type of electron distribution around the fixed hole as reported for a tPA single chain in Ref. [RL99] (see Fig. 5.1). Therefore, the electron-hole interaction, which enters the state energy via terms analogous to the two last terms on the right-hand side of Eq. 5.1, leads to the formation of well-bound electron-hole pair and such a (pinned) pair in a crystal can be described in the form of the linear combination (5.3) with only a finite amount of local excited configurations Φ_R^{R+d}.

Such localized states given by Eq. (5.3) are not eigenstates of the periodic system

as they are degenerated. To remove the degeneracy we proceed as in chapter II of Ref. [K63] that is the pinned-hole excitonic wavefunctions $\Psi_R^{\rm exc}$ are treated as rigit objects and a set of LCAO ansatz is made for the wavefunction of the excited state in the one-dimensional crystal (like in a tight-binding model):

$$\Psi_K^{\rm exc} = \sum_R {\rm e}^{iKR}\Psi_R^{\rm exc} = \sum_R {\rm e}^{iKR}\sum_d \alpha_R(d)\Phi_R^{R+d}. \tag{5.4}$$

Here K is the crystal momentum of pair made up by the hole and the electron being distributed among virtual WOs in the close vicinity of this hole. The ansatz (5.4) takes into account the periodic structure of the crystal and the excited states of the crystal can be referred to "particles" of neutral electronic excitations (which are called *excitons*) travelling through the crystal with wave vector K. The energies to produce such excited states $\varepsilon_K^{\rm exc}$ regarded as a function of K form the *excitonic* bands which can be obtained from the finite-cluster calculations.

In the $9 \times H_2$ cluster we open all 9 bonding and 9 anti-bonding orbitals to construct the singly excited configurations Φ_a^s which form the model space and 81 excited states can be obtained as linear combinations of these configurations:

$$\Psi_i^{\rm exc} = \sum_{a=1}^{9}\sum_{s=1}^{9} \alpha_i{}_a^s \Phi_a^s \tag{5.5}$$

where index a (s) denotes an occupied (virtual) localized molecular orbital. Actually this equation is just the finite-cluster version of the crystalline ansatz given in Eq. (5.2). Among all these excited states we find 9 states which are energetically well-separated from the rest and lower than all other excited states. These 9 states $\Psi_i^{\rm exc}$, $i = 1, \ldots, 9$ are strongly-bound excitons we are looking for here and can be regarded as some linear combinations of 9 suitable localized excited states. These 9 "delocalized" states $E_i^{\rm exc}$ are easily identifiable since the energies of these states only spread over an energy interval of 1.4 eV (this value is approximately equal to the excitonic band width) while they are separated by a gap of 2.1 eV from all the other excited states. In fact, we focus our attention here on the lowest excitonic

band which corresponds to the "ground state" of an exciton.

To calculate the excitonic band in the framework of our approach we have to define local excitonic matrix elements (which are stransferable from clusters to the infinite periodic system):

$$\mathrm{EX}_{ij} = H_{ij}^{\mathrm{exc}} - \delta_{ij} E_0 = \langle \Phi_i^{\mathrm{exc}} \mid H \mid \Phi_j^{\mathrm{exc}} \rangle - \delta_{ij} E_0 \tag{5.6}$$

in terms of some *localized* excitonic wavefunctions Φ_i^{exc}. The latter are obtained by a unitary transformation applied to the N^{exc} delocalized excitonic wavefunctions Ψ_i^{exc} in the cluster

$$\Phi_i^{\mathrm{exc}} = \sum_j \Psi_j^{\mathrm{exc}} u_{ji} \tag{5.7}$$

where the unitary matrix u_{ji} is determined by minimizing the total spatial spread of the electron-hole pairs

$$I^{\mathrm{exc}} = \sum_{i=1}^{N^{\mathrm{exc}}} (\sigma_i^{\mathrm{exc}})^2 \tag{5.8}$$

(cf. Eq. (3.5)). Below we provide one possible definition of the spatial spread of the excitonic wavefunction in terms of singly excited configurations.

Note that the introduction of an electron-hole pair with a pinned hole was only used to develop the idea of the quantum-chemical description of a well-bound exciton in terms of singly excited configurations. However, in both, crystals and clusters there exist no such fixed hole, and electrons and holes together are delocalized. Hence, it seems natural to describe the bound electron-hole pairs in terms of *excitonic* coordinates, i.e. a coordinate $\bar{R}$ of the "center of mass" of the exciton and a relative coordinate $\bar{r}$. They can be defined as the population-weghted average of the "centers of mass" and the relative coordinate R_a^s and r_a^s of each of the configurations Φ_a^s entering the excitonic wavefunction:

$$\bar{R}_i = \sum_{a,s} R_a^s \, (\alpha_{i\,a}^{\;\;s})^2, \qquad \bar{r}_i = \sum_{a,s} r_a^s \, (\alpha_{i\,a}^{\;\;s})^2 \tag{5.9}$$

(cf. Eq. (3.7)) where

$$R_a^s = \frac{1}{2}(R_a + R_s) \qquad \text{and} \qquad r_a^s = \frac{1}{2}(R_a - R_s), \tag{5.10}$$

R_a denotes the center of the bonding orbital φ_a and R_s the center of the anti-bonding orbital φ_s.

The spread of each electron-hole pair is defined by the average distance between the electron and the hole (given by $\bar{r}_i$) and by the average deviation of the "center of mass" of each contributing configuration R_a^s from the "center of mass" $\bar{R}_i$ of the exciton itself:

$$(\sigma_i^{\text{exc}})^2 = (\bar{r}_i)^2 + \sum_{a,s} (R_a^s - \bar{R}_i)^2 \, (\alpha_{i\,a}^{\;s})^2 \tag{5.11}$$

(cf. Eq. (3.6)).

Having obtained the unitary matrix u_{ji} which corresponds to the minimum of the functional I^{exc} in Eq. (5.8) or some other measure for the extent of the exciton, we get N^{exc} localized excitonic wavefunctions Φ_i^{exc}. Then, the matrix elements of the Hamiltonian H_{ij}^{exc} can be calculated analogously to the elements of the effective Hamiltonian for hole or electron attachment states as given by Eq. (2.62):

$$H_{ij}^{\text{exc}} = \sum_{i'} u_{i'i} \, E_{i'}^{\text{exc}} \, u_{i'j}. \tag{5.12}$$

In the periodic system one expects to find one such localized excitonic wavefunction Φ_R^{exc} in each unit cell (with R being the translation vector of this unit cell) which all together correspond to the lowest excitonic band of the crystal. Note, that here the center of the exciton is its "center of mass" $\bar{R}_R$ in contrast to the position of the fixed hole in the ansatz (5.3). The local excitonic matrix elements in the periodic system are then defined as

$$\text{EX}_R = H_R^{\text{exc}} - \delta_{0R} E_0 = \langle \Phi_0^{\text{exc}} \mid H \mid \Phi_R^{\text{exc}} \rangle - \delta_{0R} E_0 \tag{5.13}$$

The diagonal matrix element EX_0 is the (Brillouin zone averaged) energy of the exciton and the off-diagonal elements EX_R are the hopping matrix elements between the reference (zero) unit cell and the unit cell at R. As the cluster represents a finite part of the crystal one can associate the excitonic LMEs EX_{ij} obtained in the cluster (for the two localized excited configurations Φ_i^{exc} and Φ_j^{exc} with centers $\bar{R}_i$ and $\bar{R}_j$, respectively) with the crystalline LMEs $\mathrm{EX}_{\bar{R}_j-\bar{R}_i}$. The closer the centers of the chosen localized excitonic wavefunctions Φ_i^{exc} and Φ_j^{exc} are to the center of the cluster the better the LMEs EX_{ij} from the cluster approximate the corresponding crystalline LMEs EX_R.

The excitonic band finally can be obtained by the local excitonic matrix elements (5.13) being subject to a transformation similar to Eqs. (2.32) and (2.33):

$$\mathrm{EX}(k) = \sum_R \mathrm{e}^{ikR}\mathrm{EX}_R. \tag{5.14}$$

As the local off-diagonal matrix elements EX_R are expected to decay with increasing distance R between the centers of the localized electron-hole pairs Φ_0^{exc} and Φ_R^{exc}, the series (5.14) can be truncated at some cut-off radius R_{cut} such that the omitted part of the series is negligible with respect to the terms already summed up. Therefore, one only needs a finite number of the off-diagonal matrix elements to calculate the excitonic band with a given accuracy, and both, diagonal and off-diagonal excitonic matrix elements can be obtained from finite clusters.

Chapter 6

Conclusions and perspectives

The main result of the present thesis is the implementation of a multireference configuration interaction method with singly and doubly excited configurations to account for the electron correlation effects in both neutral and charged infinite periodic systems, in particular in excited electron hole and attached electron states. Our approach is one of the first approaches for solids which is purely based on the correlated wavefunction of the system. Sufficiently large basis sets (valence triple zeta) to describe the correlations especially in the anionic $(N+1)$-electron systems are used. As an output we obtain the quasiparticle band structure (all valence and the lowest conduction bands) of a non-conducting material where electron correlation is systematically taken into account which allows to extract the ionization potential, the electron affinity, the band gap and the band widths of the material as those properties which can be measured in experiments. All these quantities are obtained with *controlled* accuracy. Thus, the approach provides highly desired information on electronic properties of extended systems on a very high level of sophistication and, as we believe, will find many interesting applications. We have applied it to *trans*-polyacetylene single chains and obtained complete and *quantitatively* correct information on electronic properties of the investigated system. Further, an extension of the above approach to excitons (i.e. optical excitations) in crystals is developed which allows to use standard quantum-chemical methods to describe the

electron-hole pairs and to finally obtain *excitonic* bands.

Our method starts from the many-body wavefunction of the infinite closed-shell system obtained in the Hartree–Fock approximation. Local quantities in *real* space (namely, localized electron orbitals and local matrix elements) are then defined which are well-transferable from finite clusters to the infinite system. By the use of these local matrix elements derived from clusters the SCF band structure of the extended system is accurately reproduced. Exploiting the local character of the electron correlation we perform correlation calculations by the MRCI(SD) method in the finite clusters for the N-, $(N-1)$- and $(N+1)$-electron states and as a result obtain the change of the local SCF matrix elements due to the correlation effects which again turned out to be well-transferrable from the clusters to the periodic system.

To reach the current stage of implementation of our approach the following challenging problems were solved. A proper treatment of the $(N+1)$-particle states requires *localized* virtual SCF orbitals which are essentially the same for both infinite periodic systems and clusters. Such orbitals can not be generated in a cluster by any standard localization scheme applied to some ad hoc set of the canonical virtual orbitals of the cluster (in contrast to the occupied orbitals). Therefore, we first generate a set of localized virtual Wannier orbitals in the crystal which correspond to bands of our interest and then project them onto the space of the virtual canonical orbitals of a proper cluster. This way we are able to generate localized virtual molecular orbitals and the relevant local SCF matrix elements in the clusters which are used further in the correlation calculations.

To systematically account for the correlation effects the incremental scheme was exploited. However, this scheme (originally designed for the ground and hole states calculations) has the problem of the emergence of a divergently large number of increments when bigger clusters are considered. To handle this problem the scheme

for the hole states was reformulated in terms of orbital groups. Also, the scheme was extended to the case of attached-electron states.

We showed that within the multireference configuration interaction method one can also handle the problem of satellite states. This problem appears in systems with a relatively small band gap and leads to severe instabilities in the calculations when many-body perturbation theory is used to account for the correlation effects. In the MRCI method the satellite states can be treated together with the true hole or attached-electron states by a proper modification of the reference space however by the cost of increasing computational effort.

The use of configuration interaction methods with singly and doubly excited configurations in combination with the incremental scheme requires a very accurate handling of the size-extensivity error intrinsic to all truncated CI methods. We could show that the known Pople correction applied to the correlation energy of the neutral closed-shell system reduces this error to the required level. However, there did not exist any correction for the size-extensivity error of the MRCI(SD) method, which in case of the charged open-shell systems could lead to a comparable precision. In the present work we have developed such a correction. The analytic formula for it is derived and its performance is checked. The new correction allowed us to extract the final results with a reasonable accuracy.

The whole approach is focused on obtaining local matrix elements which correspond to correlated wavefunctions of the system and contain information on the N-, $(N-1)$- and $(N+1)$-electron states of a system when electron correlation is systematically included. Using these matrix elements we were able to compile a band structure (both valence and conduction bands) of the chosen crystal which fully takes into account correlation effects. From this band structure we extract correlation-corrected values of some characteristic electronic properties of the system which can be measured experimentally. They are the band gap, the band widths, and the ionization potential and electron affinity. We applied our method to an infinite *trans*-polyacetylene single chain. We found that upon inclusion of

electron correlation, the calculated results approved substantially as compared to those on the HF level and that they are in good accordance with the experimental data once the effect of interchain interaction and long-range polarization in *bulk* tPA are also taken into account.

As a remarkable feature of our method we emphasize the possibility to estimate the error for the obtained quantities and to systematically improve the results to any desired accuracy by just increasing the computational effort. For the calculated correlated band structure of a *trans*-polyacetylene single chain which spans an energy range of approximately 30 eV the estimated error for any band energy at any k-point does not exceed 0.3 eV.

Comparison of our results on a tPA single chain to the experimental data on the bulk crystal, composed of weakly interacting chains, indicates that the study of correlation effects in polymers can not be reduced completely to the treatment of isolated chains. There is clear evidence that accounting for the mutual interaction of the tPA chains in the bulk material improves the theoretical results with respect to the experimental data. The correlation of electrons in neighbor chains has to be considered for that purpose. This can be done with our approach. However, to calculate these effects explicitly is beyond the scope of the present study.

Finally, a new wavefunction-based approach which allows to describe well-bound excitons in crystals by means of standard quantum-chemical methods is established. Exploiting the finite dimension of a bound electron-hole pair (extending over several unit cells) we can restrict ourselves to finite clusters of a crystal to calculate the relevant properties of such a compact object. A localization scheme to generate localized excitons in clusters is proposed. Then, the local *excitonic* matrix elements as obtained in the finite clusters can be transferred to the periodic system, and, as the ultimate result of this approach, the *excitonic* bands can be calculated.

At the end we would like to discuss some perspectives of our approach. The

present study opens the possibility to apply highly accurate standard quantum chemical method, designed to account for the correlation effects in finite molecules, to a wide range of crystalline insulators and semiconductors being periodic systems. The approach provides information on the correlated wavefunction of the system and gives *quantitatively* correct results for band energies with a controlled precision which can systematically be improved by increasing the computational cost. With such a combination of highly desired features our approach has no analogue at the present moment.

In the present work the method was applied to a semiconducting polymer, i.e. to a linear system. However, this study was going hand-in-hand with the application of the same methodology to bulk diamond carried out in our laboratory. By now, that investigation of bulk diamond has also been finished successively demonstrating that our approach can equally well be applied to true three-dimensional periodic infinite non-conducting systems.

As discussed in section 3.4, the main computational efforts of our approach goes into the evaluation of a large number of individual increments (roughly two hundred) which corresponds to the calculation of several hundreds of the N-, $(N-1)$- and $(N+1)$-electron states (using a limited number of configurations only) providing us with the information on the energies and the wavefunctions. Such an amount of information requires an automatization of the calculations and data processing. An appropriate general-purpose computer tool, which automatically generates the input files for the correlation calculations with the MOLPRO program package, picks up all the relevant data from the output files and also computes the matrix elements of the effective Hamiltonians and the size-extensivity corrections to the correlation energies, evaluates the individual increments, checks for missing increments and properly sums up the increments of the correlation correction of some particular quantity, have been already developed in our laboratory. Also, some code has been designed to assist the user in generating clusters from a given crystal. Nonetheless, to become a routine tool used by many researchers studying solids

a complete automatization of our method is required. By this we mean a further automatization of the projection of the Wannier orbitals generated by the CRYSTAL code onto the clusters, a dynamic and automatic control of the convergence of the increments with the distance between the active bonds and (by this) a proper choice of suitably-sized clusters for the correlation calculations, a grouping of molecular bonds, the summing up of the increments to both the SCF and the correlation-corrected local matrix elements and finally the compiling of the bands by the use of these LMEs. Many programm tools to tackle these tasks for some particular classes of systems have already been established but most of them are not yet fully general-purpose codes.

On the other hand, there is an increasing activity in the implementation of quantum-chemical correlation methods for extended systems (MP2, say) into existing packages for the SCF calculations which account for the electron correlation directly in the periodic systems using local representations of the single-particle wavefunctions and exploiting the predominantly local character of the correlation effects. The main difference of these approaches to our one is the requirement of *all* the virtual orbitals in the periodic system being localized. Then, by some cutoff criteria on the mutual distance of the localized orbitals the problem is effectively reduced to the case of correlation calculations in clusters (or some other suitable finite subspace). Thus, our experience will be very useful for the developers of such new codes.

Let us finally turn to our approach to excitons in crystals which was established in the present work. Here, a completely new direction in the use of standard quantum-chemical program packages is opened. Further development and an explicit implementation of this approach seems to be a very attractive task since this way the optical properties of non-conducting crystals can be studied by the already existing highly accurate quantum-chemical methods providing quantitatively correct results. There are many open question in this new field of research and, as we believe, they can be answered soon.

Bibliography

[A02] M. Albrecht. Local-orbital-based correlated ab initio band structure calculations in insulating solids: LiF. *Thoer. Chem. Acc.* **107**, 71, 2002.

[AA+99] A. Abdurahman, M. Albrecht, A. Shukla, and M. Dolg. Ab initio study of structural and cohesive properties of polymers. Polyiminoborane and polyaminoborane. *J. Chem. Phys.* **110**, 8819, 1999.

[AF02] M. Albrecht and P. Fulde. Local ab inition schemes to include correlationsin the calculated band structure of semiconductors and insulators. *Phys. Stat. Sol.* **234**, 313, 2002.

[AFS00] M. Albrecht, P. Fulde, H. Stoll. Ab initio estimates of correlation effect on the band gap of covalent semiconductors: diamond and silicon. *Chem. Phys. Lett.* **319**, 355, 2000.

[AI01] M. Albrect and J. Igarashi. Local-orbital based correlated ab initio band structure calculations in insulatig solids. *J. Phys. Soc. Japan* **70**, 1035, 2001.

[AKS01] P.Y. Ayala, K.N. Kudin and G.E. Scuseria. Atomic orbital Laplace-transformed second-order Møller–Plesset theory for periodic systems. *J Chem. Phys.* **115**, 9698, 2001.

[AMI00] L. Adamowicz, J.-P. Malrieu, V.V. Ivanov. New approach to the state-specific multireference coupled-cluster formalism. *J. Chem. Phys.* **112**, 10075, 2000.

[ARM98] M. Albrecht, P. Reinhardt, J.P. Malrieu. Ab initio correlation corrections to the Hartree–Fock quasi band-structure of periodic systems employing Wannier-type orbitals. *Theor. Chem. Acc.* **100**, 241, 1998.

[ASD00a] A. Abdurahman, A. Shukla, and M. Dolg. Correlated ground-state ab initio calculations of polymethineimine. *Chem. Phys.* **257**, 301, 2000.

[ASD00b] A. Abdurahman, A. Shukla, and M. Dolg. Ab initio treatment of electron correlations in polymers: lithium hydride chain and beryllium hydride polymer. *J. Chem. Phys.* **112**, 4801, 2000.

[B50] S.F. Boys. A general method of calculation for the stationary states of any molecular system. *Proc. R. Soc. London* **A 200**, 542, 1950.

[BF87] W. Borrmann and P. Fulde. Exchange and correlation effects on the band structure of semiconductors. *Phys. Rev.* **B 35**, 9569, 1987.

[BF+87] D.D.C. Bradley, R.H. Friend, T. Hartmann, E.A. Marseglia, M.M. Sokolowski and P.D. Townsend. Structural studies of oriented precursor route conjugated polymers. *Synth. Met.* **17**, 473, 1987.

[BZ+01] Ph. Baranek, C.M. Zicovich-Wilson, C. Roetti, R. Orlando and R. Dovesi. Well localized crystalline orbitals obtained from Bloch functions: The case of $KNbO_3$. *Phys. Rev.* **B 64**, 125102, 2001.

[CD88] R.J. Cave and E.R. Davidson. Quasidegenerate variational perturbation theory and the calculation of first-order properties from variational perturbation theory wave functions. *J. Chem. Phys.* **89**, 6798, 1988.

[CRY98] V.R. Saunders, R. Dovesi, C. Roetti, M. Causà, N.M. Harrison, R. Orlando and C.M. Zicovich-Wilson. *CRYSTAL98 User's manual.* University of Torino, Torino, 1998.

[CRYREAD] M. von Arnim, U. Birkenheuer and W. Alsheimer. Embedding calculations with the program CRYREAD. Unpublished.

[D75] E.R. Davidson. Iterative calculation of a few of lowest eigenvalues and corresponding eigenvectors of large real-symmetric matrices. *J. Comp. Phys* **17**, 87, 1975.

[D89] T. Dunning. Gaussian basis sets for use in correlated molecular calculations. I. The atoms boron through neon and hydrogen. *J. Chem. Phys.* **90**, 1007, 1989.

[DD94] W. Duch and G.H.F. Diercksen. Size-extensivity corrections in configuration interaction methods. *J. Chem. Phys.* **101**, 3018, 1994.

[DDFS97] K. Doll, M. Dolg, P. Fulde, and H. Stoll. Quantum chemical approach to cohesive properties of NiO. *Phys. Rev.* **B 55**, 10282, 1997.

[E88] H. Eschrig. *Optimized LCAO Method and the electronic structure of Extended Systems.* Akademie Verlag, Berlin, 1988.

[EF80] J.H. Edwards and W.J. Feast. A new synthesis of poly(acetylene). *Polymer* **21**, 595, 1980.

[EFB84] J.H. Edwards, W.J. Feast and D.C. Bott. New routes to conjugated polymers .1. A 2 step route to polyacetylene. *Polymer* **25**, 395, 1984.

[ER65] C. Edmiston and K. Ruedenberg. Localized atomic and molecular orbitals. *J. Chem. Phys.* **43**, S97, 1965.

[F02] P. Fulde. Wavefunction methods in electronic-structure theory of solids. *Adv. Phys.* **51**, 909, 2002.

[F95] P. Fulde. *Electron correlations in Molecules and solids.* Springer, Berlin, 1995.

[FB60] J.M. Foster and S.F. Boys. Canonical configuration interaction procedure. *Rev. Mod. Phys.* **32**, 300, 1960.

[FC+82] C.R. Fincher, Jr., C.-E. Chen, A.J. Heeger, A.G. MacDiarmid and J.B. Hastings. Structural determination of the symmetry-breaking parameter in *trans*-$(CH)_x$. *Phys. Rev. Lett.* **48**, 100, 1982.

[FG+99] R.H. Friend, R.W. Gymer, A.B. Holmes, J.H. Burroughes, R.N. Marks, C. Taliani, D.D.C. Bradley, D.A. Dos Santos, J.L. Brédas, M. Lödglung and W.R. Salaneck. Electroluminescence in conjugated polymers. *Nature* **397**, 121, 1999.

[FL86] J. Fimk and G. Leising. Momentum-dependent dielectric functions of oriented *trans*-polyacetylene. *Phys. Rev.* **B 34**, 5320, 1986.

[FO+79] C.R. Fincher, Jr., M. Ozaki, M. Tanaka, D. Peebles, L. Lauchlan, A.J. Heeger and A.G. MacDiarmid. Electronic structure of polyacetylene: Optical and infrared studies of undoped semiconducting $(CH)_x$ and heavely doped metallic $(CH)_x$. *Phys. Rev.* **B 20**, 1589, 1979.

[Fr31] J. Frenkel. On the transformation of light into heat in solids. *Phys. Rev.* **37**, 17, 1931.

[G98] M.J. Frisch, G.W. Trucks, H.B. Schlegel, G.E. Scuseria, M.A. Robb, J.R. Cheeseman, V.G. Zakrzewski, J.A. Montgomery, R.E. Stratmann, J.C. Burant, S. Dapprich, J.M. Millam, A.D. Daniels, K.N. Kudin, M.C. Strain, O. Farkas, J. Tomasi, V. Barone, M. Cossi, R. Cammi, B. Mennucci, C. Pomelli, C. Adamo, S. Clifford, J. Ochterski, G.A. Petersson, P.Y. Ayala, Q. Cui, K. Morokuma, D.K. Malick, A.D. Rabuck, K. Raghavachari, J.B. Foresman, J. Cioslowski, J.V. Ortiz, B.B. Stefanov, G. Liu, A. Liashenko, P. Piskorz, I. Komaromi, R. Gomperts, R.L. Martin, D.J. Fox, T. Keith, M.A. Al-Laham, C.Y. Peng, A. Nanayakkara, C. Gonzalez, M. Challacombe, P.M.W. Gill, B.G. Johnson, W. Chen, M.W. Wong, J.L. Andres, M. Head-Gordon, E.S. Replogle and J.A. Pople. *Gaussian 98* (Revision A.6). Gaussian, Inc., Pittsburgh PA, 1998.

[GA88] R.J. Gdanitz and R. Ahlrichs. The averaged coupled-cluster functional (ACPF): a size-extensive modificaion of MRCI(SD). *Chem. Phys. Lett.* **143**, 413, 1988.

[GSF93] J. Gräfenstein, H. Stoll, P. Fulde. Computation of the valence band of diamonds by means of local increments. *Chem. Phys. Lett.* **215**, 611, 1993.

[GSF97] J. Gräfenstein, H. Stoll, P. Fulde. Valence-band structure of group-IV semiconductors by means of local increments. *Phys. Rev.* **B 55**, 13588, 1997.

[H65] L. Hedin. New method for calculating the one-particle Green's function with application to the electron-gas problem. *Phys. Rev.* **139**, A796, 1965.

[HHF84] S. Horsch, P. Horsch and P. Fulde. Electronic excitations in semiconductors. II. Application of the theory to diamond. *Phys. Rev.* **B 29**, 1870, 1984.

[HK64] P. Hohenberg and W. Kohn. Inhomogeneous electron gas. *Phys. Rev.* **136**, B864, 1964.

[HW76] A.F. Holleman and E. Wiberg. *Lehrbuch der Anorganische Chemie.* Walter de Gruyter, Berlin, 1976.

[IB] D. Izotov and U. Birkenheuer. Unpublished.

[K63] R.S. Knox. *Theory of excitons.* Academic Press, New York, 1963.

[Ko34] T. Koopmans. Über die Zuordnung von Wellenfunktionen und Eigenwerten zu den ienzelnen Elektronen eines Atoms. *Physica* **1**, 104, 1934.

[KLL87] H. Kahlert, O. Leitner and G. Leising. Structural-properties of *trans*-$(CH)_x$ and *cis*-$(CH)_x$. *Synth. Met.* **17**, 467, 1987.

[KP+89] R.B. Kaner, S.J. Porter, D.P. Nairns and A.G. MacDiarmid. The application of electrochemistry to the measurement of selected intrinsic properties of polyacetylene. *J. Chem. Phys.* **90**, 5102, 1989.

[KPFS97] S. Kaldova, B. Paulus, P. Fulde and H. Stoll. Influence of electron correlations on ground-state properties of III-V semiconductors. *Phys. Rev.* **B 55**, 4027, 1997.

[KS65] W. Kohn and L.J. Sham. Self-consistent equations including exchange and correlation effects. *Phys. Rev.* **140**, A1133, 1965.

[KW88] P.J. Knowles, H.-J. Werner. An efficient method for the evaluation of coupling coefficients in configuration interaction calculations. *Chem. Phys. Lett.* **145**, 514, 1988.

[KW92] P.J. Knowles, H.-J. Werner. Internally contracted multiconfiguration-reference configuration-interaction calculations for excited-states. *Theor. Chim. Acta* **84**, 95, 1992.

[L88] G. Leising. Anisotropy of the optical constants of pure and metallic polyacetylene. *Phys. Rev.* **B 38**, 10313, 1988.

[LBT87] S.R. Langhoff, C.W. Bauschlicher Jr. and P.R. Taylor. Accurate ab initio calculations for the ground states of N_2, O_2 and F_2. *Chem. Phys. Lett.* **135**, 543, 1987.

[LD74] S.R. Langhoff and E.R. Davidson. Configuration interaction calculations on nitrogen molecule. *Int. J. Quantum Chem.* **8**, 61, 1974.

[LE+81] L. Lauchlan, S. Etemad, T.-C. Chung, A.J. Heeger and A.G. MacDiarmid. Photoexcitations in polyacetylene. *Phys. Rev.* **B 24**, 3701, 1981.

[LL77] L.D. Landau and E.M. Lifshitz. *Quantum mechanics. Non-relativistic theory.* Pergamon press, Oxford, 1977.

[LM86] I. Lindgren and J. Morrison. *Atomic many-bogy theory.* Springer-Verlag, Berlin, 1986.

[LS+93] M. Löndlund, W.R. Salaneck, F. Meyers, J.L. Brédas, G.A. Arbuckle, R.H. Friend, A.B. Holmes and G. Froyer. Evolution of the electronic structure in a conjugated polymer series: polyacetylene, poly(*p*-phenylene), and poly(*p*-phenylenevinylene). *Macromol.* **26**, 3815, 1993.

[M2000] H.-J. Werner and P.J. Knowles. *MOLPRO User's manual.* University of Birmingham, Birmingham, 1999.

[MOLDEN] G.Schaftenaar and J.H.Noordik. Molden: a pre- and post-processing program for molecular and electronic structures. *J. Comput.-Aided Mol. Design*, **14**, 123, 2000.

[MV97] N. Marzari and D. Vanderbilt. Maximally localized generalized Wannier functions for composite energy bands. *Phys. Rev.* **B 56**, 12847, 1997.

[OB82] J. Orenstein and G.L. Baker. Photogenerated gap states in polyacetylene. *Phys. Rev. Lett.* **49**, 1043, 1982.

[P03] J. Pittner. Continuous transition between Brillouin-Wigner and Rayleigh-Schrodinger perturbation theory, generalized Bloch equation, and Hilbert space multireference coupled cluster. *J. Chem. Phys.* **118**, 10876, 2003.

[P55] R.E. Peierls. *Quantum theory of solids.* Clarendon, London, 1955.

[PB99] P. Piecuch, R.J. Bartlett. EOMXCC: A new coupled-cluster method for electronic excited states. *Adv. Quant. Chem.* **34**, 295, 1999.

[PDR88] C. Pisani, R. Dovesi and C. Roetti. *Hartree-Fock ab initio treatment of crystalline systems.* Springer-Verlag, Berlin, 1988.

[PFS95] B. Paulus, P. Fulde and H. Stoll. Electron correlations for ground-state properties of group-IV semiconductors. *Phys. Rev.* **B 51**, 10572, 1995.

[PFS96] B. Paulus, P. Fulde and H. Stoll. Cohesive energies of cubic III-V semiconductors. *Phys. Rev.* **B 54**, 2556, 1996.

[PM89] J. Pipek and P.G. Mezey. A fast intrinsic localization procedure applicable for ab initio and semiempirical linear combination of atomic orbital wavefunctions. *J. Chem. Phys.* **90**, 4916, 1989.

[PS99] M. Pope and C.E. Swenberg. *Electronic processes in organic crystals and polymers.* Oxford University Press, New York, Oxford, 1999.

[PSK77] J.A. Pople, R. Seeger and R. Krishnan. Variational configuration interaction methods and comparision with perturbation theory. *Int. J. Quantum Chem.* **11**, 149, 1977.

[RL99] M. Rohlfing and S.G. Louie. Optical excitations in conjugated polymers. *Phys. Rev. Lett.* **82**, 1959, 1999.

[RP+83] P. Robin, J.P. Pouget, R. Comès, H.W. Gibson and A.J. Epstein. Structural study of the *cis*-to-*trans* thermal isomerization in polyacetylene. *Phys. Rev.* **B 27**, 3938, 1983.

[RTL00] M. Rohlfing, M.L. Tiago and S.G. Louie. First-principles calculation of optical absorption spectra in conjugated polymers: role of electron-hole interaction. *Synth. Met.* **116**, 101, 2000.

[S92] S. Suhai. Structural and electronic properties of infinite *cis* and *trans* polyenes: perturbation theory of electron correlation effects. *Int. J. Quant. Chem.* **42**, 193, 1992.

[SB96] J.-Q. Sun and R.J. Bartlett. Second-order many-body perturbation-theory calculations in extended systems. *J Chem. Phys.* **104**, 8553, 1996.

[SHW99] M. Schütz, G. Hetzer and H.-J. Werner. Low-order scaling local electron correlation methods. I. Linear scaling local MP2. *J. Chem. Phys.* **111**, 5691, 1999.

[SI79/80] H. Shirakawa, S. Ikeda. Preparation and morphology of as-prepared and highly stretch-aligned polyacetylene. *Synth. Met.* **1**, 175, 1979/1980.

[SMV01] I. Souza, N. Marzari and D. Vanderbilt. Maximally localized Wannier functions for entangled energy bands. *Phys. Rev.* **B 65**, 035109, 2001.

[SO96] A. Szabo and N.S. Ostlund. *Modern Quantum Chemistry.* Dover, New York, 1996.

[SSH79] W.P. Su, J.R. Schrieffer, and A.J. Heeger, Soliton excitations in polyacetylene. *Phys. Rev. Lett.* **42**, 1698, 1979.

[SSH80] W.P. Su, J.R. Schrieffer, and A.J. Heeger, Soliton excitations in polyacetylene. *Phys. Rev.* **B 22**, 2099,1980.

[St92a] H. Stoll. The correlation energy of crystalline silicon. *Chem. Phys. Lett.* **191**, 548, 1992.

[St92b] H. Stoll. Correlation energy of diamond. *Phys. Rev.* **B 46**, 6700, 1992.

[SY+82] C.V. Shank, R. Yen, R.L. Fork, J. Orenstein and G.L. Baker. Picosecond dynamics of photoexcited gap states in polyacetylene. *Phys. Rev. Lett.* **49**, 1660, 1982.

[TG+80] T. Tani, P.M. Grant, W.D. Grill, G.B. Street and T.C. Clarke. Phototransport effects in polyacetylene, $(CH)_x$. *Solid Stat. Comm.* **33**, 499, 1980.

[UTLK87] R. Uitz, G. Temmel, G. Leising and H. Kahlert. Infrared optical constants and dichroism of thin polymer films: *trans*-polyacetylene. *Z. Phys. B - Cond. Matt.* **67**, 459, 1987.

[W34] G.H. Wannier. The structure of electronic excitation levels in insulating crystals. *Phys. Rev.* **52**, 191, 1937.

[WK88] H.-J. Werner, P.J. Knowles. An efficient internally contracted multiconfiguration-reference configuration interaction method. *J. Chem. Phys.* **89**, 5803, 1988.

[WMK03] H.-J. Werner, F.R. Manby and P.J. Knowles. Fast linear scaling second-order Møller–Plesset perturbation theory (MP2) using local and density fitting approximations. *J. Chem. Phys.* **118**, 8149, 2003.

[YC83] C.S. Yannoni and T.C. Clarke. Molecular geometry of *cis*- and *trans*-polyacetylene by nutation NMR Spectroscopy. *Phys. Rev. Lett.* **51**, 1191, 1983.

[YKD97] M. Yu, S. Kalvoda, and M. Dolg. An incremental approach for correlation contributions to the structural and cohesive properties of polymers. Coupled-cluster study of trans-polyacetylene. *Chem. Phys.* **224**, 121, 1997.

[Z72] J.M. Ziman. *Princeples of the theory of solids.* At the university press, Cambridge, 1972.

[ZWDS01] C.M. Zicovich-Wilson, R. Dovesi and V.R. Saunders. A general method to obtain well localized Wannier functions for composite energy bands in linear combinations of atomic orbital periodic calculations. *J. Chem. Phys.* **115**, 9708, 2001

Acknowledgements

I am deeply grateful to Prof. Dr. Peter Fulde, director of the Max Planck Institute for the Physics of Complex Systems in Dresden, for his kind invitation to work in this modern international research centre with its impressive computing facilities and very friendly working atmosphere. He drew my attention to this fascinating field of research which brings together physics, chemistry and computer science and for that I would like to give him my special thanks. I am also grateful to him for the encouragement and continuous interest in my work during the whole time of my study at the Institute and for the many illuminating and helpful discussions.

I am very grateful to my advisor Dr. habil. Uwe Birkenheuer, head of the Quantum Chemistry group, for introducing me to my current research field and for his constant and patient guidance of my work. Many of the ideas presented in this thesis emerged in discussions with him. I came to appreciate his very kind personality. He could always find the time for the listening to my little problems and never refused to provide any kind of help or advice. Also I am indebted to him for the developed computer tools which enormously speeded up the data processing. Owing to all mentioned above it was possible to complete the study in a rather limited amount of time.

I would like to thank all my co-laborators Dr. Dmitry Izotov, Dr. Malte von Arnim, Dr. Walter Alsheimer, Dr. Liudmila Siurakshina, J. Prof. Dr. Martin Albrecht, Dr. Christa Willnauer and Dr. Beate Paulus for providing codes and many helpful discussions.

I am also thankful to Prof. Dr. Hermann Stoll and Prof. Cesare Pisani for their very helpful discussions.

Separately I would like to thank Dr. Uwe Birkenheuer, Dr. Aleksey Bezuglyj and Prof. Peter Fulde for the critical reading of the manuscript of this thesis.

I also gratefully acknowledge the generous financial support by the Max Planck Society.

Last, but not least, I am deeply grateful to my parents Aleksey and Galina, my wife Evgeniya and my son Alyosha for their understanding and support during the whole time of my work in Dresden.

HSSS AdminTools (c) 2001, last visited: Mon Apr 26 15:52:02 GMT+02:00 2004